

# Optimal Design of Inductive Components Based on Accurate Loss and Thermal Models

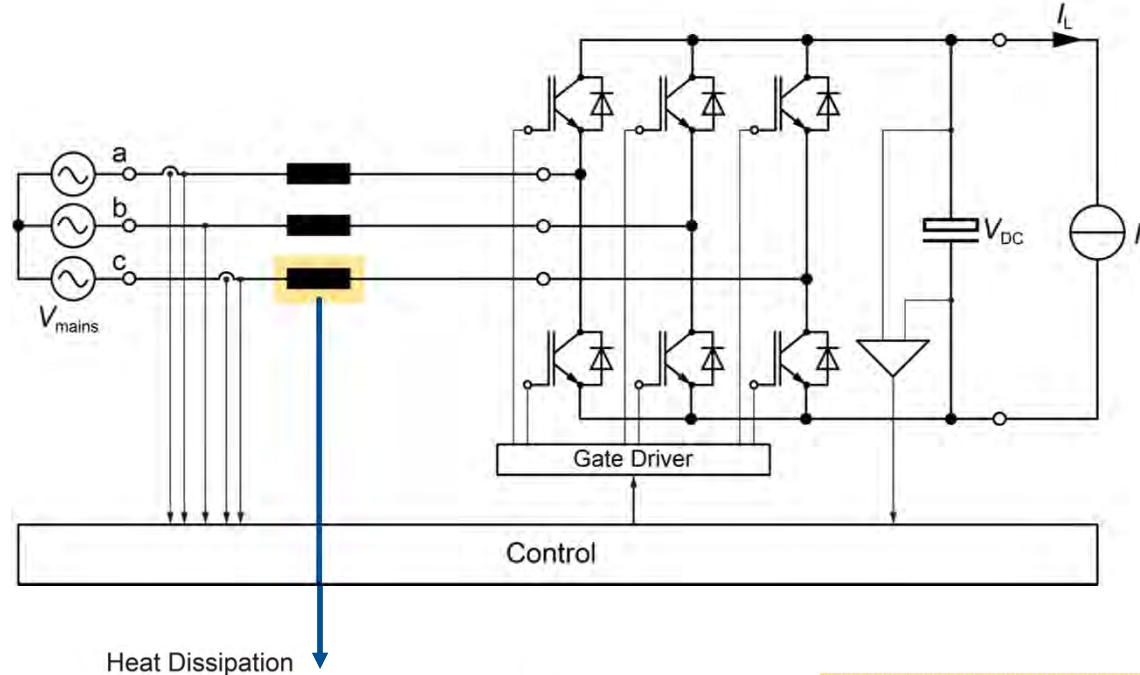
Jonas Mühlethaler and Johann W. Kolar

Power Electronic Systems Laboratory, ETH Zurich

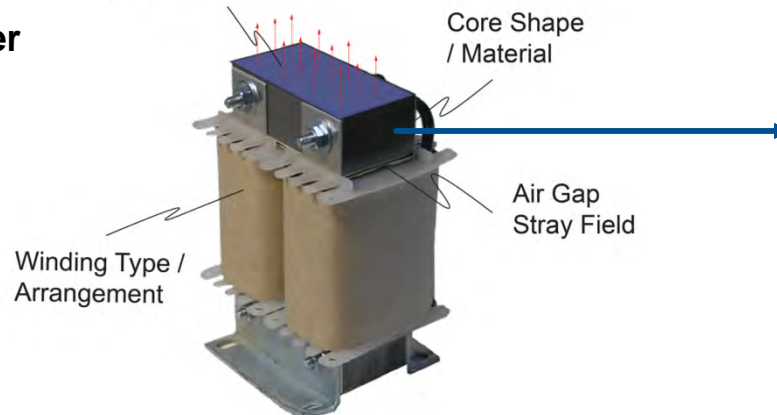


# Introduction

## System Layer



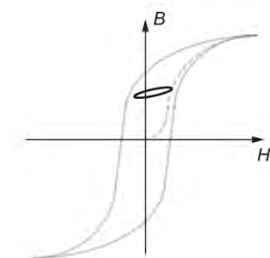
## Component Layer



## Material Layer



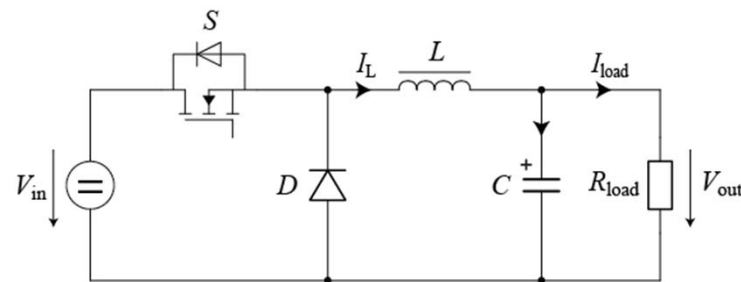
[www.ferroxcube.com](http://www.ferroxcube.com)



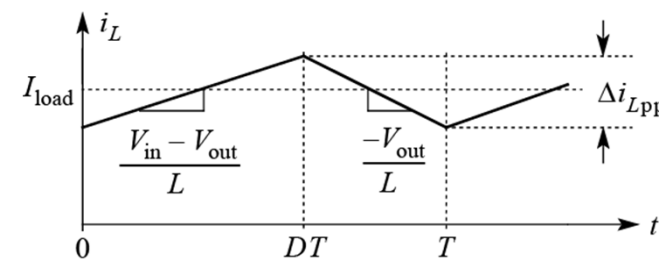
# Introduction

## Application of Inductive Components (1) : Buck Converter (DC Current + HF Ripple)

**Schematic**



**Current / Flux Waveform**



### Modeling Difficulties

- Non-sinusoidal current / flux waveform
- Current / flux is DC biased

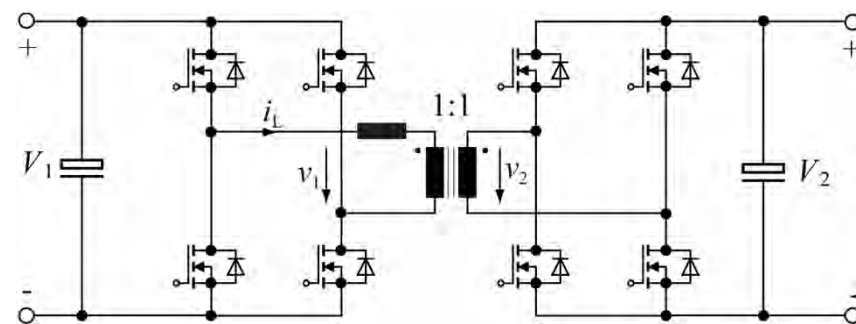
### Solutions

- FFT of current waveform for the calculation of winding losses
- Determine core loss energy for each segment and for each corner point in the piecewise-linear flux waveform
- Loss Map enables to consider a DC bias

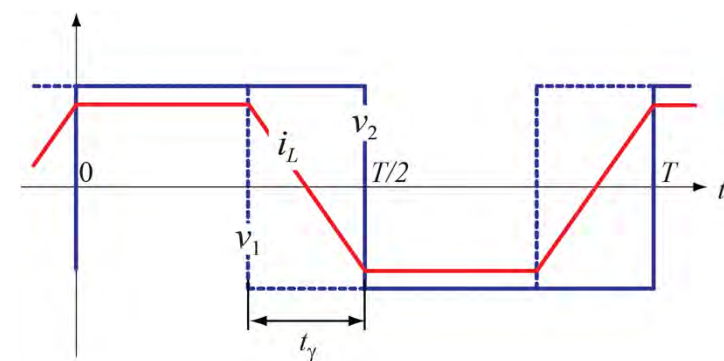
# Introduction

## Application of Inductive Components (2) : Inductor of DAB Converter (Non-Sinusoidal AC Current)

Schematic



Current / Flux Waveform



### Modeling Difficulties

- Non-sinusoidal current / flux waveform
- Core losses occur in the interval of constant flux

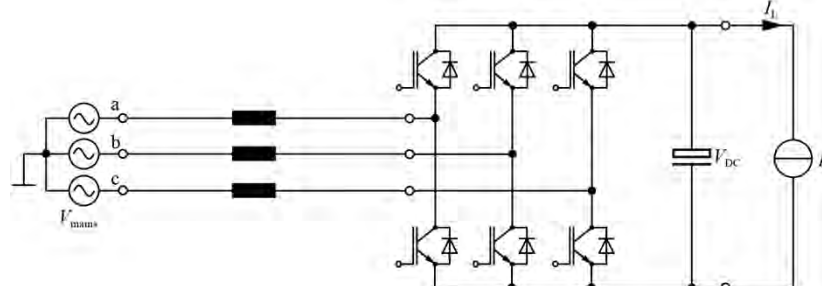
### Solutions

- FFT of current waveform for the calculation of winding losses
- Improved core loss equation that considers relaxation effects

# Introduction

## Application of Inductive Components (3) : Three-Phase PFC (Sinusoidal Current + HF Ripple)

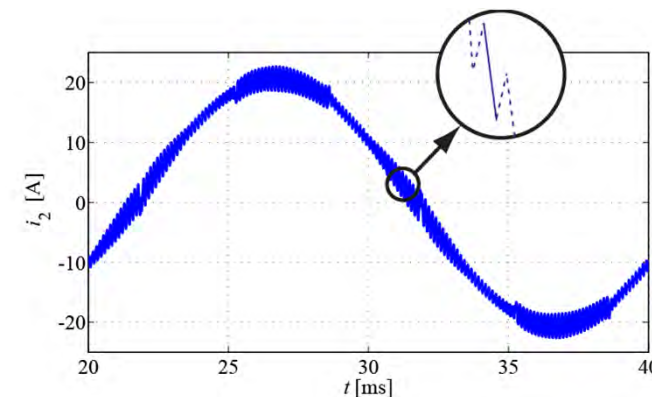
**Schematic**



### Modeling Difficulties

- Non-sinusoidal current / flux waveform
- Major loop and many (DC biased) minor loops

**Current / Flux Waveform**



### Solutions

- FFT of current waveform for the calculation of winding losses
- Determine core loss energy for each segment and for each corner point in the piecewise-linear flux waveform (-> minor loop losses)
- Add major loop losses

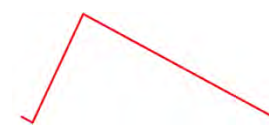
## Introduction

### Overview About Different Flux Waveforms

**Sinusoidal**



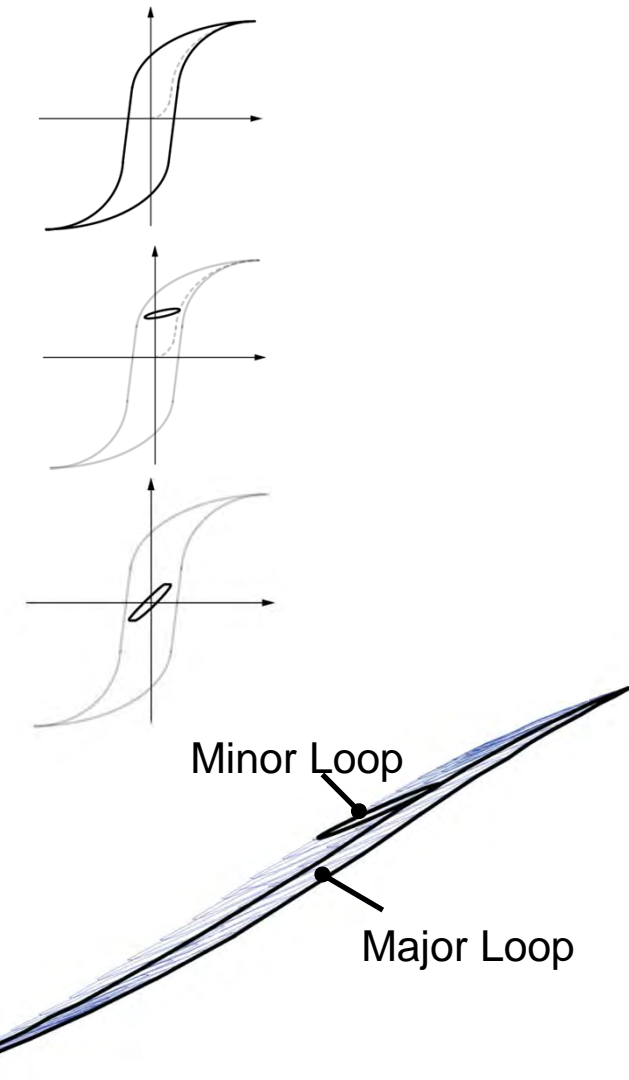
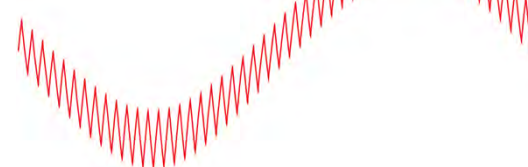
**DC Current +  
HF Ripple**



**Non-Sinusoidal AC  
Current**

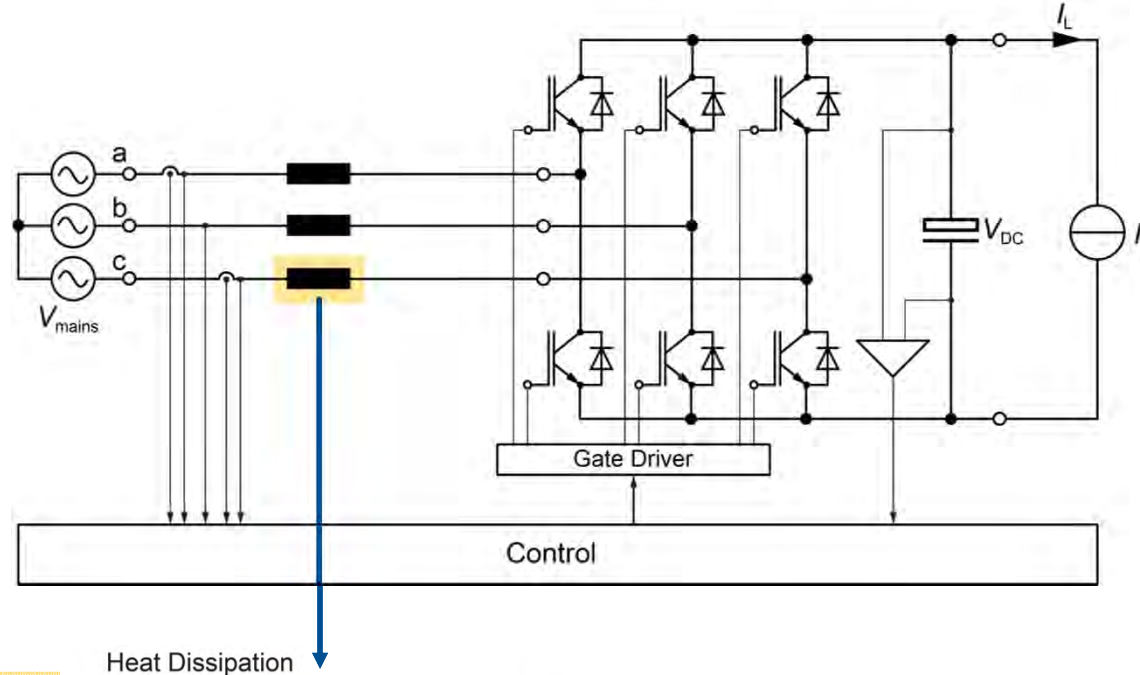


**Sinusoidal Current  
+ HF Ripple**

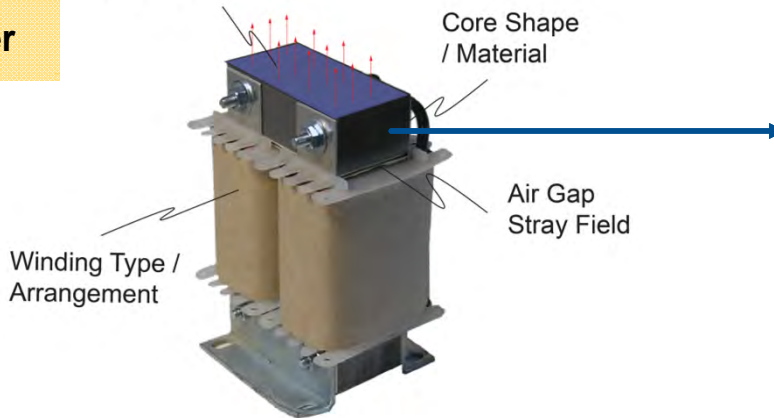


# Introduction

## System Layer



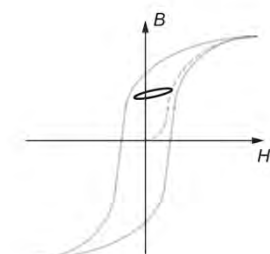
## Component Layer



## Material Layer

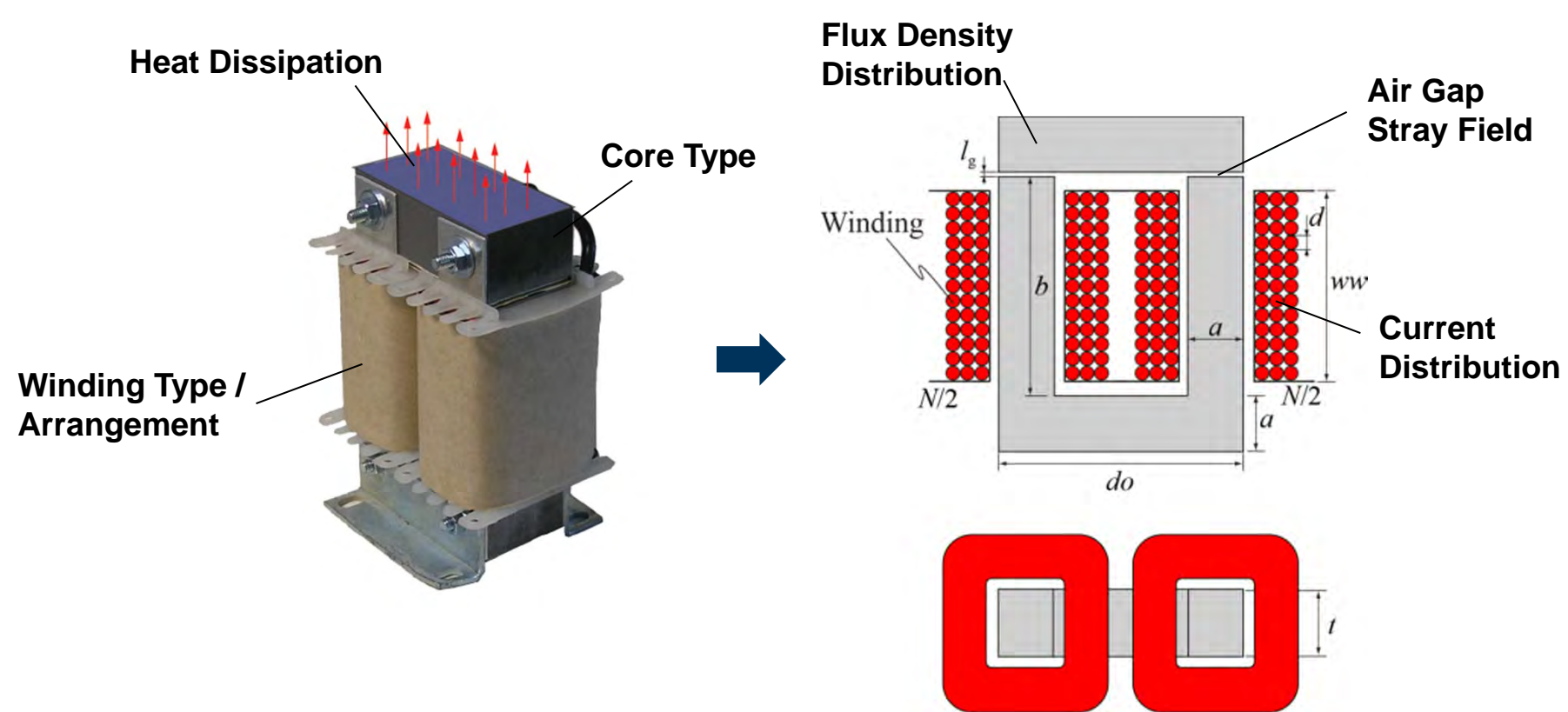


[www.ferroxcube.com](http://www.ferroxcube.com)



## Introduction

### Overview About Other Modeling Issues



# Introduction

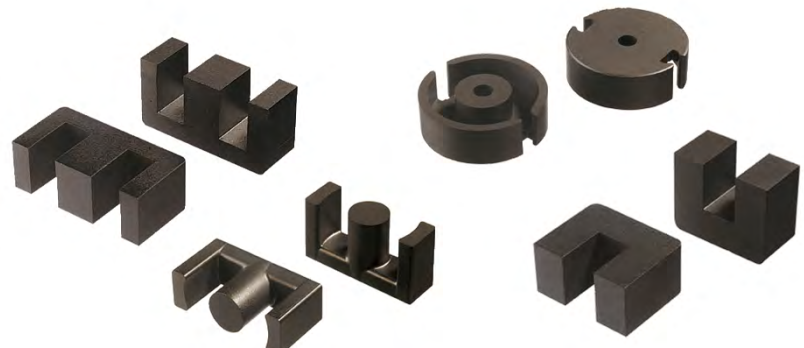
## Wide Range of Realization Options

### Inductors / Transformers



[www.wagnergrimm.ch](http://www.wagnergrimm.ch), [www.ferroxcube.com](http://www.ferroxcube.com)

### Core Shapes



[www.ferroxcube.com](http://www.ferroxcube.com)

### Conductor Shapes



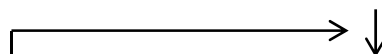
[www.pack-feindraehte.de](http://www.pack-feindraehte.de), [www.jiricek.de](http://www.jiricek.de)

# Introduction

## Modeling Inductive Components (1)

### Procedure

- 1) A reluctance model is introduced to describe the electric / magnetic interface, i.e.  $L = f(i)$ .



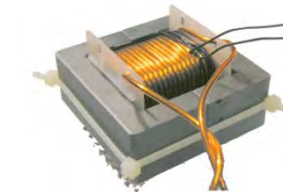
- 2) Core losses are calculated.



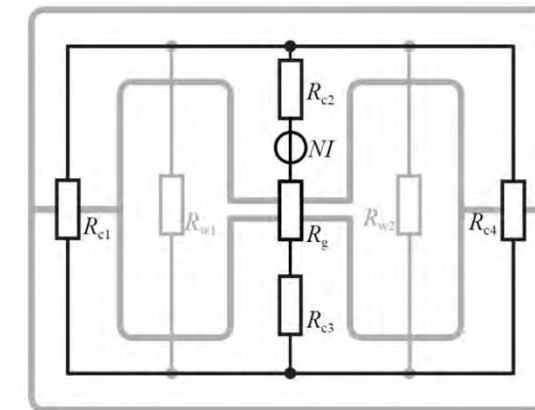
- 3) Winding losses are calculated.



- 4) Inductor temperature is calculated.



Reluctance Model



# Introduction

## Modeling Inductive Components (2)

The following effects will be taken into consideration:

### Magnetic Circuit Model (e.g. for Inductance Calculation):

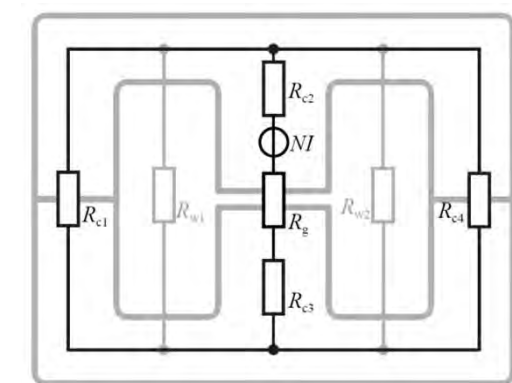
- Air gap stray field
- Non-linearity of core material

### Core Losses:

- DC Bias
- Different flux waveforms (link to circuit simulator)
- Wide range of flux densities and frequencies
- Different core shapes

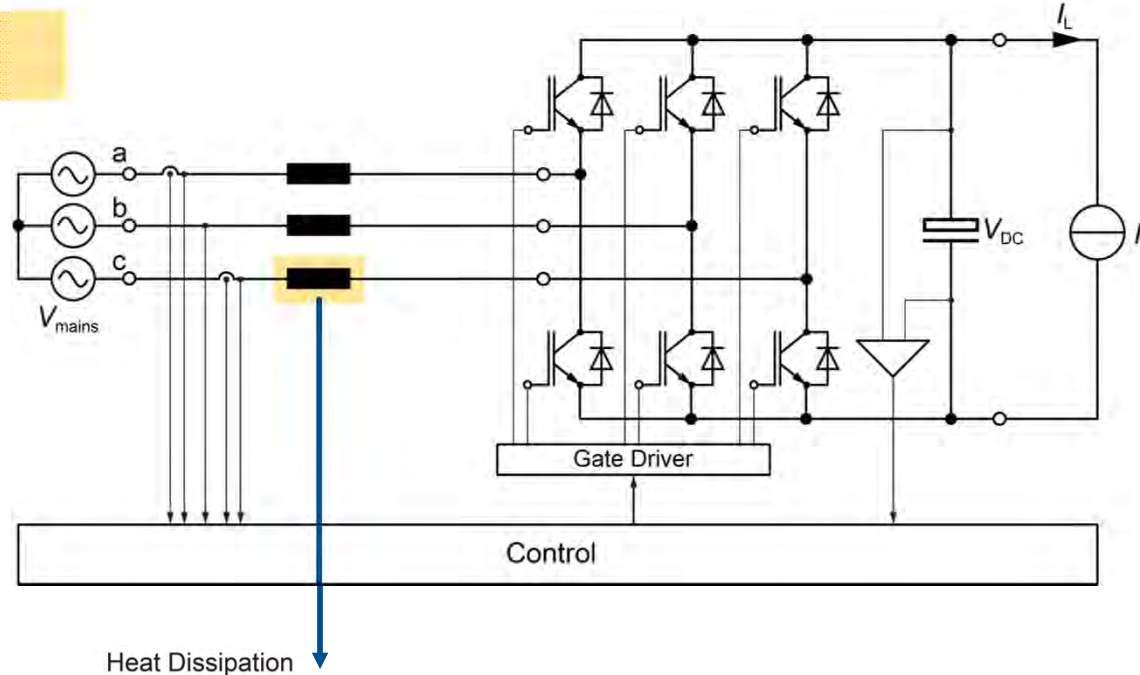
### Winding Losses:

- Skin and proximity effect
- Stray field proximity effect
- Effect of core on magnetic field distribution
- Litz, solid, and foil conductors

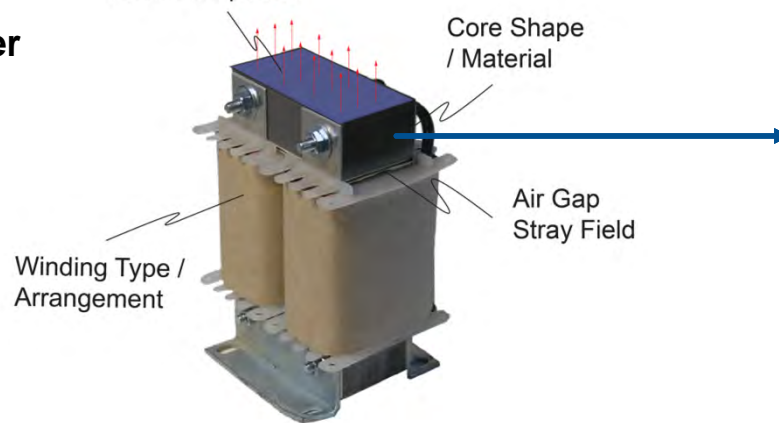


# Introduction

## System Layer



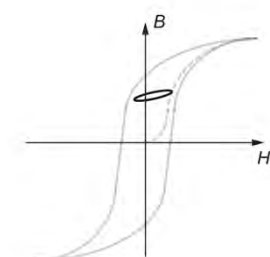
## Component Layer



## Material Layer



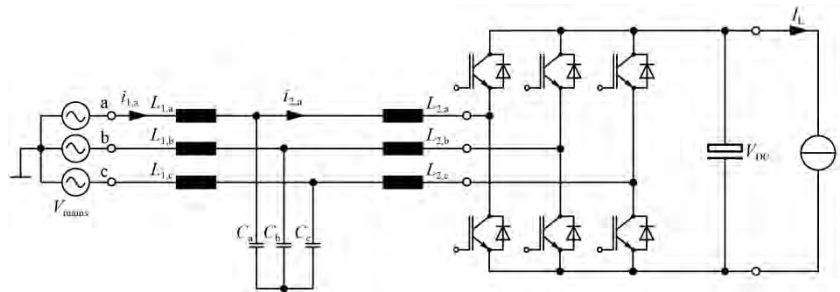
[www.ferroxcube.com](http://www.ferroxcube.com)



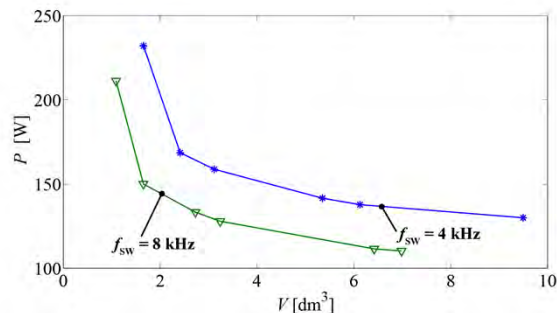
# Introduction

## Motivation for an Accurate Loss Modeling : Multi-Objective Optimization (1)

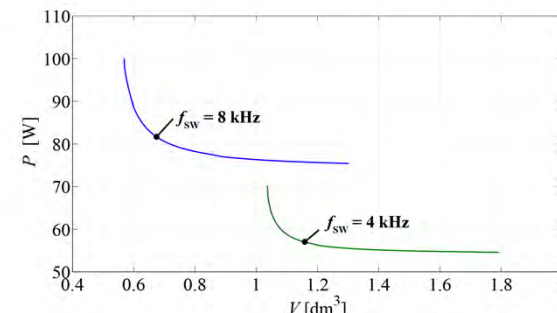
PFC Rectifier with Input LCL filter



Filter Losses vs. Filter Volume



Converter Losses vs. Converter Volume

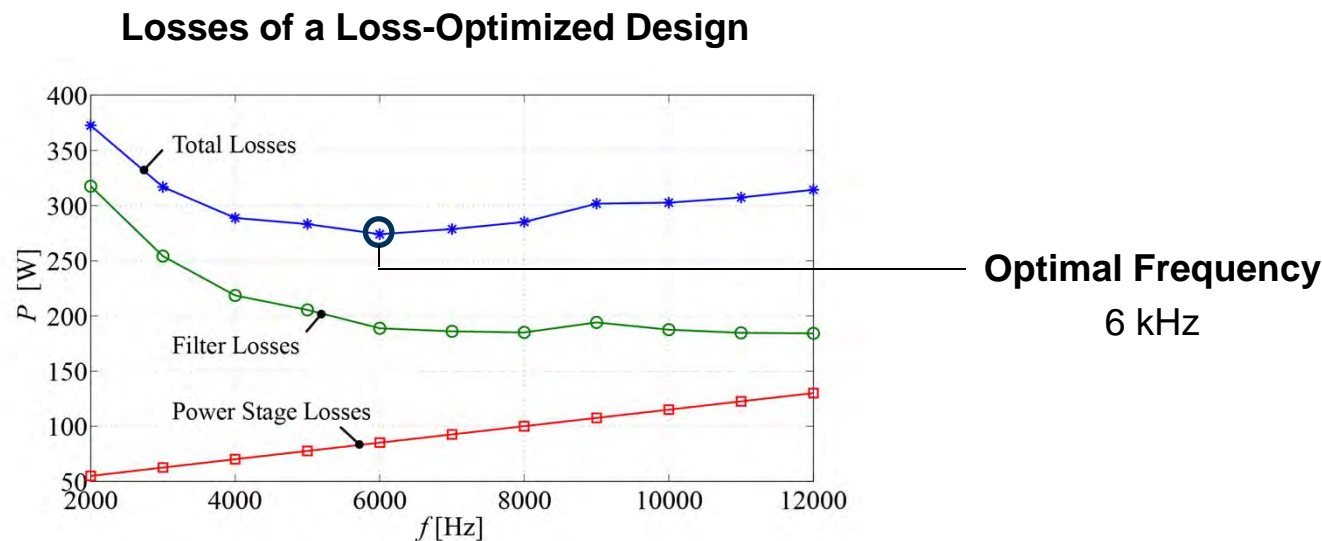


**Converter =**  
Cooling System  
+ Switches

- Sometime there are parameters that bring advantages for one subsystem while deteriorating another subsystem (e.g. frequency in above example).

## Introduction

### Motivation for an Accurate Loss Modeling : Multi-Objective Optimization (2)

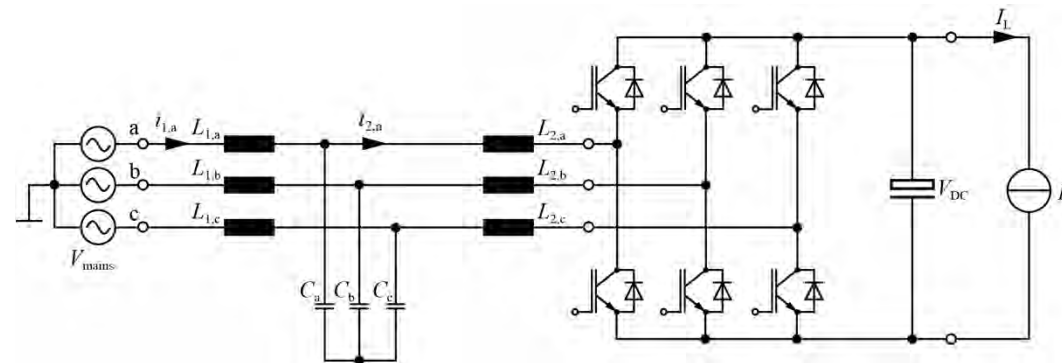


- In order to get an optimal system design, an overall system optimization has to be performed.
- It is (often) not enough to optimize subsystems independent of each other.

# Introduction

## Motivation for an Accurate Loss Modeling : Multi-Objective Optimization (3)

PFC Rectifier with Input LCL filter



### Limits concerning mains

- Tolerable mains harmonics.
- Max. admissible VAr consumption.

### Limits concerning rectifier

- Max. admissible  $T_{j,\max}$
- Max. cooling system vol.  $V_{CS,\max}$

### Limits concerning filter structure

- Max. admissible volume
- Max. admissible losses

### Optimize for

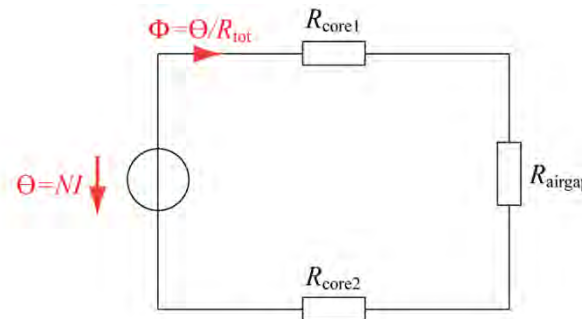
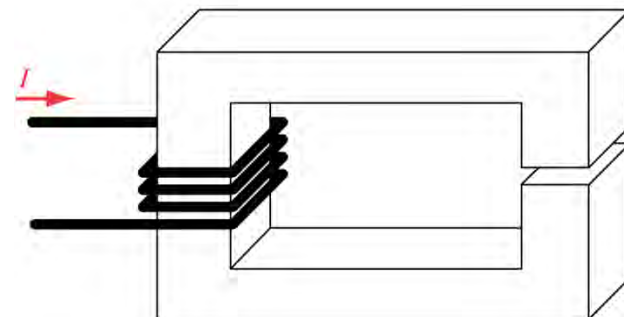
- Overall PFC rectifier volume
- Overall PFC rectifier losses
- (PFC system cost)

# Outline

- **Magnetic Circuit Modeling**
- **Core Loss Modeling**
- **Winding Loss Modeling**
- **Thermal Modeling**
- **Multi-Objective Optimization**
- **Summary & Conclusion**

# Magnetic Circuit Modeling

## Reluctance Model



**Electric Network      Magnetic Network**

**Conductivity / Permeability**

$\kappa$

$\mu$

**Resistance / Reluctance**

$$R = l / (\kappa A)$$

$$R_m = l / (\mu A)$$

**Voltage / MMF**

$$V = \int_{P_1}^{P_2} \vec{E} \cdot d\vec{s}$$

$$V_m = \int_{P_1}^{P_2} \vec{H} \cdot d\vec{s}$$

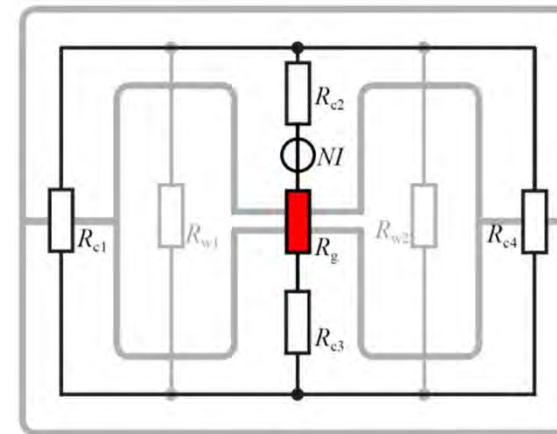
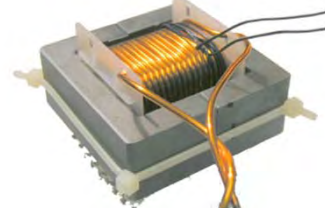
**Current / Flux**

$$I = \iint_A \vec{J} \cdot d\vec{A}$$

$$\Phi = \iint_A \vec{B} \cdot d\vec{A}$$

# Magnetic Circuit Modeling

## Why a Reluctance Model is Needed

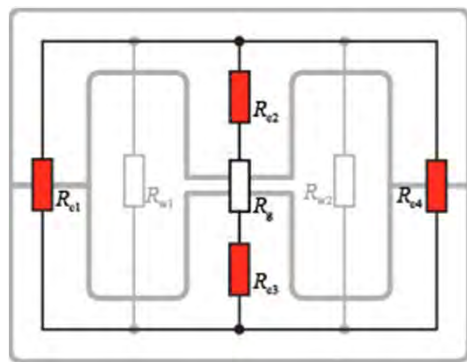


A reluctance model is needed in order to

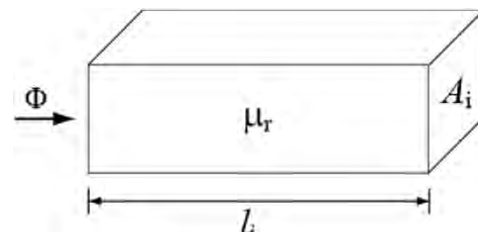
- calculate the inductance ( $L = N^2/R_{\text{tot}}$ )
- calculation the saturation current
- calculate the air gap stray field
- calculate the core flux density

# Magnetic Circuit Modeling

## Core Reluctance

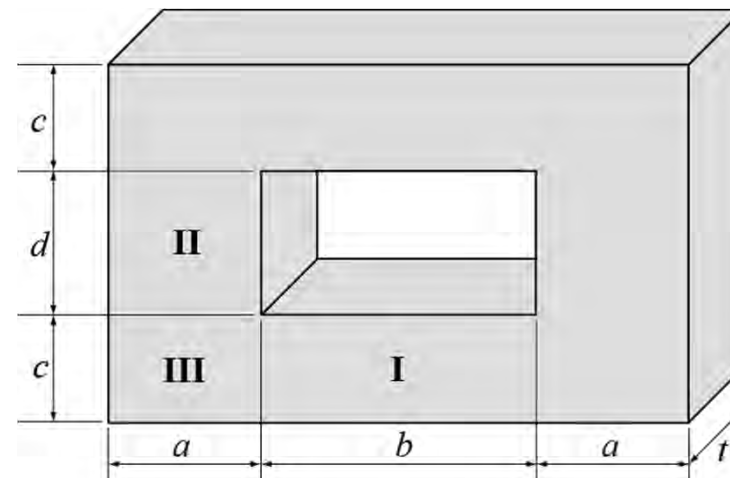


### Reluctance Calculation



$$R_m = \frac{l_i}{\mu_0 \mu_r A_i}$$

### Core Reluctance Dimensions



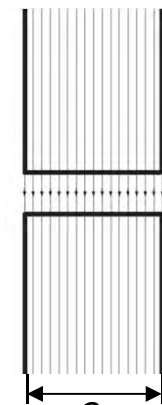
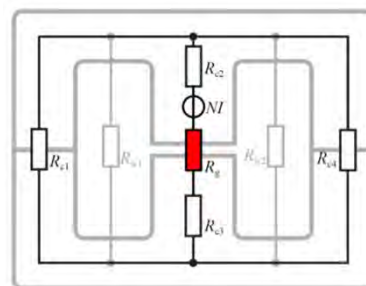
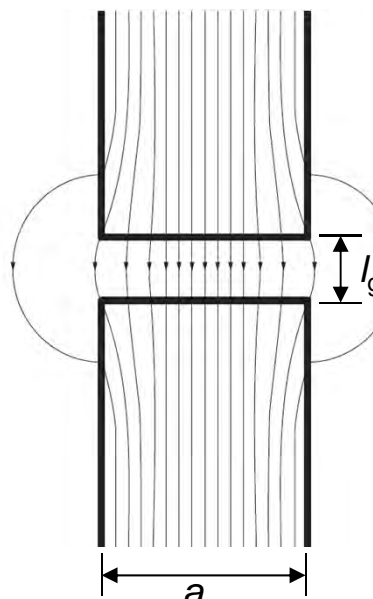
Section	$l_i$	$A_i$
I	$b$	$c \cdot t$
II	$d$	$a \cdot t$
III	$\frac{2\pi}{4} \cdot \frac{(a+c)}{4} = \frac{\pi}{8}(a+c)$	$\frac{t(a+c)}{2}$

Mean magnetic  
length

Mean magnetic  
cross-sectional  
area

# Magnetic Circuit Modeling

## Air Gap Reluctance : Different Approaches (1)

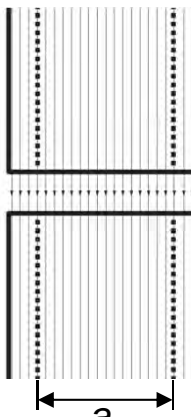


**Assumption of Homogeneous Field Distribution**

$$R_m = \frac{l_g}{\mu_0 A_g}$$

$l_g$  Air gap length

$A_g$  Air gap cross-sectional area



**Increase of the Air Gap Cross-Sectional Area**

e.g. [1] (for a cross section with dimension  $a \times t$ ):

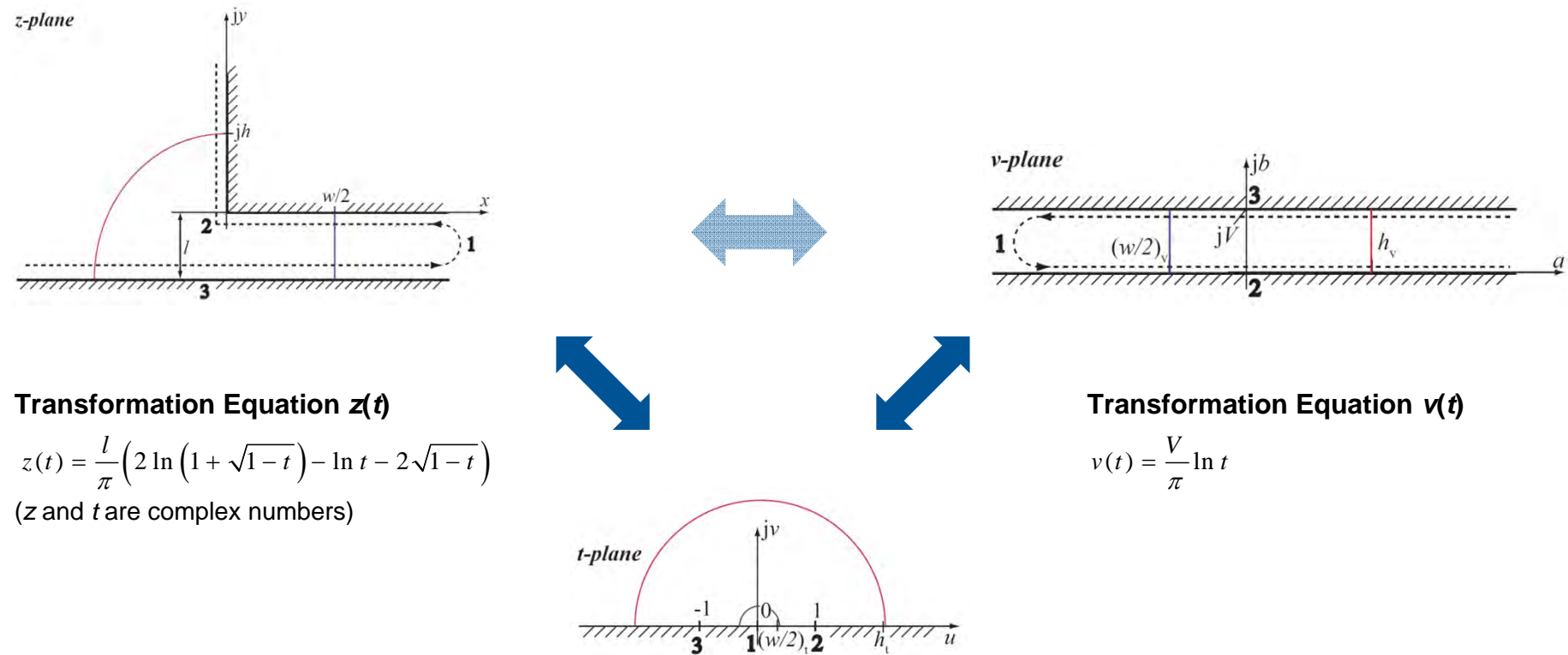
$$R_m = \frac{l_g}{\mu_0 (a + l_g)(t + l_g)}$$

- [1] N. Mohan, T. M. Undeland, and W. P. Robbins - "Power Electronics – Converter, Applications, and Design", John Wiley & Sons, Inc., 2003

# Magnetic Circuit Modeling

## Air Gap Reluctance : Different Approaches (2)

### Schwarz-Christoffel Transformation



- [2] K. J. Binns, P. J. Lawrenson, and C. W. Trowbridge, «The Analytical and Numerical Solution of Electric and Magnetic Fields», John Wiley & Sons, Inc., 1992

# Magnetic Circuit Modeling

## Air Gap Reluctance : Different Approaches (3)

**Solution to 2-D problems found in literature, e.g. in [3]**

Can't be directly applied to 3-D problems.

**Some 3-D solution to problem found in literature; however, they are **complex** [4] and/or limited to one air gape shape [5]**

More simple and universal model desired.

- [3] A. Balakrishnan, W. T. Joines, and T. G. Wilson - "Air-gap reluctance and inductance calculations for magnetic circuits using a Schwarz-Christoffel transformation", IEEE Transaction on Power Electronics, vol. 12, pp. 654—663, July 1997.
- [4] P. Wallmeier, "Automatisierte Optimierung von induktiven Bauelementen für Stromrichteranwendungen", PhD Thesis, Universität – Gesamthochschule Paderborn, 2001.
- [5] E. C. Snelling, "Soft Ferrites - Properties and Applications", 2<sup>nd</sup> edition, Butterworths, 1988

# Magnetic Circuit Modeling

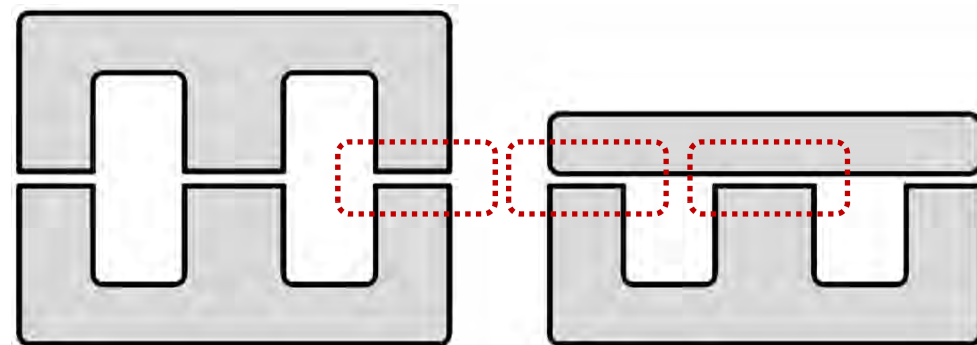
## Aim of New Model

Air gap reluctance calculation that

- considers the **three dimensionality**,
- is reasonable **easy-to-handle**,
- is capable of modeling **different shapes** of air gaps,
- while still achieving a high **accuracy**.



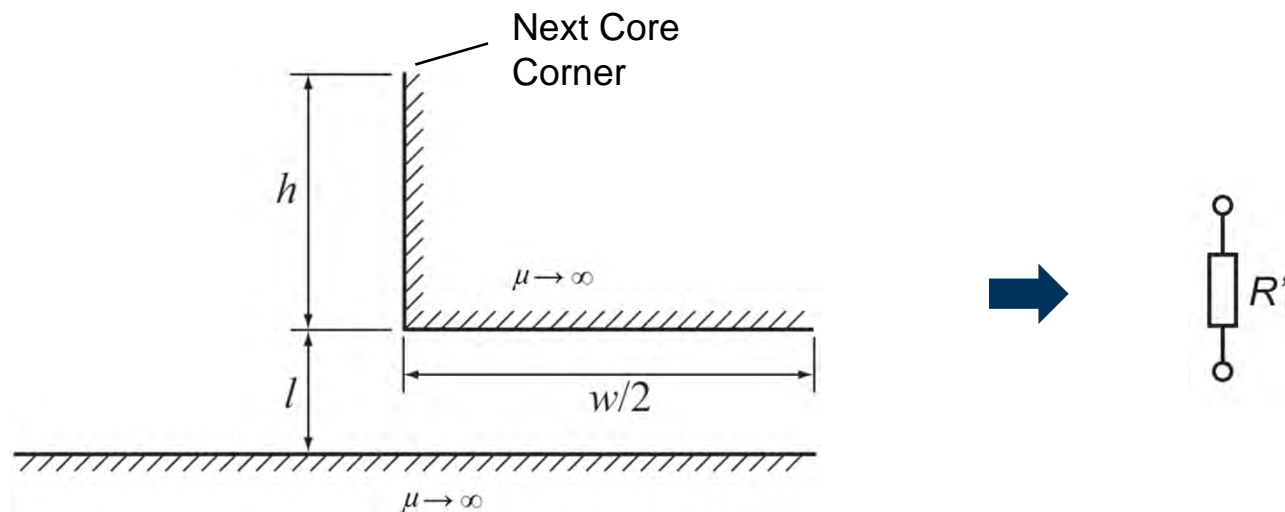
### Illustration of Different Air Gap Shapes:



# Magnetic Circuit Modeling

## New Model (1)

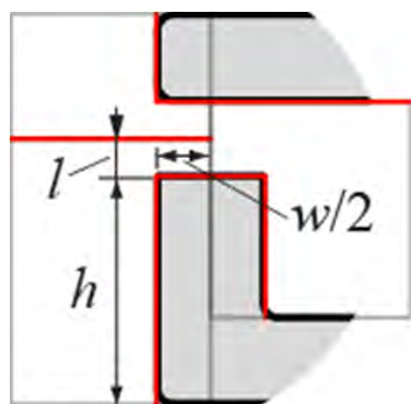
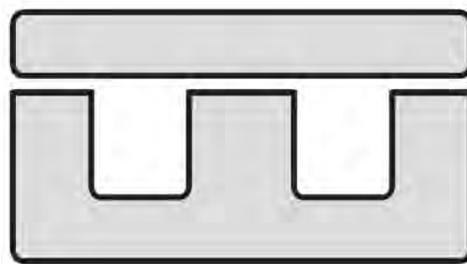
Basic Structure for the Air Gap Calculation (2-D) [3]



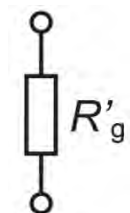
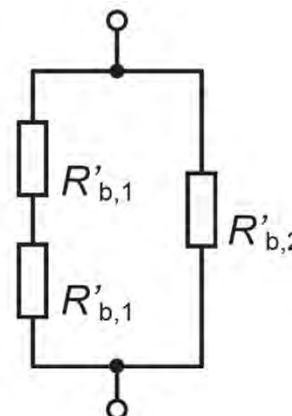
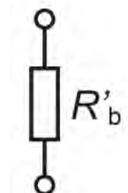
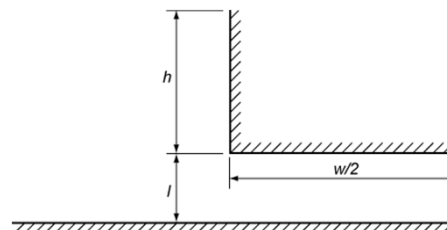
$$R'_{\text{basic}} = \frac{1}{\mu_0 \left[ \frac{w}{2l} + \frac{2}{\pi} \left( 1 + \ln \frac{\pi h}{4l} \right) \right]}$$

## Magnetic Circuit Modeling New Model (2)

2-D (1)



Basic Structure for the Air Gap Calculation

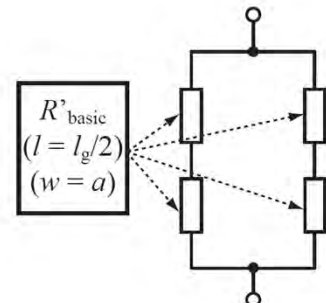
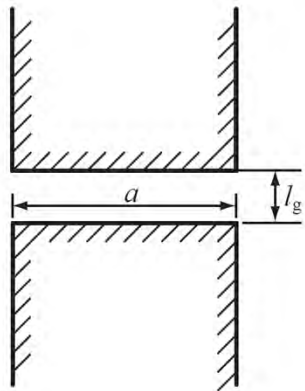


# Magnetic Circuit Modeling

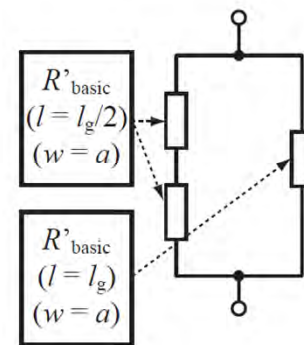
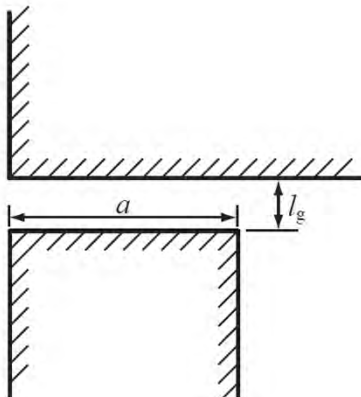
## New Model (3)

2-D (2)

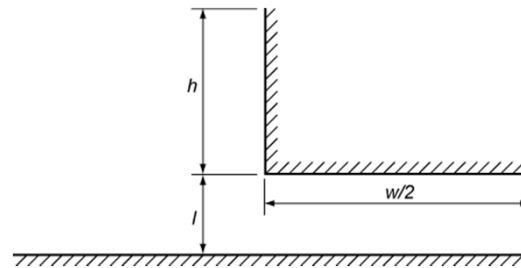
### Air Gap Type 1



### Air Gap Type 2

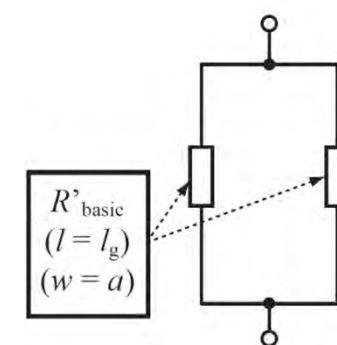
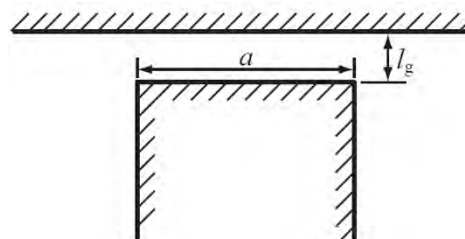


### Basic Structure for the Air Gap Calculation



$$R'_{\text{basic}} = \frac{1}{\mu_0 \left[ \frac{w}{2l} + \frac{2}{\pi} \left( 1 + \ln \frac{\pi h}{4l} \right) \right]}$$

### Air Gap Type 3

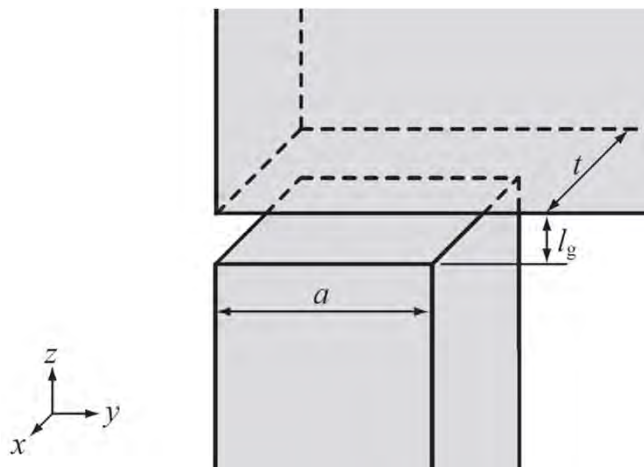


# Magnetic Circuit Modeling

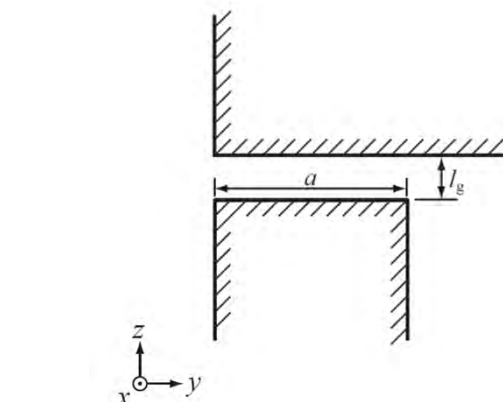
## New Model (4)

2D → 3D : Fringing Factor (1)

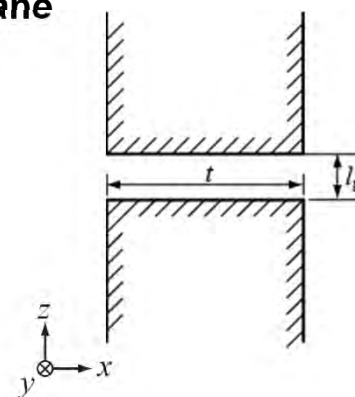
### Illustrative Example



### zy-plane



### zx-plane



Air gap per unit length

$$\rightarrow R_{zy} \rightarrow \sigma_y = \frac{R'_{zy}}{\frac{l_g}{\mu_0 a}}$$

“Idealized” air gap  
(no fringing flux)

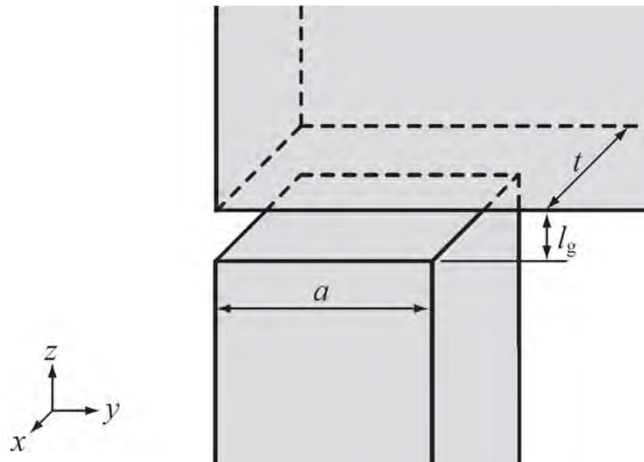
$$\rightarrow R'_{zx} \rightarrow \sigma_x = \frac{R'_{zx}}{\frac{l_g}{\mu_0 t}}$$

# Magnetic Circuit Modeling

## New Model (5)

2D → 3D : Fringing Factor (2)

### Illustrative Example



### 3-D Fringing Factor:

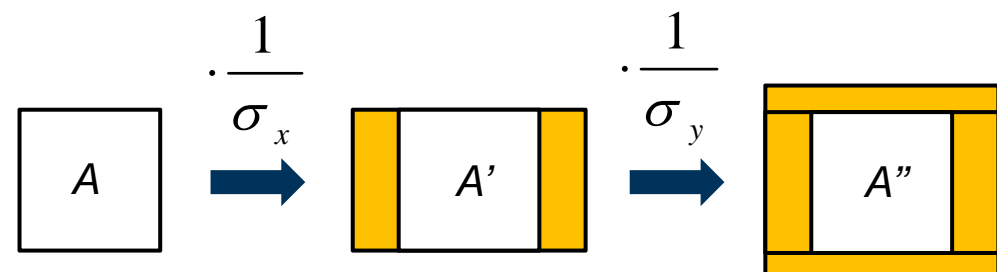
$$\sigma = \sigma_x \sigma_y$$

$$R_g = \sigma \frac{l_g}{\mu_0 a t}$$

"Idealized" air gap  
(no fringing flux)

### Alternative Interpretation:

Increase of air gap cross sectional area



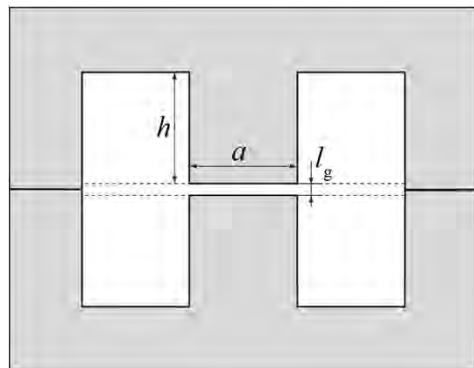
- [6] J. Mühlethaler, J.W. Kolar, and A. Ecklebe, "A Novel Approach for 3D Air Gap Reluctance Calculations", in Proc. of the ICPE - ECCE Asia, Jeju, Korea, 2011

# Magnetic Circuit Modeling

## FEM Results

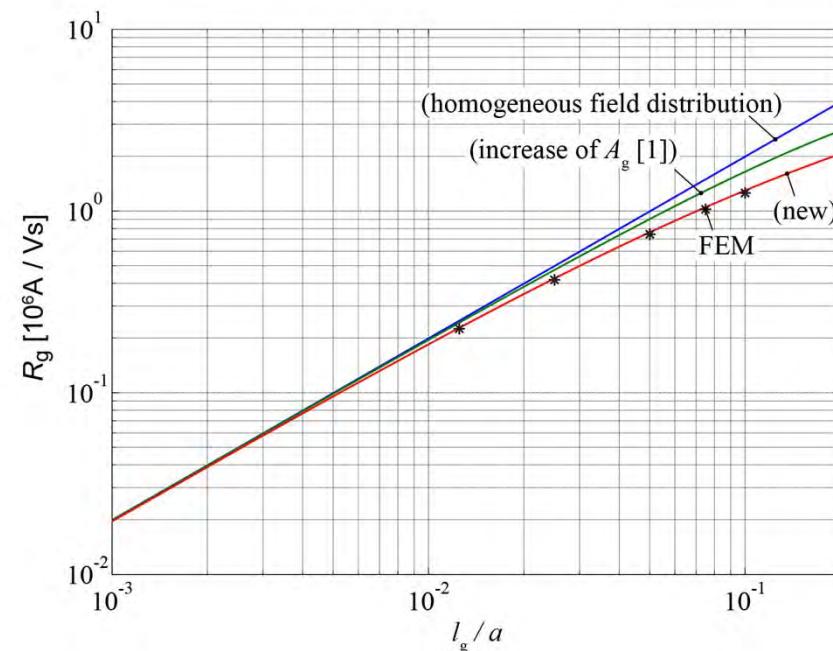
### 3-D FEM Simulation

#### Modeled Example



$a = 40 \text{ mm}$ ;  $h = 40 \text{ mm}$

#### Results



# Magnetic Circuit Modeling

## Experimental Results

### Inductance Calculation

EPCOS E55/28/21,  $N = 80$

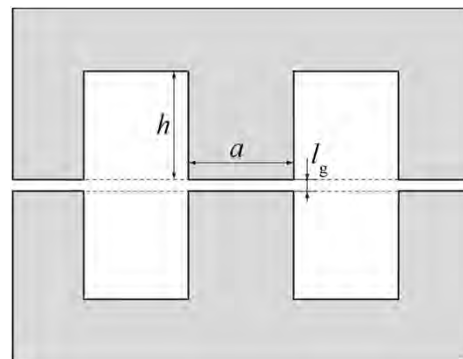


TABLE I  
MEASUREMENT RESULTS OF E-CORE

Air Gap Length $l_g$	Calculated classically (3)	Calculated with new approach (12)	Measured
1.0 mm	1.42 mH	1.97 mH	2.07 mH
1.5 mm	0.96 mH	1.47 mH	1.58 mH
2.0 mm	0.72 mH	1.22 mH	1.26 mH

### Saturation Calculation

EPCOS E55/28/21,  $N = 80$ ,

$$l_g = 1 \text{ mm}, B_{\text{sat}} = 0.45 \text{ T}$$

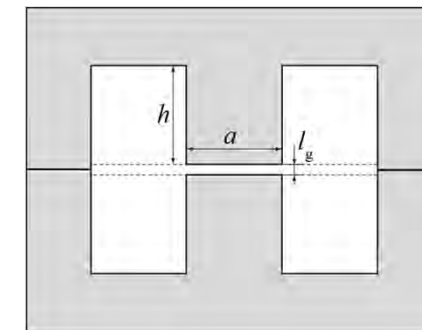
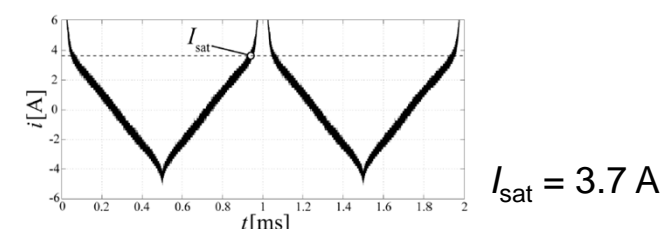


TABLE II  
MEASUREMENT RESULTS OF E-CORE

	Calculated classically (3)	Calculated with new approach (12)
$L$	2.75 mH	3.55 mH
$I_{\text{sat}}$	4.6 A	3.6 A

### Measurement



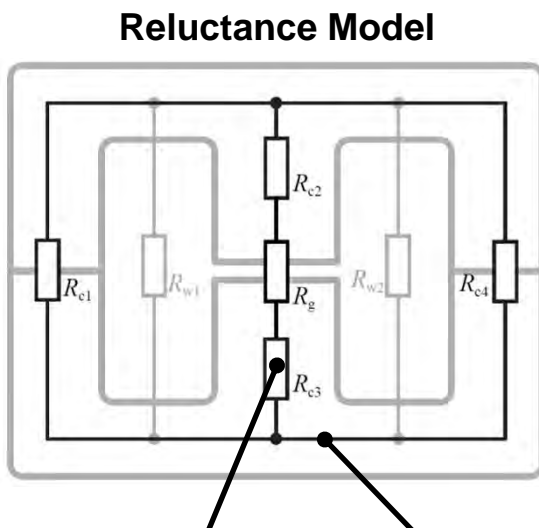
# Magnetic Circuit Modeling

## Non-Linearity of the Core Material

### Flux and Reluctance Calculation

$$\emptyset = f(R_m(\emptyset), I)$$

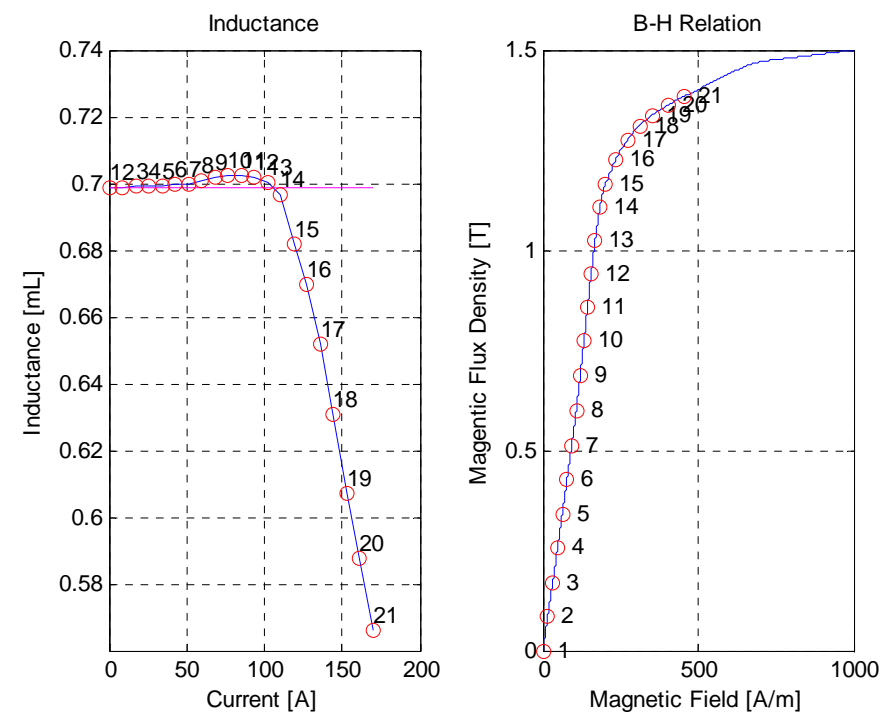
This equation must be solved iteratively by using a numerical solving method, e.g. the Newton's method.



$$R_m = f(\emptyset) \quad \emptyset = f(R_m(\emptyset), I) = f(\emptyset, I)$$

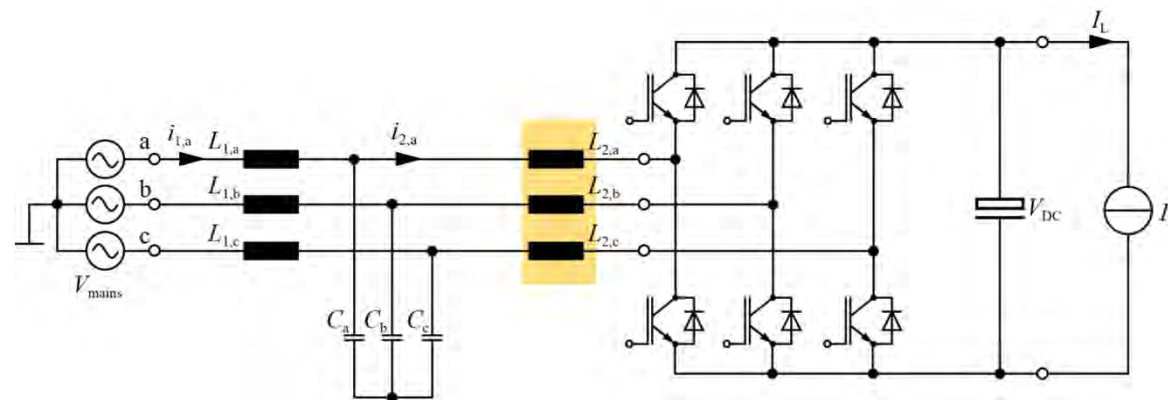
### Inductance Calculation

$$L = \frac{N^2}{R_{\text{tot}}(I)}$$



## Example Introduction

Schematic



### Aim

Design PFC rectifier system.

Show trade-off between losses and volume.

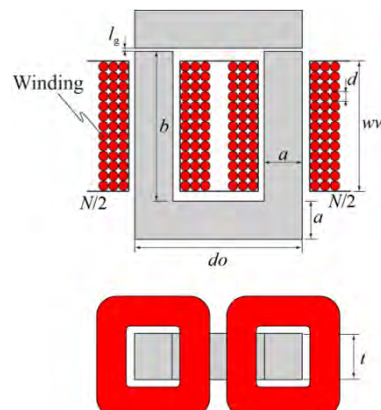
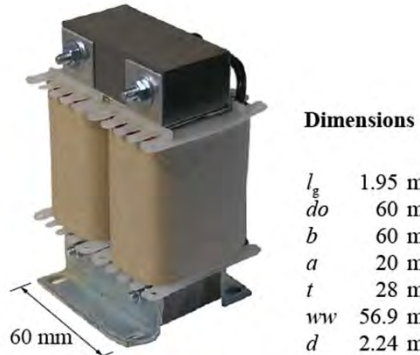
Illustrative example.

**Modeling of boost inductors (three individual inductors  $L_{2a} = L_{2b} = L_{2c}$ ) will be step-by-step illustrated in the course of this presentation.**

## Example

### Reluctance Model (1)

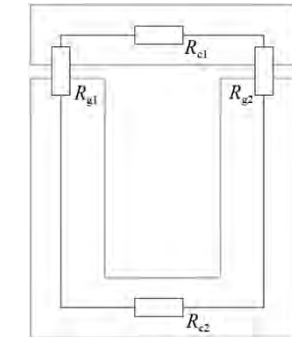
#### Photo & Dimensions



#### Material

Grain-oriented steel (M165-35S)

#### Reluctance Model



#### Calculation of Core Reluctances

$$R_{c1} = \frac{do - 2a}{\mu_0 \mu_r a t} + 2 \frac{\frac{\pi}{8}(2a)}{\mu_0 \mu_r t \frac{(2a)}{2}}$$

$$= \frac{60\text{mm} - 2 \cdot 20\text{mm}}{\mu_0 \cdot 20'000 \cdot 20\text{mm} \cdot 28\text{mm}} + 2 \frac{\frac{\pi}{8}(2 \cdot 20\text{mm})}{\mu_0 \cdot 20'000 \cdot 28\text{mm} \frac{(2 \cdot 20\text{mm})}{2}} = 3654 \frac{\text{A}}{\text{Vs}}$$

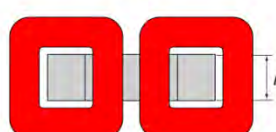
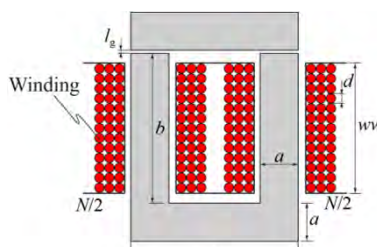
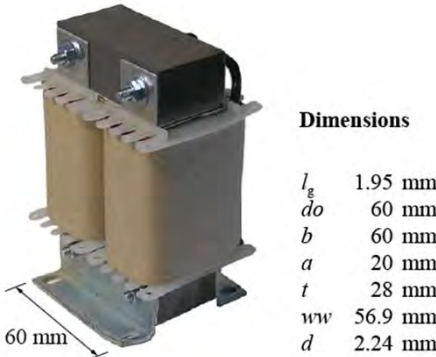
$$R_{c2} = \frac{do - 2a + 2b}{\mu_0 \mu_r a t} + 2 \frac{\frac{\pi}{8}(2a)}{\mu_0 \mu_r t \frac{(2a)}{2}}$$

$$= \frac{60\text{mm} - 2 \cdot 20\text{mm} + 2 \cdot h}{\mu_0 \cdot 20'000 \cdot 20\text{mm} \cdot 28\text{mm}} + 2 \frac{\frac{\pi}{8}(2 \cdot 20\text{mm})}{\mu_0 \cdot 20'000 \cdot 28\text{mm} \frac{(2 \cdot 20\text{mm})}{2}} = 12184 \frac{\text{A}}{\text{Vs}}$$

## Example

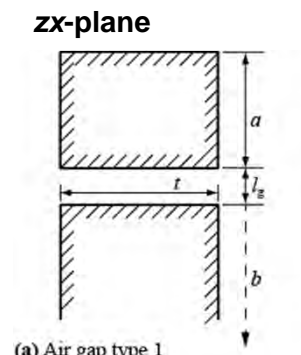
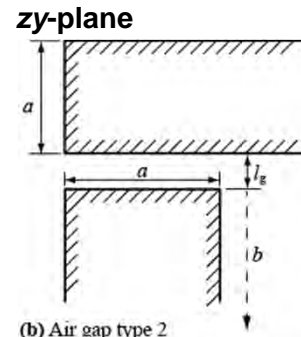
### Reluctance Model (2)

#### Photo & Dimensions

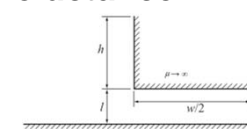


**Material**  
Grain-oriented steel (M165-35S)

#### Calculation Air Gap Reluctances



#### Basic Reluctance



$$R_{\text{basic}} = \frac{1}{\mu_0 \left[ \frac{w}{2l} + \frac{2}{\pi} \left( 1 + \ln \frac{\pi h}{4l} \right) \right]}$$

$$\Rightarrow R_{zy,1} = \frac{1}{\mu_0 \left[ \frac{a}{2l_g} + \frac{2}{\pi} \left( 1 + \ln \frac{\pi a}{4l_g} \right) \right]} \quad R_{zy,2} = \frac{1}{\mu_0 \left[ \frac{a}{2l_g} + \frac{2}{\pi} \left( 1 + \ln \frac{\pi(b+a)}{4l_g} \right) \right]}$$

$$R_{zy,3} = \frac{1}{\mu_0 \left[ \frac{a}{2l_g} + \frac{2}{\pi} \left( 1 + \ln \frac{\pi b}{4l_g} \right) \right]} \Rightarrow R_{zy} = \frac{(R_{zy,1} + R_{zy,2})R_{zy,3}}{R_{zy,1} + R_{zy,2} + R_{zy,3}}$$

$$\Rightarrow \sigma_y = \frac{R_{zy}}{l_g} = 0.72$$

$$R_{zx,1} = \frac{1}{\mu_0 \left[ \frac{t}{2l_g} + \frac{2}{\pi} \left( 1 + \ln \frac{\pi a}{4l_g} \right) \right]} \quad R_{zx,2} = \frac{1}{\mu_0 \left[ \frac{t}{2l_g} + \frac{2}{\pi} \left( 1 + \ln \frac{\pi(b+a)}{4l_g} \right) \right]}$$

$$\Rightarrow R_{zx} = \frac{R_{zx,1} + R_{zx,2}}{2} \quad \Rightarrow \sigma_x = \frac{R_{zx}}{l_g} = 0.84$$

$$R_g = \sigma_x \sigma_y \frac{l_g}{\mu_0 at} = 1.66 \frac{\text{MA}}{\text{Wb}}$$

#### Inductance

$$L = \frac{N^2}{R_{c1} + R_{c2} + R_{g1} + R_{g2}} = 2.66 \text{ mH}$$

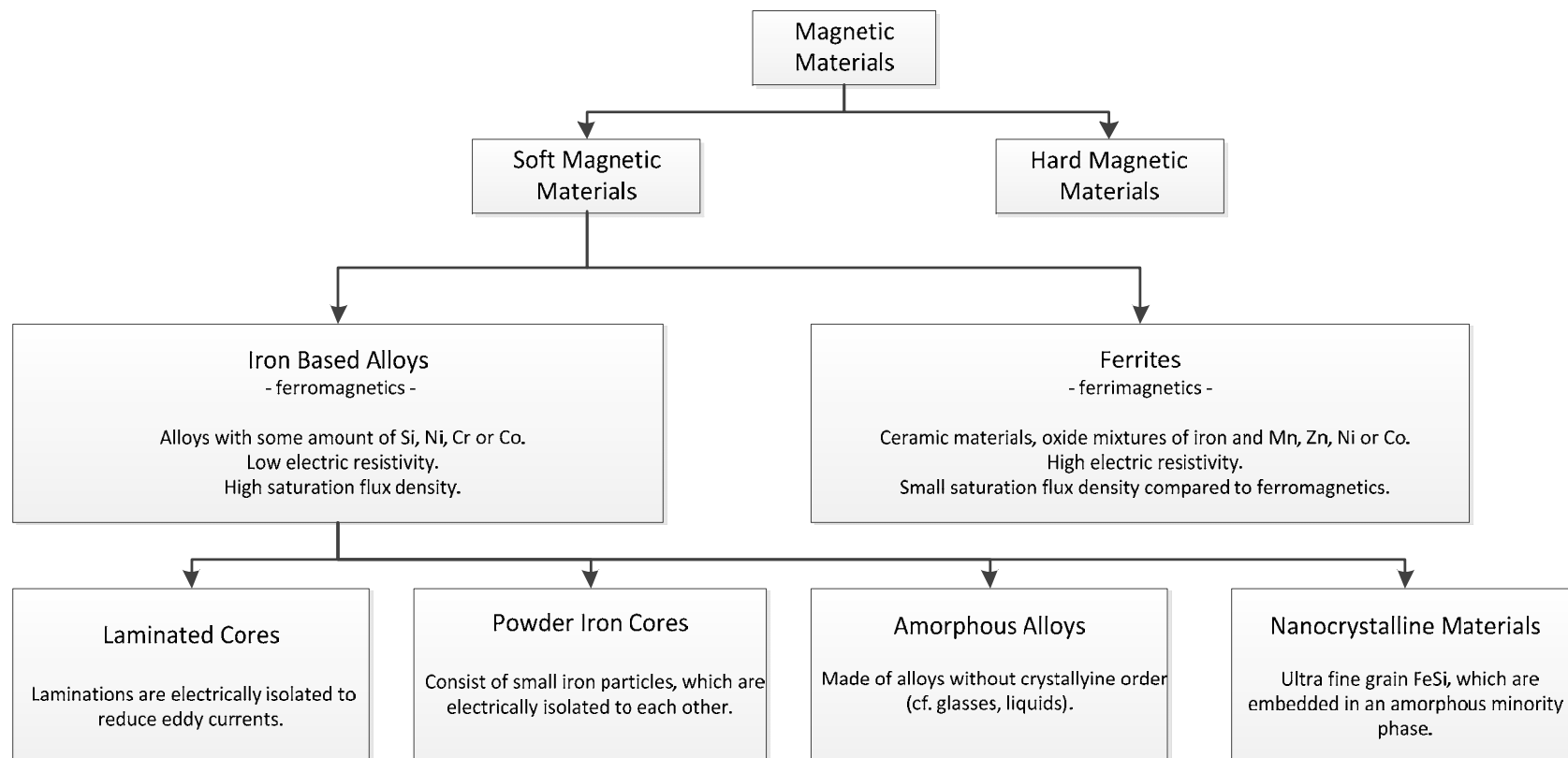
**meas.**  
2.69 mH

# Outline

- **Magnetic Circuit Modeling**
- **Core Loss Modeling**
- **Winding Loss Modeling**
- **Thermal Modeling**
- **Multi-Objective Optimization**
- **Summary & Conclusion**

# Core Loss Modeling

## Overview of Different Core Materials (1)



# Core Loss Modeling

## Overview of Different Core Materials (2)

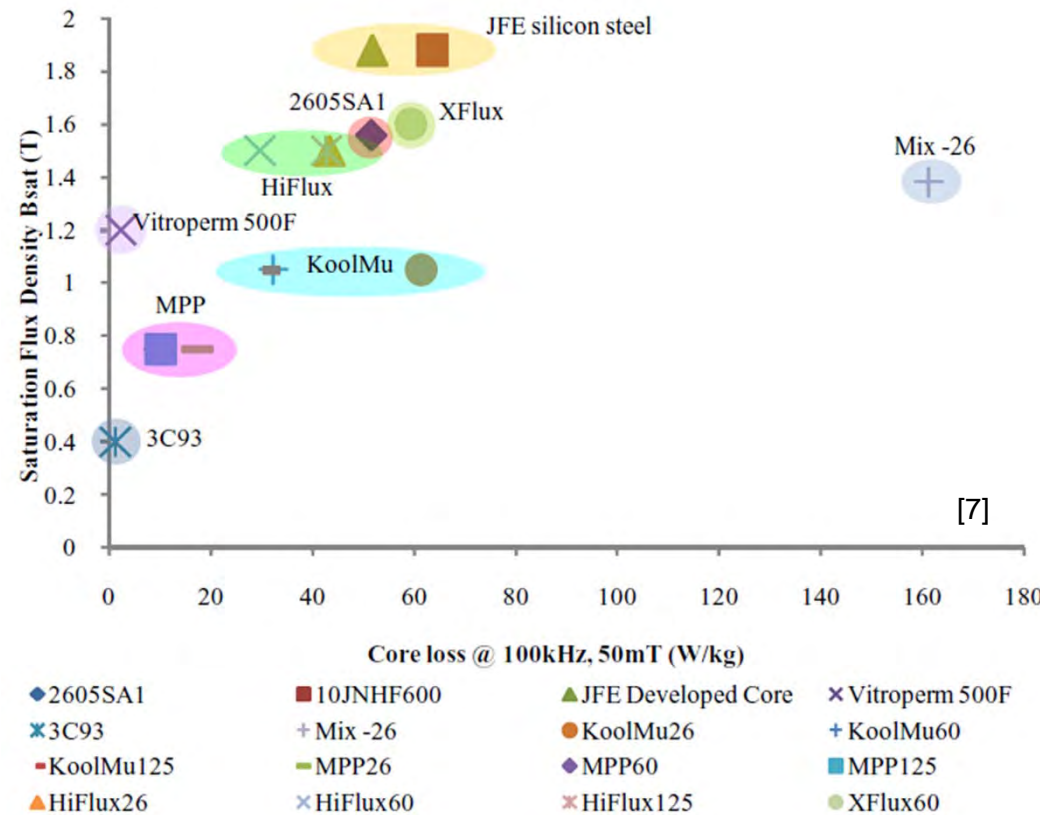
Selection Criteria	Ferrite	Powder Iron Core
Saturation Flux Density	Low Sat. Flux Density (0.45 T)	High Sat. Flux Density (1.5 T)
Power Loss Density (Frequency Range)	Low Losses	Moderate Losses
Price	Low Price	Low Price
etc.	Many Different Shapes	Many Different Shapes
	Very Brittle	Distributed Air Gap (low rel. permeability)
<b>Laminated Steel Cores</b>	<b>Amorphous Alloys</b> 	<b>Nanocrystalline Materials</b> 
Very High Sat. Flux Density (2.2T)	High Sat. Flux Density (1.5T)	High Sat. Flux Density (1.1T)
High Losses	Low Losses	Very Low Losses
Low Price	High Price	Very High Price
Many Different Shapes	Limited Available Shapes	Limited Available Shapes

**LF:**  $B_{SAT} = B_{max}$ .

**HF:**  $B_{max}$  is limited by core losses.

## Core Loss Modeling

### Overview of Different Core Materials (3)

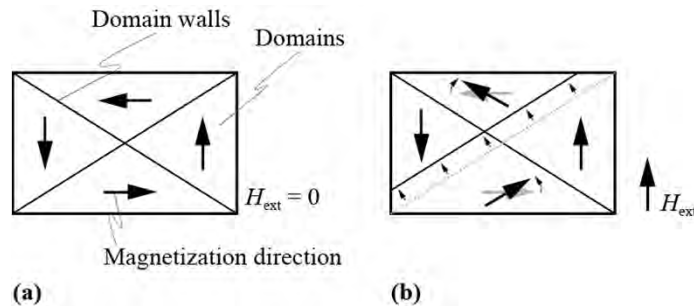


[7] M. S. Rylko, K. J. Hartnett, J. G. Hayes, M.G. Egan, "Magnetic Material Selection for High Power High Frequency Inductors in DC-DC Converters", in Proc. of the APEC 2009.

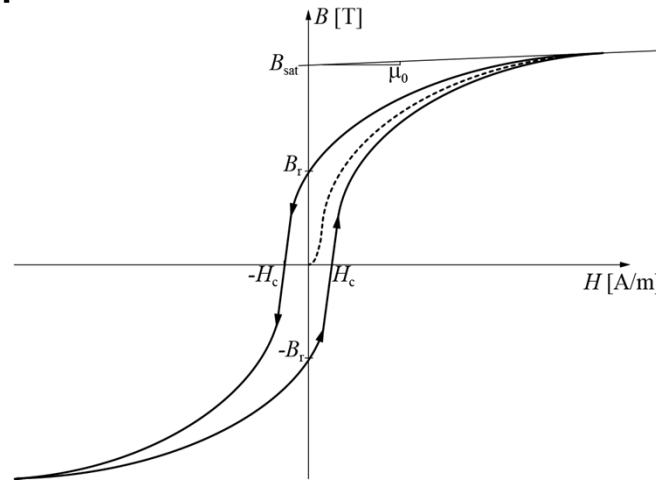
# Core Loss Modeling

## Physical Origin of Core Losses (1)

### Weiss Domains / Domain Walls



### B-H-Loop



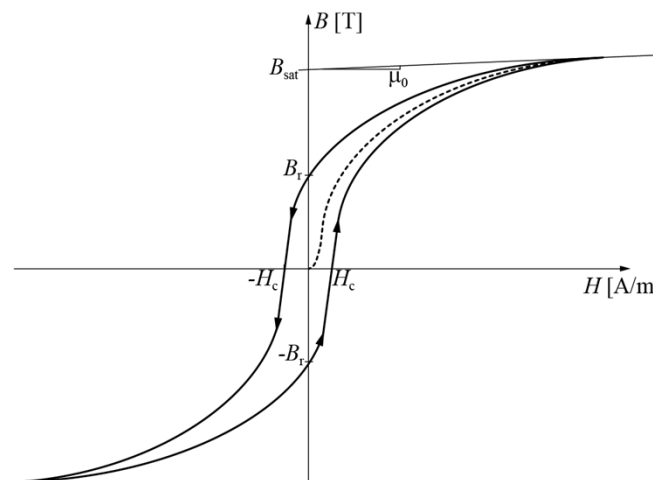
- Spontaneous magnetization.
- Material is divided to saturated domains (Weiss domains).
- In case an external field is applied, the domain walls are shifted or the magnetic moments within the domains change their direction. → The net magnetization becomes greater than zero.

- The flux change is partly irreversible, i.e. energy is dissipated as heat.
- The reason for this are the so called Barkhausen jumps, that lead to local eddy current losses.
- In case the loop is traversed very slowly, these Barkhausen jumps lead to the *static hysteresis losses*.

## Core Loss Modeling

### Physical Origin of Core Losses (2)

#### B-H-Loop



- If the process would be fully reversible, going from  $B_1$  to  $B_2$  would store potential energy in the magnetic material that is later released (i.e. the area of the closed loop would be zero).
- Since the process is partly irreversible, the area of the closed loop represents the energy loss per cycle

$$W = \oint H dB$$

# Core Loss Modeling

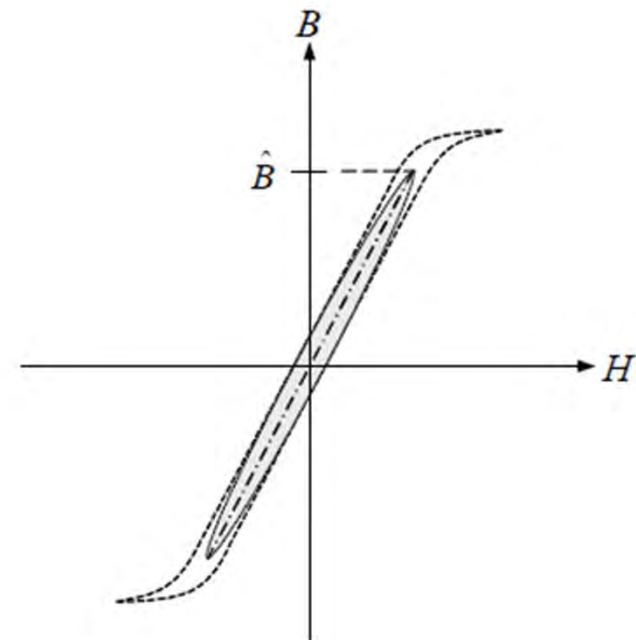
## Classification of Losses (1)

- **(Static) hysteresis loss**

- Rate-independent  $BH$  Loop.
- Loss energy per cycle is constant.
- Irreversible changes each within a small region of the lattice (Barkhausen jumps).
- These rapid, irreversible changes are produced by relatively strong local fields within the material.

- **Eddy current losses**

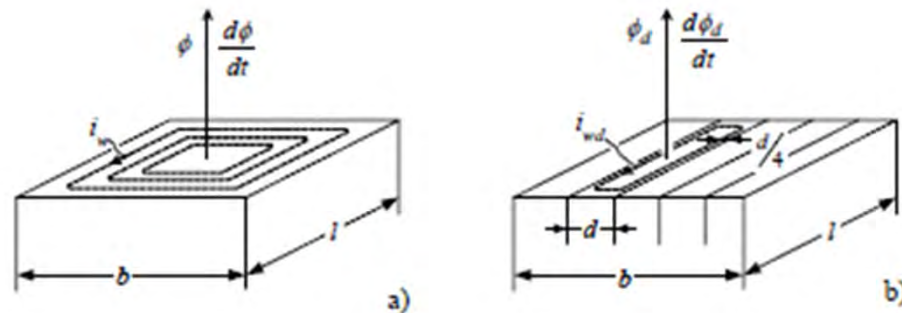
- **Residual Losses – Relaxation losses**



# Core Loss Modeling

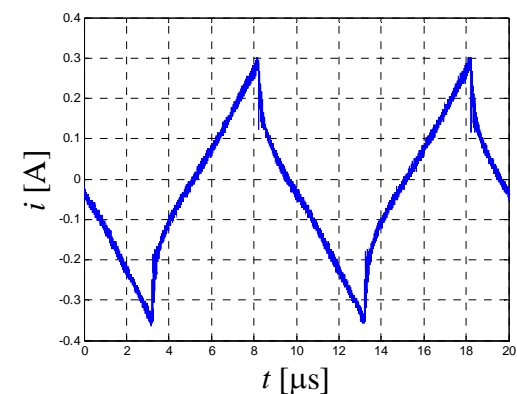
## Classification of Losses (2)

- (Static) hysteresis loss
- Eddy current losses
  - Depend on material conductivity and core shape.
  - Affect  $BH$  loop.
- Residual Losses – Relaxation losses



### Measurements

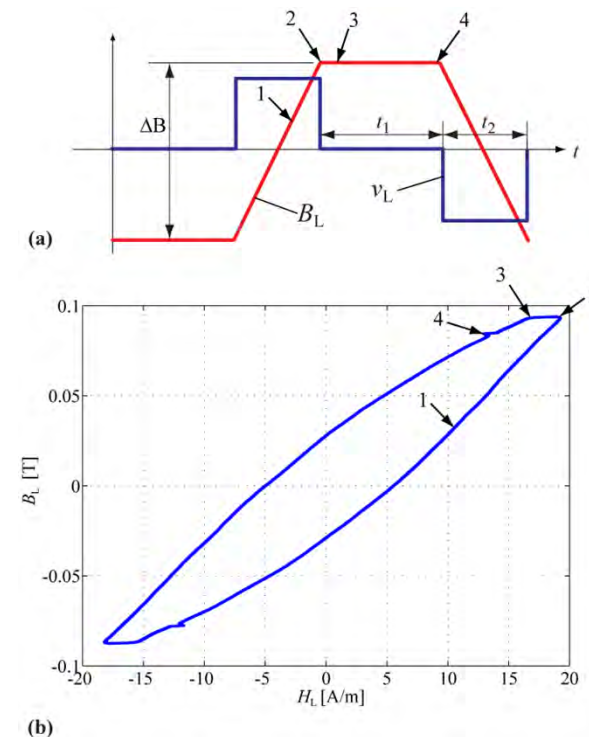
VITROPERM 500F



# Core Loss Modeling

## Classification of Losses (3)

- **(Static) hysteresis loss**
- **Eddy current losses**
- **Residual losses – Relaxation losses**
  - Rate-dependent  $BH$  Loop.
  - Reestablishment of a thermal equilibrium is governed by relaxation processes.
  - Restricted domain wall motion.



# Core Loss Modeling

## Typical Flux Waveforms

**Sinusoidal**



e.g. 50/60 Hz isolation transformer

**Triangular**



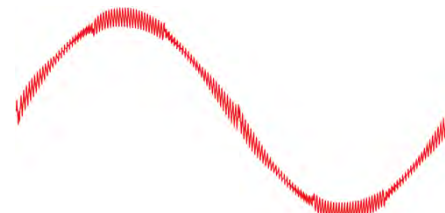
e.g. Buck / Boost converter

**Trapezoidal**



e.g. boost inductor of Dual Active Bridge

**Combination**



e.g. Boost inductor in PFC

# Core Loss Modeling

## Outline of Different Modeling Approaches

### Steinmetz Approach

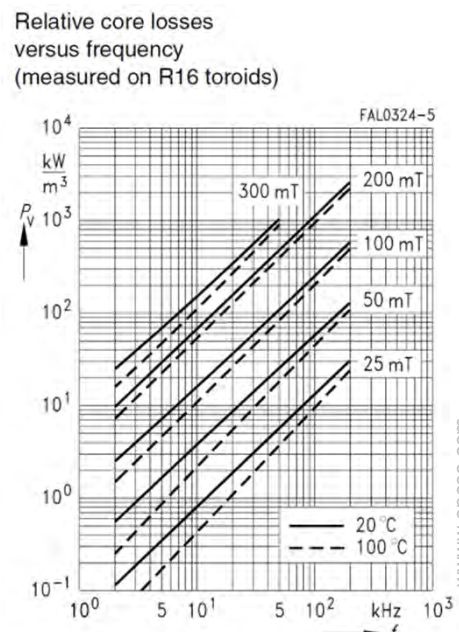
$$P = k f^\alpha B^\beta$$

- Simple
- Steinmetz parameter are valid only in a limited flux density and frequency range
- DC Bias not considered
- (Only for sinusoidal flux waveforms)

### Loss Separation

$$P = P_{\text{hyst}} + P_{\text{eddy}} + P_{\text{residual}}$$

- Needed parameters often unknown
- Model is widely applicable
- Increases physical understanding of loss mechanisms



### Loss Map Approach

#### (Loss Database)

- Measuring core losses is indispensable to overcome limits of Steinmetz approach

### Hysteresis Model

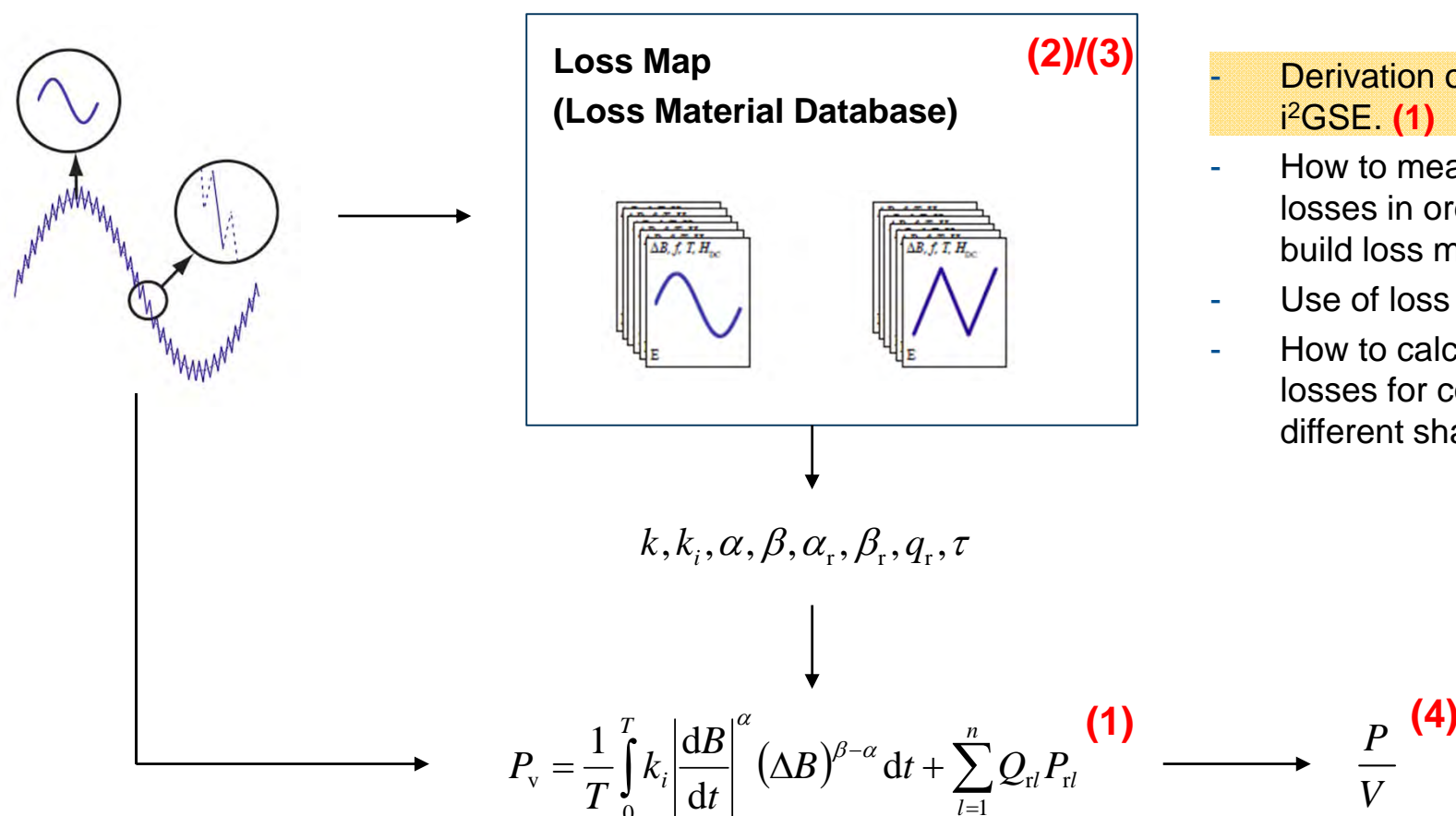
(e.g. Preisach Model, Jiles-Atherton Model)

- Difficult to parameterize
- Increases physical understanding of loss mechanisms

# Core Loss Modeling

## Overview of Hybrid Modeling Approach

“The best of both worlds” (Steinmetz & Loss Map approach)



### Outline of Discussion

- Derivation of the  $i^2GSE$ . (1)
- How to measure core losses in order to build loss map. (2)
- Use of loss map. (3)
- How to calculate core losses for cores of different shapes? (4)

# Core Loss Modeling

## Derivation of the i<sup>2</sup>GSE – Motivation (1)

### Steinmetz Equation SE

$$P_v = k f^\alpha \hat{B}^\beta$$

- Only sinusoidal waveforms ( $\rightarrow$  iGSE).

$P_v$  : time-average power loss per unit volume



### iGSE

$$P_v = \frac{1}{T} \int_0^T k_i \left| \frac{dB}{dt} \right|^\alpha (\Delta B)^{\beta-\alpha} dt$$

$$k_i = \frac{k}{(2\pi)^{\alpha-1} \int_0^{2\pi} |\cos \theta|^\alpha 2^{\beta-\alpha} d\theta}$$

- DC bias not considered
- Relaxation effect not considered ( $\rightarrow$  i<sup>2</sup>GSE)
- Steinmetz parameter are valid only for a limited flux density and frequency range

# Core Loss Modeling

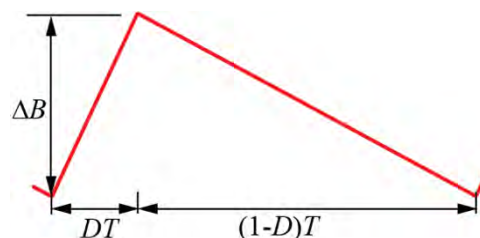
## Derivation of the $i^2GSE$ – Motivation (2)

iGSE [8]

$$P_v = \frac{1}{T} \int_0^T k_i \left| \frac{dB}{dt} \right|^\alpha (\Delta B)^{\beta-\alpha} dt$$

$$k_i = \frac{k}{(2\pi)^{\alpha-1} \int_0^{2\pi} |\cos \theta|^\alpha 2^{\beta-\alpha} d\theta}$$

How to apply the formula?



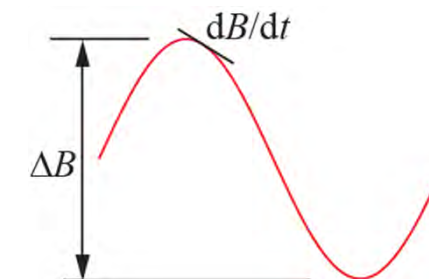
$$P_v = \frac{k_i}{T} \left[ DT \left( \frac{\Delta B}{DT} \right)^\alpha (\Delta B)^{\beta-\alpha} + (1-D)T \left( \frac{\Delta B}{(1-D)T} \right)^\alpha (\Delta B)^{\beta-\alpha} \right] = \dots$$

Idea

- Generalized formula that is applicable for different flux waveforms
- Losses depend on  $dB/dt$

For Sinusoidal Waveforms

$$P_v = \frac{1}{T} \int_0^T k_i \left| \frac{dB}{dt} \right|^\alpha (\Delta B)^{\beta-\alpha} dt = kf^\alpha \left( \frac{\Delta B}{2} \right)^\beta$$

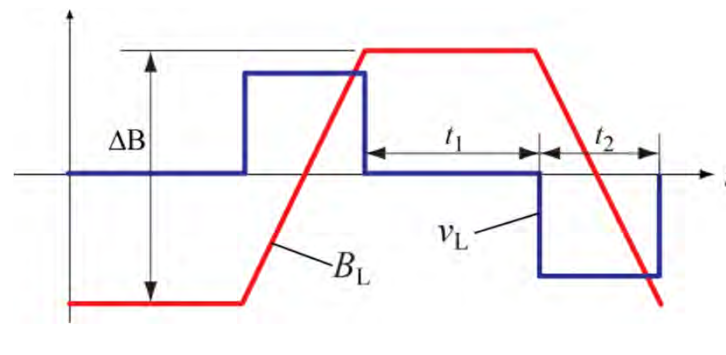


[8] K. Venkatachalam, C. R. Sullivan, T. Abdallah, and H. Tacca, "Accurate prediction of ferrite core loss with nonsinusoidal waveforms using only Steinmetz parameters", in Proc. of IEEE Workshop on Computers in Power Electronics, pp. 36-41, 2002.

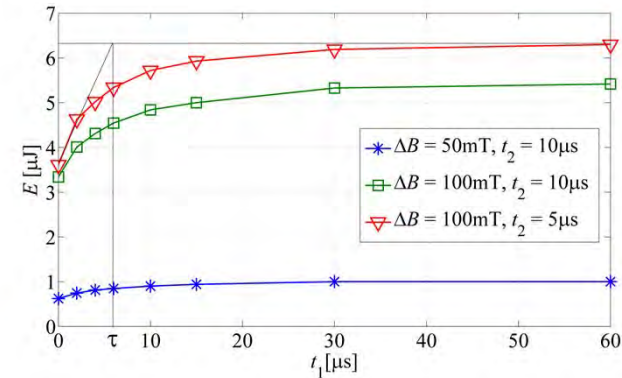
# Core Loss Modeling

## Derivation of the i<sup>2</sup>GSE – Motivation (3)

### Waveform



### Results



### iGSE

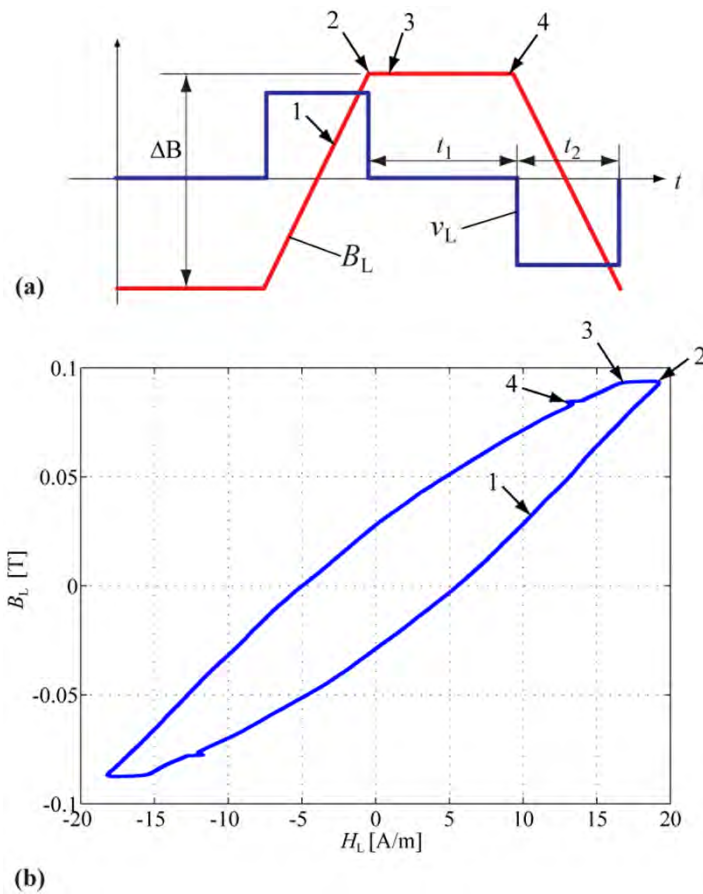
$$P_v = \frac{1}{T} \int_0^T k_i \left| \frac{dB}{dt} \right|^{\alpha} (\Delta B)^{\beta-\alpha} dt$$

### Conclusion

Losses in the phase of constant flux!

## Core Loss Modeling

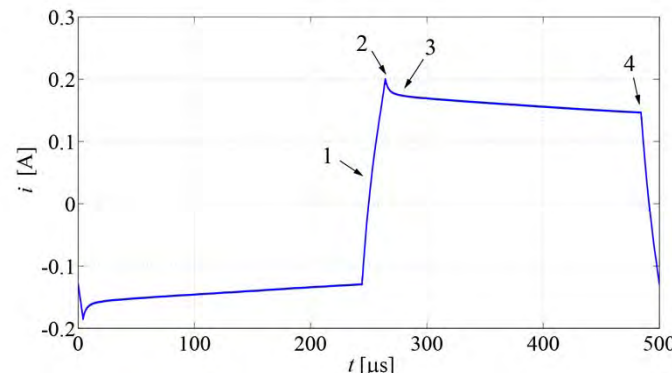
### Derivation of the $i^2GSE - B-H$ -Loop



### Relaxation Losses

- Rate-dependent  $BH$  Loop.
- Reestablishment of a thermal equilibrium is governed by relaxation processes.
- Restricted domain wall motion.

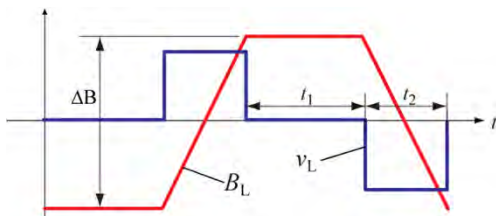
### Current Waveform



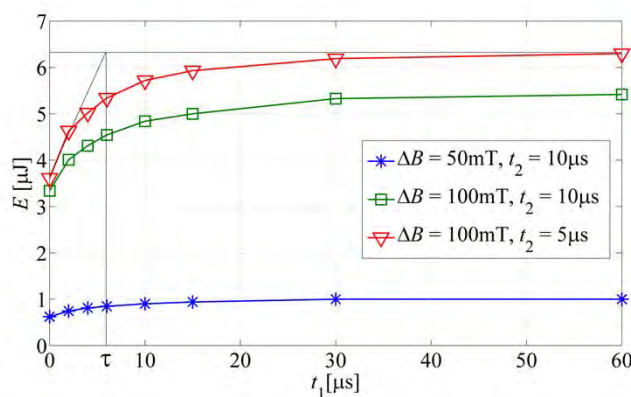
# Core Loss Modeling

## Derivation of the i<sup>2</sup>GSE – Model Derivation 1 (1)

### Waveform



### Loss Energy per Cycle



### Derivation (1)

Relaxation loss energy can be described with

$$E = \Delta E \left( 1 - e^{-\frac{t_1}{\tau}} \right)$$

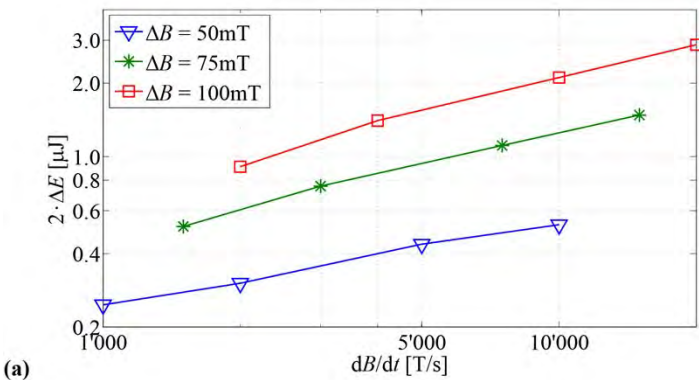
$\tau$  is independent of operating point.

How to determine  $\Delta E$ ?

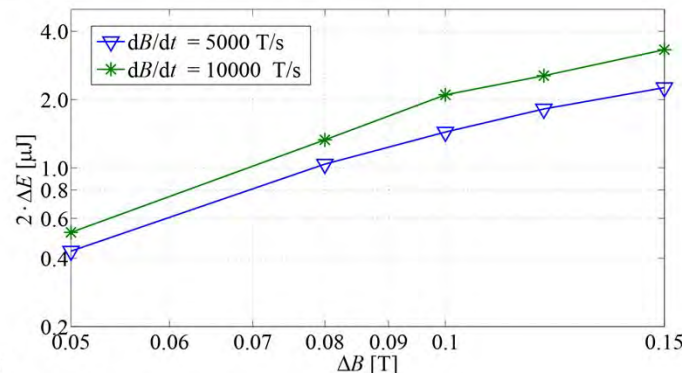
# Core Loss Modeling

## Derivation of the i<sup>2</sup>GSE – Model Derivation 1 (2)

$\Delta E$  – Measurements

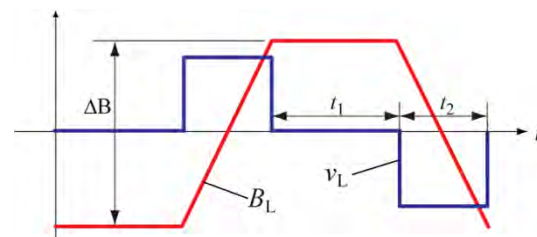


(a)



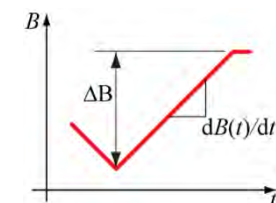
(b)

Waveform



## Conclusion

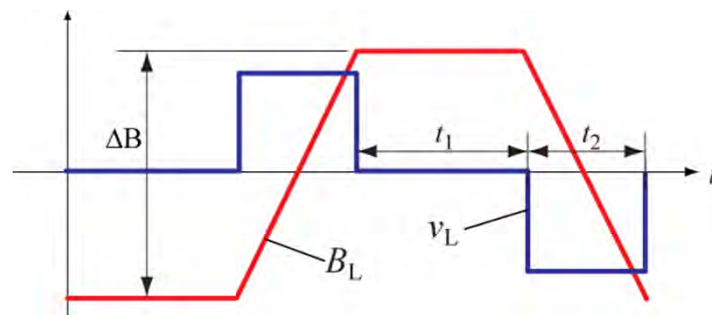
→  $\Delta E$  follows a power function!



$$\Delta E = k_r \left| \frac{d}{dt} B(t) \right|^{\alpha_r} (\Delta B)^{\beta_r}$$

# Core Loss Modeling

## Derivation of the i<sup>2</sup>GSE – Model Derivation 1 (3)



### Model Part 1

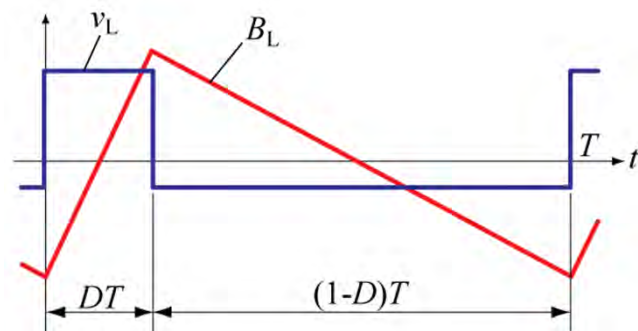
$$P_v = \frac{1}{T} \int_0^T k_i \left| \frac{dB}{dt} \right|^\alpha (\Delta B)^{\beta-\alpha} dt + \sum_{l=1}^n P_{rl}$$

$$P_{rl} = \frac{1}{T} k_r \left| \frac{d}{dt} B(t) \right|^{\alpha_r} (\Delta B)^{\beta_r} \left( 1 - e^{-\frac{t_1}{\tau}} \right)$$

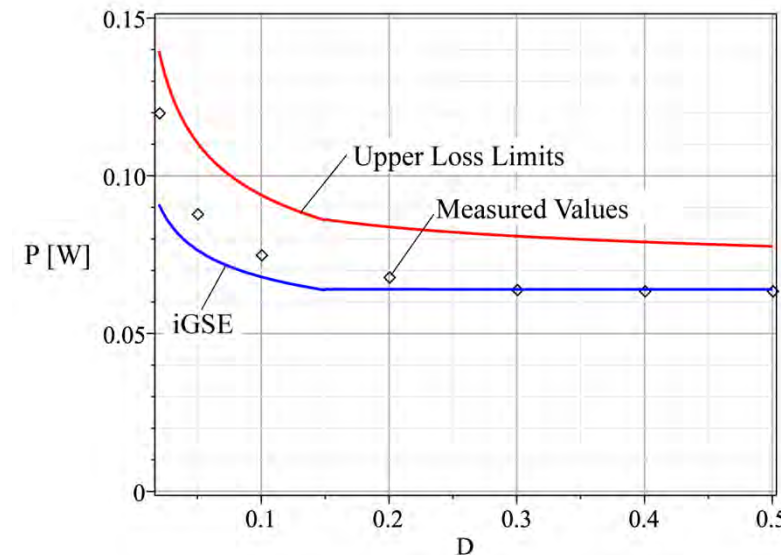
# Core Loss Modeling

## Derivation of the i<sup>2</sup>GSE – Model Derivation 2 (1)

Waveform



Power Loss



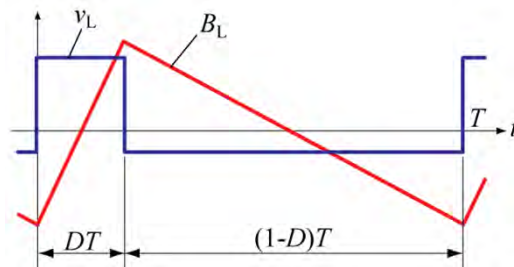
### Explanation

- 1) For values of  $D$  close to 0 or close to 1 a loss underestimation is expected when calculating losses with iGSE (no relaxation losses included).
- 2) For values of  $D$  close to 0.5 the iGSE is expected to be accurate.
- 3) Adding the relaxation term leads to the upper loss limit, while the iGSE represents the lower loss limit.
- 4) Losses are expected to be in between the two limits, as has been confirmed with measurements.

# Core Loss Modeling

## Derivation of the i<sup>2</sup>GSE – Model Derivation 2 (2)

### Waveform



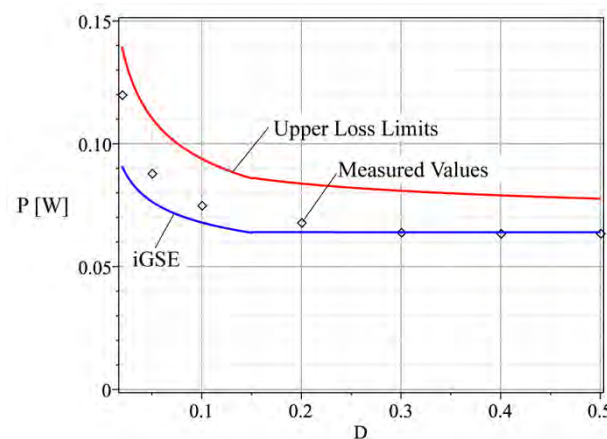
### Model Adaption

$$P_v = \frac{1}{T} \int_0^T k_i \left| \frac{dB}{dt} \right|^{\alpha} (\Delta B)^{\beta-\alpha} dt + \sum_{l=1}^n Q_{rl} P_{rl}$$

$Q_{rl}$  should be 1 for  $D = 0$

$Q_{rl}$  should be 0 for  $D = 0.5$

### Power Loss



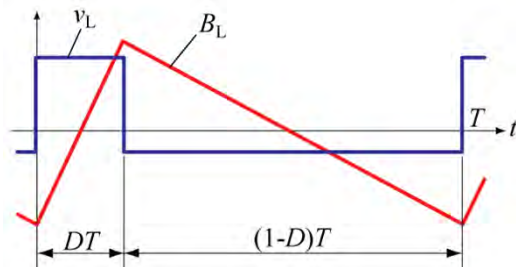
$Q_{rl}$  should be such that calculation fits a triangular waveform measurement.

$$Q_{rl} = e^{-q_r \left| \frac{dB(t+)}{dB(t-)} \right|} \left( = e^{-q_r \frac{D}{1-D}} \right)$$

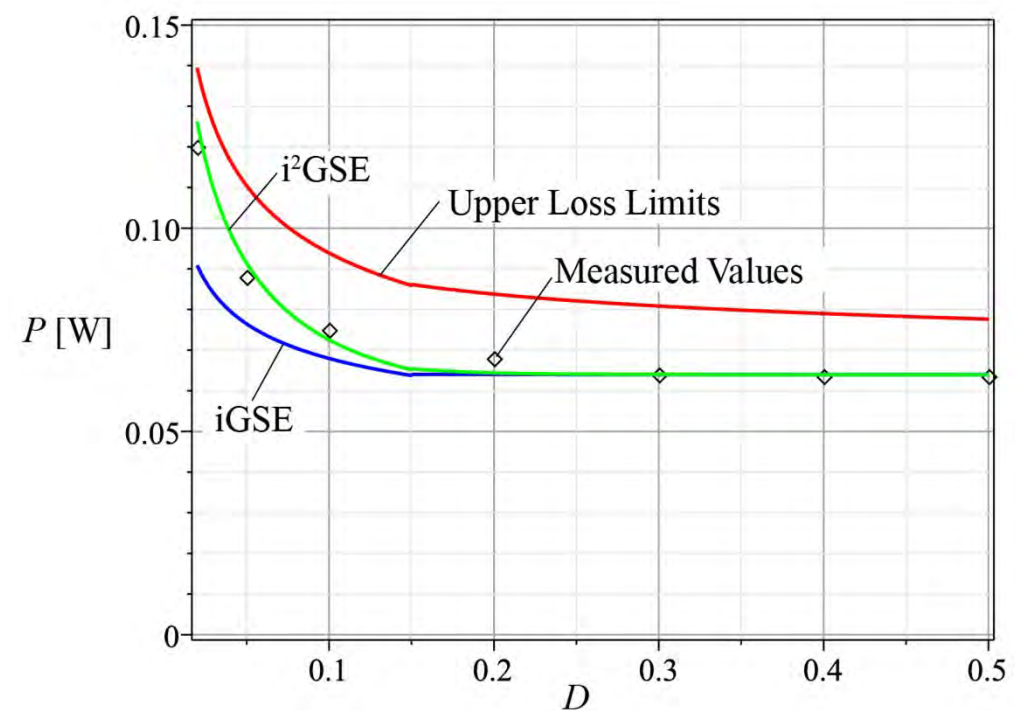
## Core Loss Modeling

### Derivation of the $i^2GSE$ – Model Derivation 2 (3)

Waveform



Power Loss



# Core Loss Modeling

## Derivation of the i<sup>2</sup>GSE – Summary

The **improved-improved Generalized Steinmetz Equation (i<sup>2</sup>GSE)** [9]

$$P_v = \frac{1}{T} \int_0^T k_i \left| \frac{dB}{dt} \right|^\alpha (\Delta B)^{\beta-\alpha} dt + \sum_{l=1}^n Q_{rl} P_{rl}$$

with

$$P_{rl} = \frac{1}{T} k_r \left| \frac{d}{dt} B(t) \right|^{\alpha_r} (\Delta B)^{\beta_r} \left( 1 - e^{-\frac{t_1}{\tau}} \right)$$

and

$$Q_{rl} = e^{-q_r \left| \frac{dB(t+)/dt}{dB(t-)/dt} \right|}$$



- [9] J. Mühlethaler, J. Biela, J.W. Kolar, and A. Ecklebe, "Improved Core Loss Calculation for Magnetic Components Employed in Power Electronic Systems", in Proc. of the APEC, Ft. Worth, TX, USA, 2011.

# Core Loss Modeling

## Derivation of the $i^2GSE$ – Example

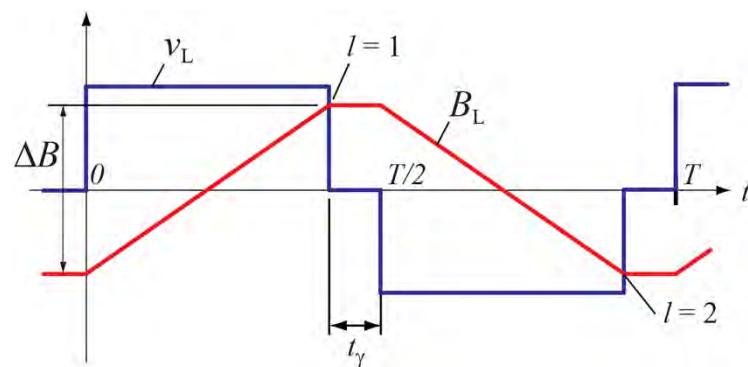
$i^2GSE$

Evaluated for each piecewise-linear flux segment

$$P_v = \frac{1}{T} \int_0^T k_i \left| \frac{dB}{dt} \right|^\alpha (\Delta B)^{\beta-\alpha} dt + \sum_{l=1}^n Q_{rl} P_{rl}$$

Evaluated for each voltage step, i.e. for each corner point in a piecewise-linear flux waveform.

Example



$$\frac{dB}{dt} = \begin{cases} \frac{\Delta B}{T/2 - t_\gamma} & \text{for } t \geq 0 \text{ and } t < T/2 - t_\gamma \\ 0 & \text{for } t \geq T/2 - t_\gamma \text{ and } t < T/2 \\ -\frac{\Delta B}{T/2 - t_\gamma} & \text{for } t \geq T/2 \text{ and } t < T - t_\gamma \\ 0 & \text{for } t \geq T - t_\gamma \text{ and } t < T \end{cases}$$

$$P_v = \frac{T - 2t_\gamma}{T} k_i \left| \frac{\Delta B}{T/2 - t_\gamma} \right|^\alpha (\Delta B)^{\beta-\alpha} + \sum_{l=1}^2 Q_{rl} P_{rl} \quad \text{with} \quad Q_{r1} = Q_{r2} = 0$$

$$P_{r1} = P_{r2} = \frac{1}{T} k_r \left| \frac{\Delta B}{T/2 - t_\gamma} \right|^{\alpha_r} (\Delta B)^{\beta_r} \left( 1 - e^{-\frac{t_\gamma}{\tau}} \right)$$

# Core Loss Modeling

## Derivation of the $i^2GSE$ – Conclusion

$i^2GSE$

$$P_v = \frac{1}{T} \int_0^T k_i \left| \frac{dB}{dt} \right|^\alpha (\Delta B)^{\beta-\alpha} dt + \sum_{l=1}^n Q_{rl} P_{rl}$$

Evaluated for each piecewise-linear flux segment

Evaluated for each voltage step, i.e. for each corner point in a piecewise-linear flux waveform.

### Remaining Problems

Steinmetz parameter are valid only in a limited flux density and frequency range.

Core Losses vary under DC bias condition.

Modeling relaxation and DC bias effects need parameters that are not given by core material manufacturers.

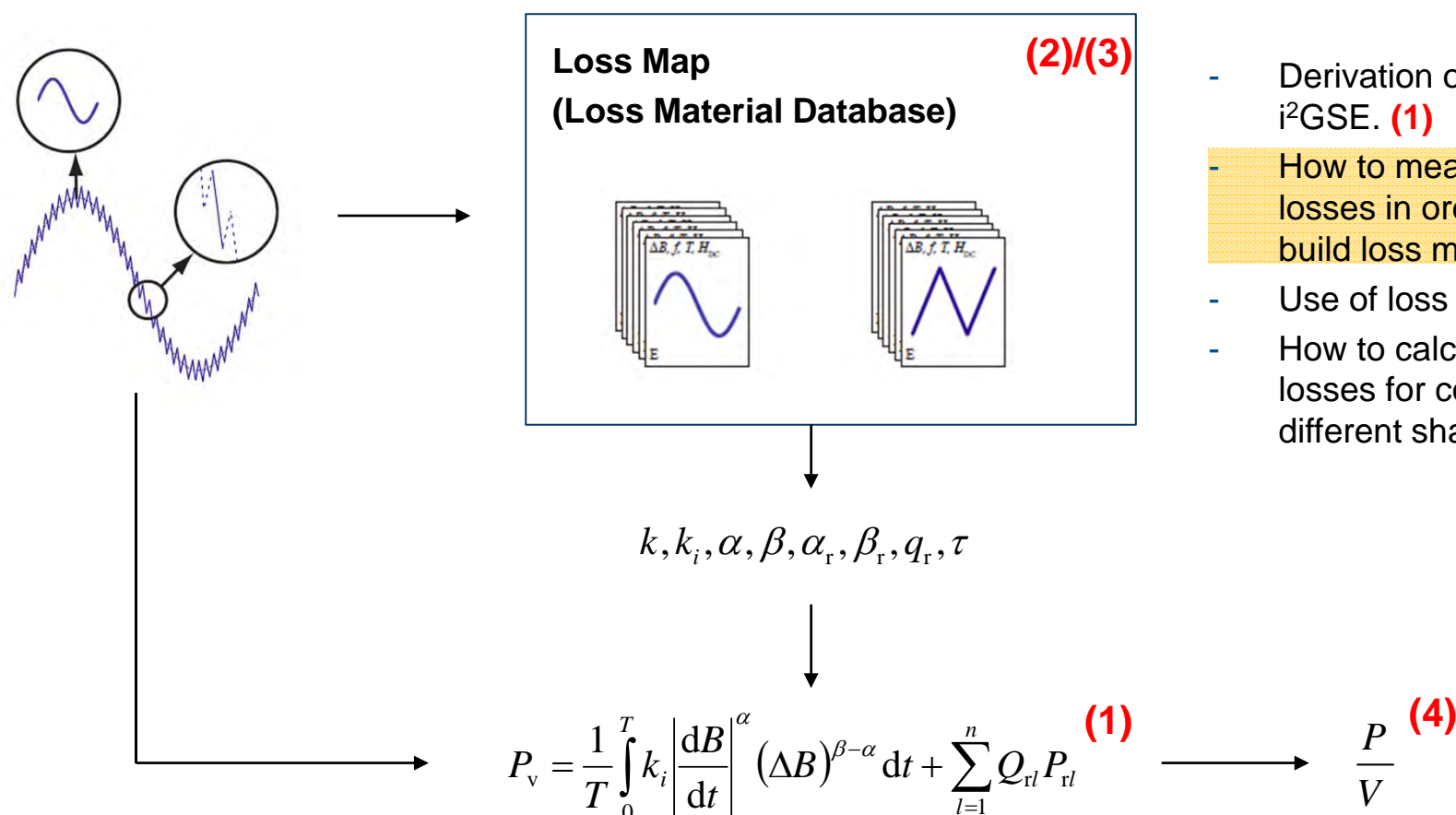


**Measuring core losses is indispensable!**

# Core Loss Modeling

## Overview of Hybrid Modeling Approach

“The best of both worlds” (Steinmetz & Loss Map approach)



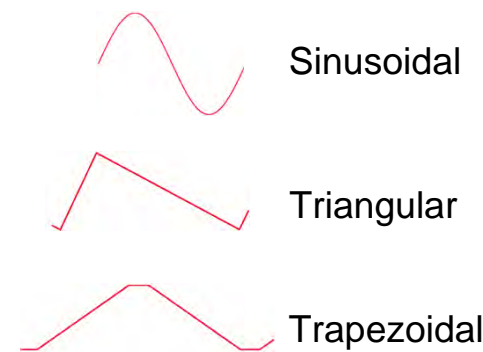
### Outline of Discussion

- Derivation of the  $i^2GSE$ . (1)
- How to measure core losses in order to build loss map. (2)
- Use of loss map. (3)
- How to calculate core losses for cores of different shapes? (4)

# Core Loss Modeling

## Core Loss Measurement – Measurement Principle

### Waveforms

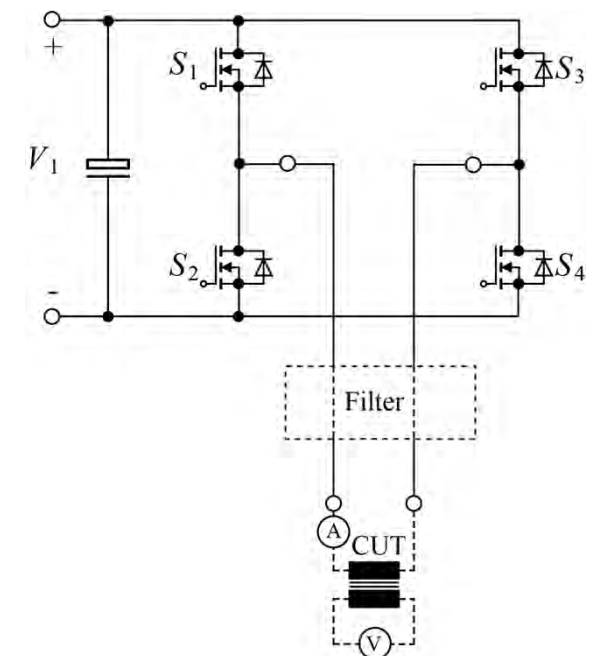


### Excitation System



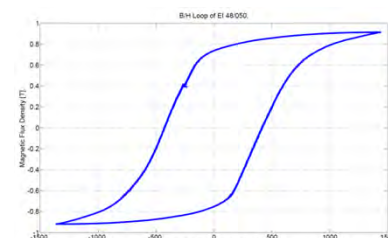
*Voltage* 0 ... 450 V  
*Current* 0 ... 25 A  
*Frequency* 0 ... 200 kHz

### Schematic



### Loss Extraction

$$\left. \begin{aligned} B(t) &= \frac{1}{N_2 \cdot A_e} \int_0^t u(\tau) d\tau \\ H(t) &= \frac{N_1 \cdot i(t)}{l_e} \end{aligned} \right\}$$

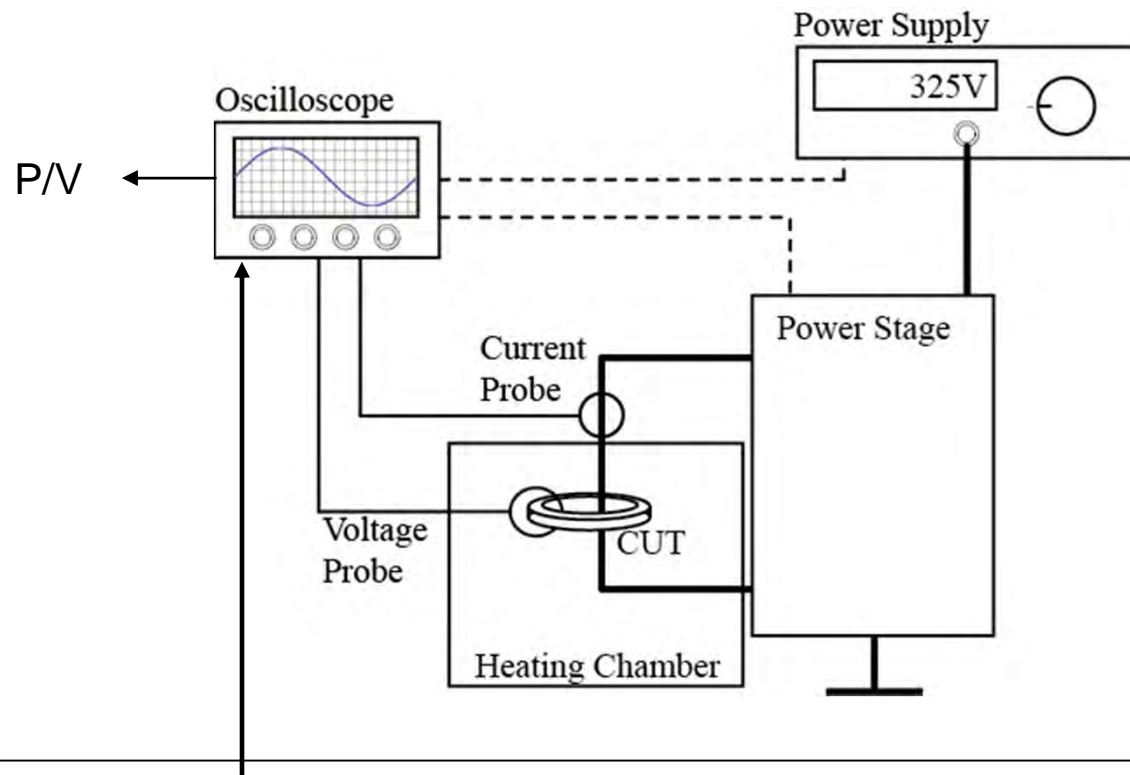


$$\frac{P[W]}{V[m^3]} = f \oint H dB$$

# Core Loss Modeling

## Core Loss Measurement - Overview

### System Overview

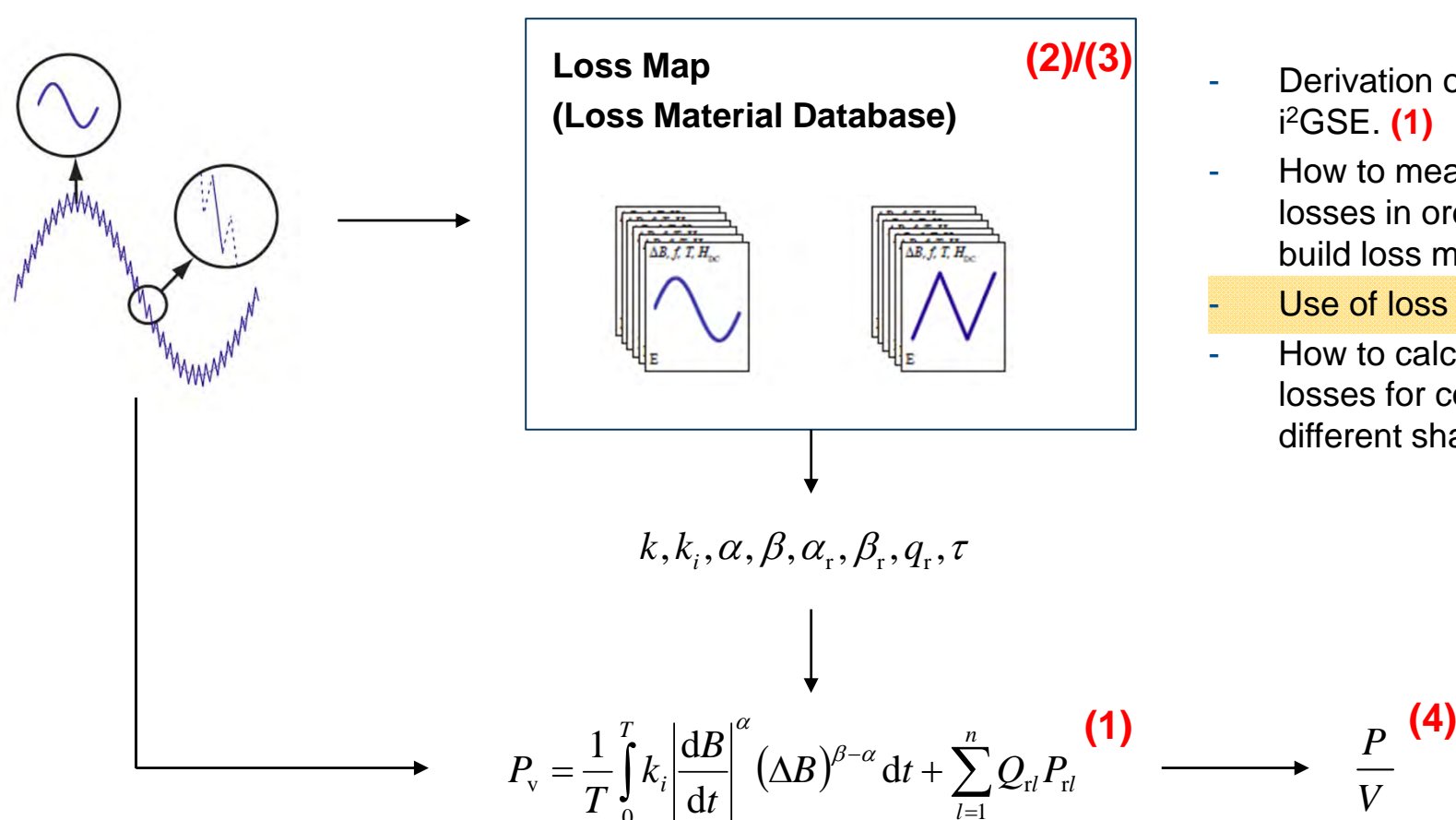


$$\frac{P}{V} = \frac{\int_0^T i_1(t) \frac{N_1}{N_2} v_2(t) dt}{A_e l_e} = \frac{\int_0^T \frac{H(t)l_e}{N_1} \frac{N_1}{N_2} N_2 A_e \frac{dB(t)}{dt} dt}{A_e l_e} = \int_{B(0)}^{B(T)} H(B) dB = f \oint H dB$$

# Core Loss Modeling

## Overview of Hybrid Modeling Approach

“The best of both worlds” (Steinmetz & Loss Map approach)

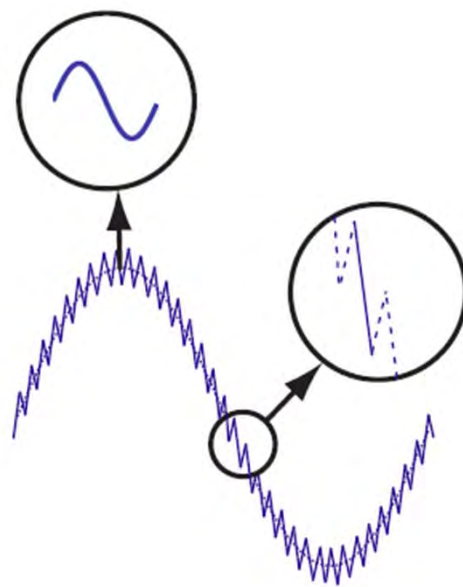


### Outline of Discussion

- Derivation of the  $i^2GSE$ . **(1)**
- How to measure core losses in order to build loss map. **(2)**
- Use of loss map. **(3)**
- How to calculate core losses for cores of different shapes? **(4)**

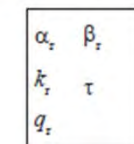
## Core Loss Modeling Needed Loss Map Structure

Typical flux waveform



Content of Loss Map

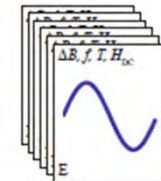
Relaxation



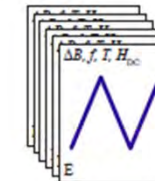
B-H-Relation



LF



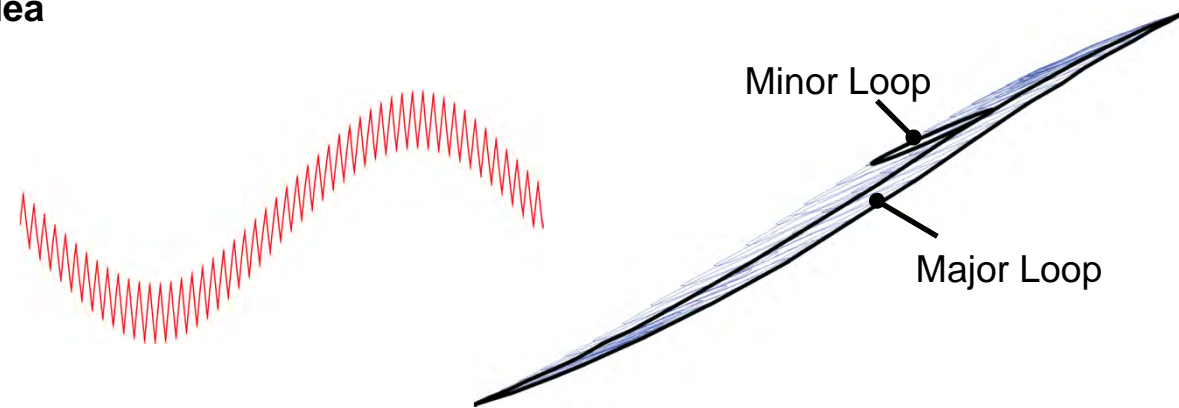
HF



# Core Loss Modeling

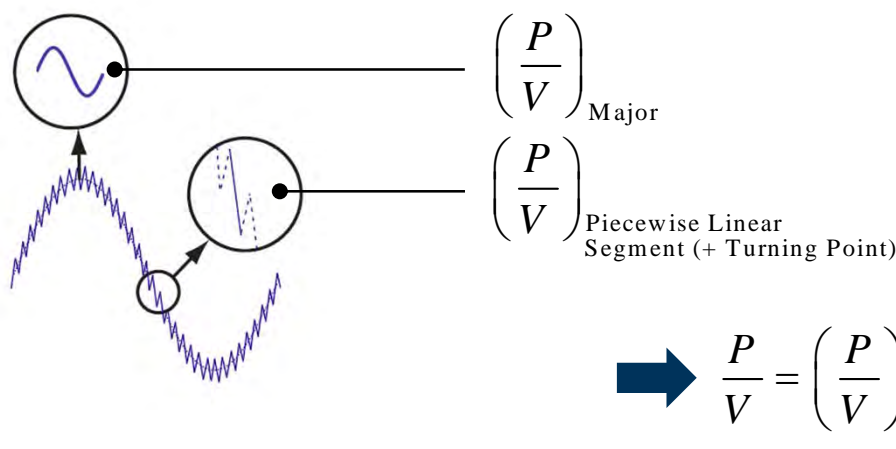
## Minor and Major Loops

### Idea



Losses due to Minor and Major Loops are calculated independent of each other and summed up.

### Implementation

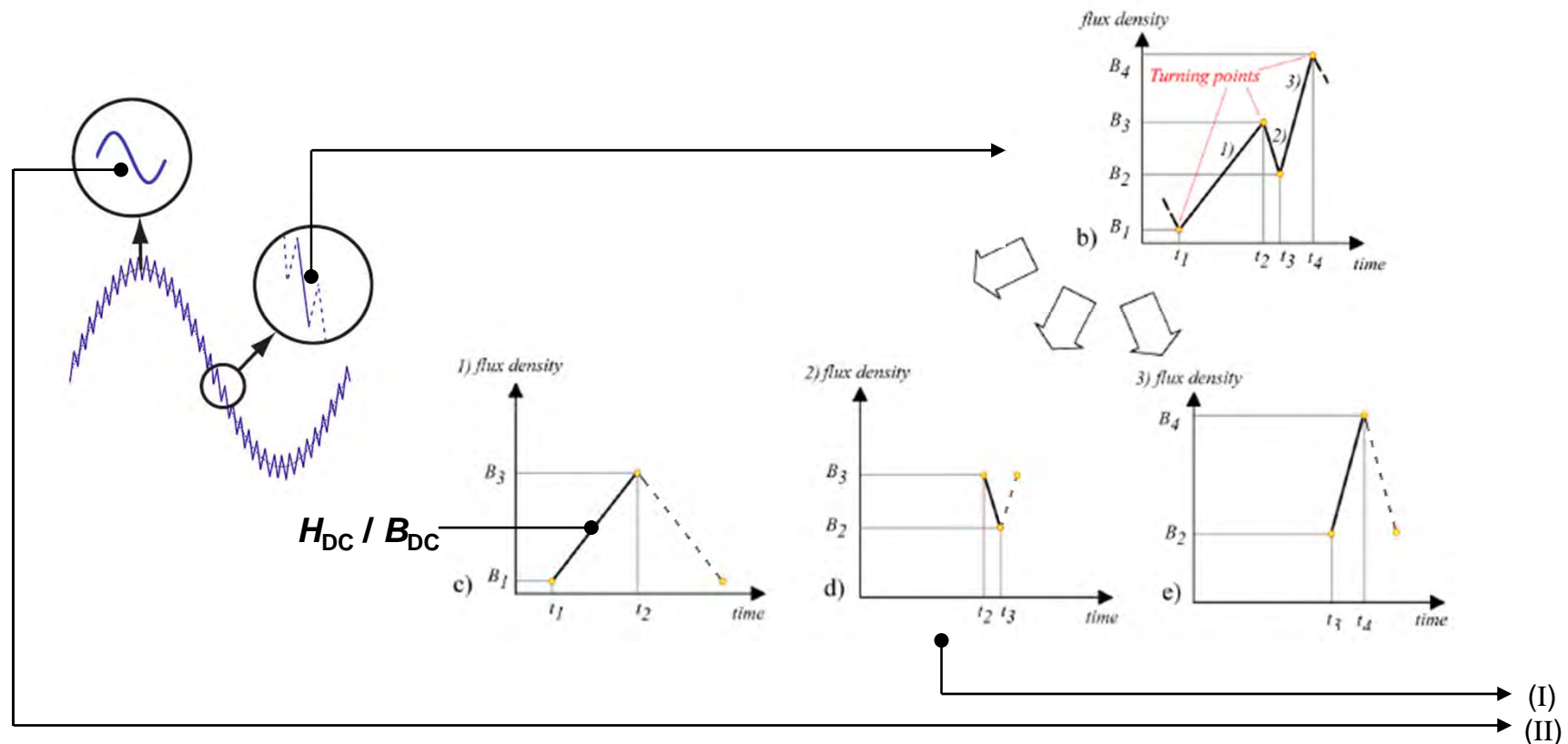


Actually, it is not considered how the minor loop closes: each piecewise linear segment is modeled as having half the losses of its corresponding closed loop (cf. next slides).

$$\rightarrow \frac{P}{V} = \left( \frac{P}{V} \right)_{\text{Major}} + \sum \left( \frac{P}{V} \right)_{\text{Piecewise Linear Segment (+ Turning Point)}}$$

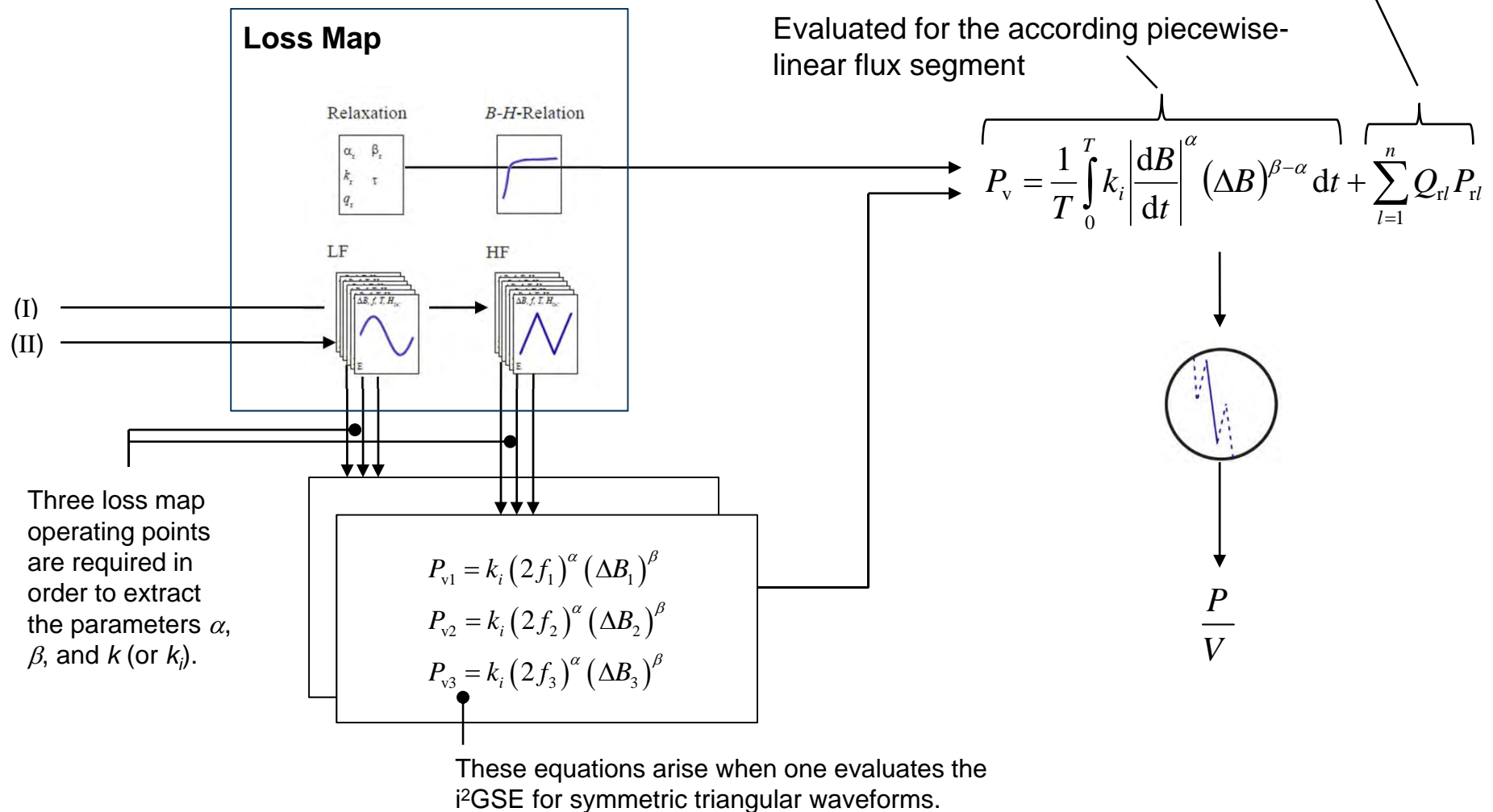
# Core Loss Modeling

## Hybrid Loss Modeling Approach (1)



## Core Loss Modeling

### Hybrid Loss Modeling Approach (2)



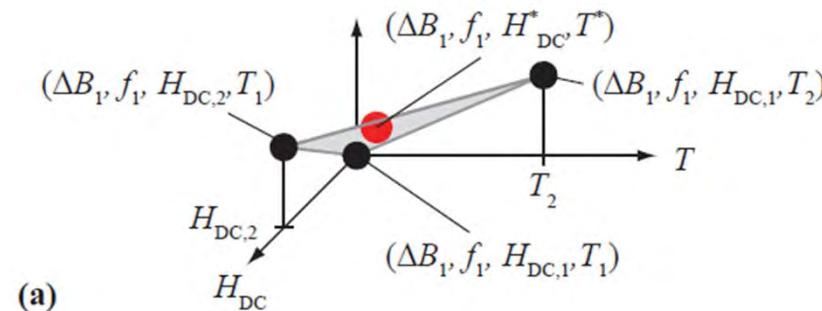
# Core Loss Modeling

## Hybrid Loss Modeling Approach (3)

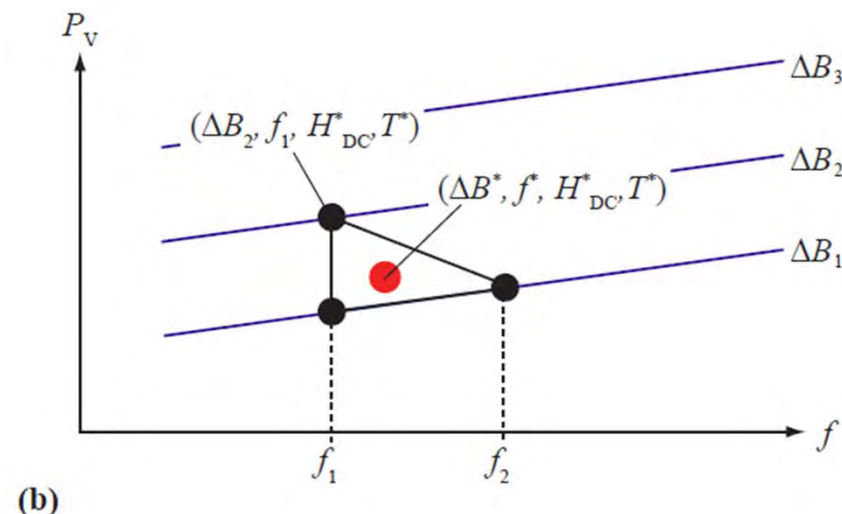
### Interpolation and Extrapolation

$(H_{DC}^*, T^*, \Delta B^*, f^*)$

#### $H_{DC}$ and $T$



#### $\Delta B$ and $f$



## Core Loss Modeling

### Hybrid Loss Modeling Approach (4)

**Advantages of Hybrid Approach (Loss Map and i<sup>2</sup>GSE):**

Relaxation effects are considered (i<sup>2</sup>GSE).

A good interpolation and extrapolation between premeasured operating points is achieved.

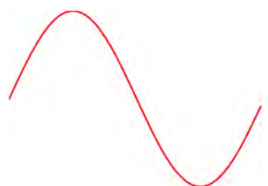
Loss map provides accurate i<sup>2</sup>GSE parameters for a wide frequency and flux density range.

A DC bias is considered as the loss map stores premeasured operating points at different DC bias levels.

# Core Losses

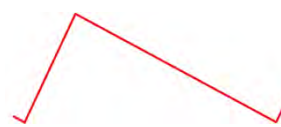
## Summary of Loss Density Calculation

**Sinusoidal**



$$P = k f^\alpha B^\beta$$

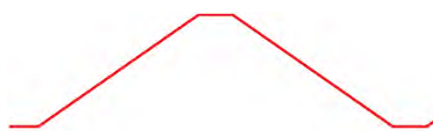
**Triangular**



$$P_v = \frac{1}{T} \int_0^T k_i \left| \frac{dB}{dt} \right|^\alpha (\Delta B)^{\beta-\alpha} dt + \sum_{l=1}^n Q_{rl} P_{rl}$$

with  $Q \geq 0, n = 1$

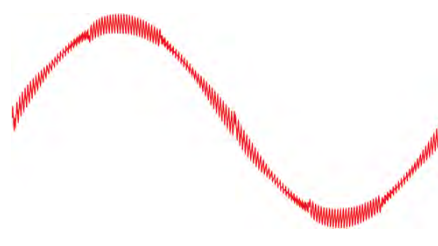
**Trapezoidal**



$$P_v = \frac{1}{T} \int_0^T k_i \left| \frac{dB}{dt} \right|^\alpha (\Delta B)^{\beta-\alpha} dt + \sum_{l=1}^n Q_{rl} P_{rl}$$

with  $Q = 1, n = 2$

**Combination**



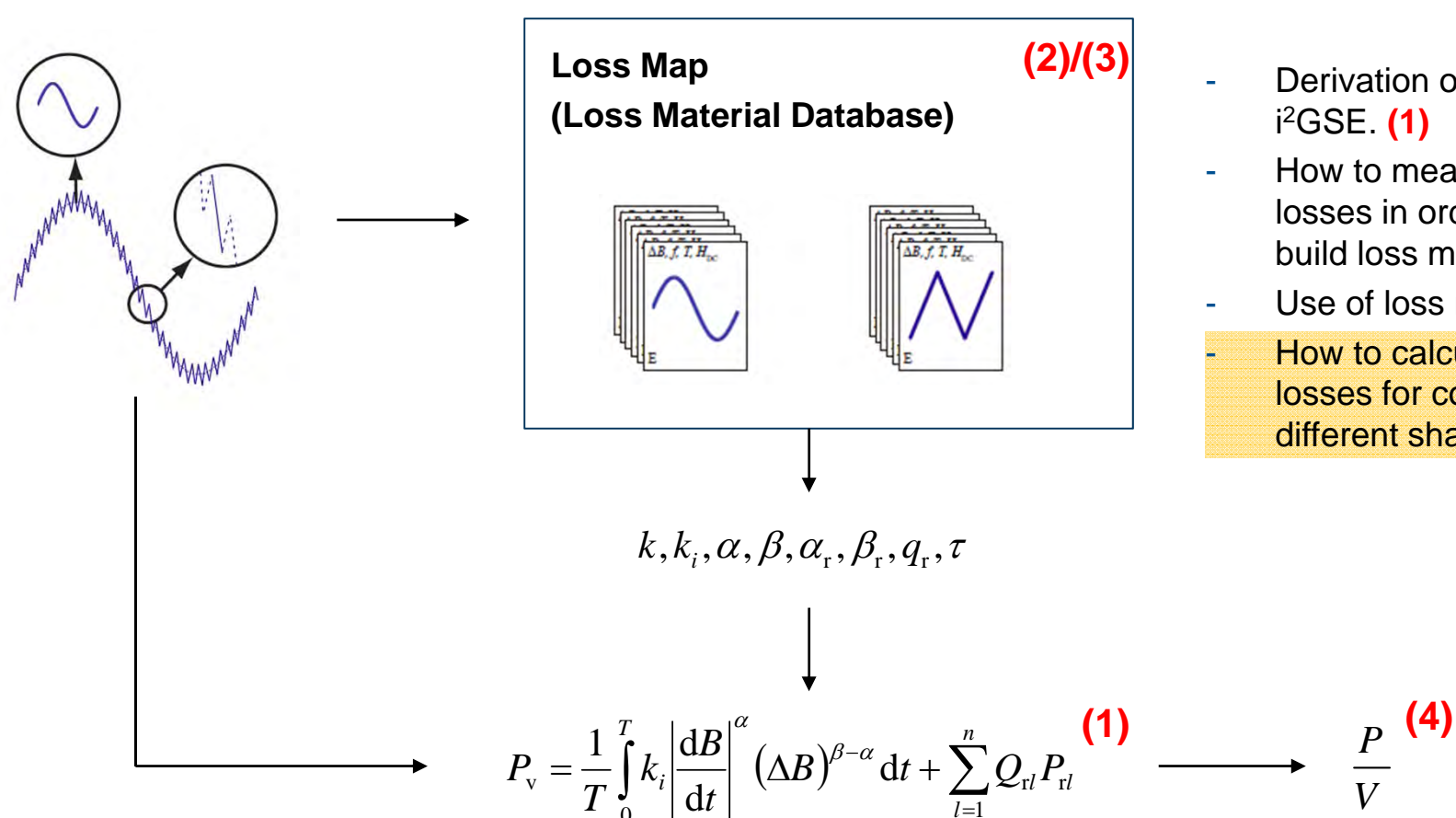
$$P_v = \frac{1}{T} \int_0^T k_i \left| \frac{dB}{dt} \right|^\alpha (\Delta B)^{\beta-\alpha} dt + \sum_{l=1}^n Q_{rl} P_{rl}$$

with different  $Q$ 's and  $n \gg 0$ .

# Core Loss Modeling

## Overview of Hybrid Modeling Approach

“The best of both worlds” (Steinmetz & Loss Map approach)



### Outline of Discussion

- Derivation of the  $i^2GSE$ . **(1)**
- How to measure core losses in order to build loss map. **(2)**
- Use of loss map. **(3)**
- How to calculate core losses for cores of different shapes? **(4)**

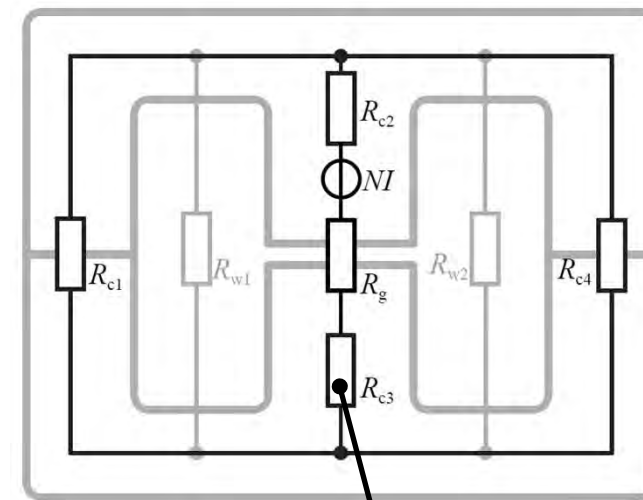
# Core Loss Modeling

## Effect of Core Shape

### Procedure

- 1) The **flux density in every core section** of (approximately) homogenous flux density is calculated.
- 2) The **losses of each section** are calculated.
- 3) The **core losses** of each section are then **summed-up** to obtain the total core losses.

### Reluctance Model



$$\phi = f(R_m(\phi), I) = f(\phi, I)$$

# Core Loss Modeling

## Effective Core Dimensions of Toroid

### Motivation for Effective Core Dimensions

Core loss *densities* are needed to model core losses. It is difficult to determine these loss densities from a toroid, since the flux density is not distributed homogeneously in a toroid.

### Definition: Ideal Toroid

A toroid is ideal when it has a homogenous flux density distribution over the radius ( $r_1 \approx r_2$ ).

### Idea for Real Toroid

Find effective core magnetic length and cross section, so one can calculate as if it were an ideal toroid, i.e. as if the flux density distribution were homogenous.

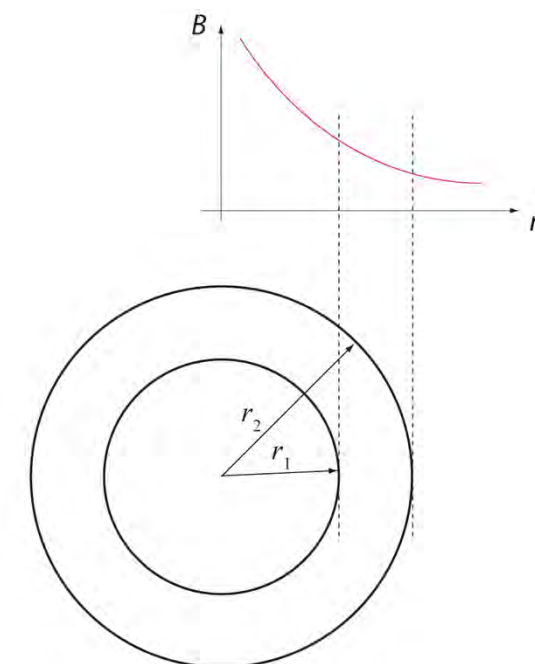
**Effective magnetic length**

$$l_e = \frac{2\pi \ln r_2 / r_1}{1 / r_1 - 1 / r_2}$$

**Effective magnetic cross-section**

$$A_e = \frac{h \ln^2 r_2 / r_1}{1 / r_1 - 1 / r_2}$$

### Illustration



# Core Loss Modeling

## Impact of Core Shape on Eddy Current Losses

Eddy current loss density can be determined as [5]

$$P_{\text{eddy}} = \frac{(\pi \hat{B} f d)^2}{k_{\text{ec}} \rho}$$

Geometry	$k_{\text{ec}}$
laminations of thickness $d$	6
cylinder of diameter $d$	16
sphere of diameter $d$	20

For a laminated core it is

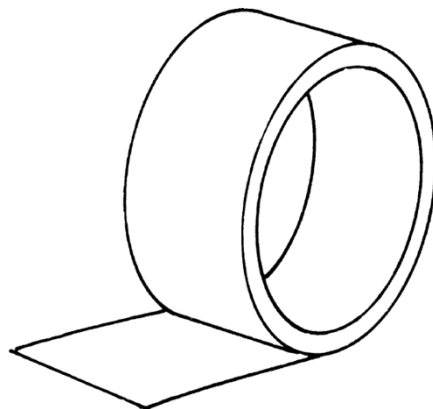
$$P_{\text{eddy}} = \frac{(\pi \hat{B} f d)^2}{6 \rho}$$



- The eddy current losses per unit volume depend not on the shape of the bulk material, but on the size and geometry of the insulated regions.
- In case of laminated iron cores, it is still appropriate to calculate with core loss densities that have been measured on a sample core with a geometrically different bulk material, but with the same lamination or tape thickness.

[5] E. C. Snelling, "Soft Ferrites - Properties and Applications", 2<sup>nd</sup> edition, Butterworths, 1988

## Core Loss Modeling Effect in Tape Wound Cores



[www.vacuumschmelze.de](http://www.vacuumschmelze.de)



Thin ribbons (approx. 20  $\mu\text{m}$ )  
Wound as toroid or as double C core.  
Amorphous or nanocrystalline materials.

**Losses in gapped tape wound cores higher than expected!**

## Core Loss Modeling

### Effect in Tape Wound Cores - Cause 1 : Interlamination Short Circuits

#### Machining process

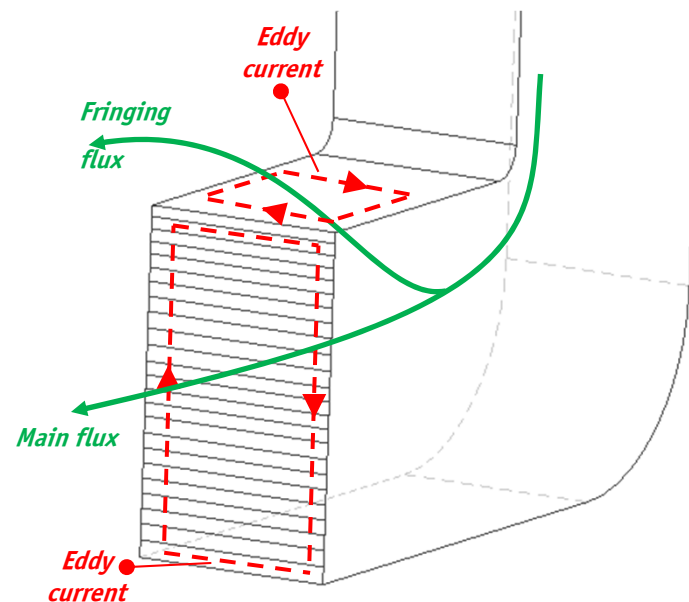
Surface short circuits introduced by machining  
(particular a problem in in-house production).



After treatment may reduce this effect. At ETH, a core was put in an 40% ferric chloride  $\text{FeCl}_3$  solution after cutting, which substantially (more than 50%) decreased the core losses.

## Core Loss Modeling

### Effect in Tape Wound Cores - Cause 2 : Orthogonal Flux Lines (1)



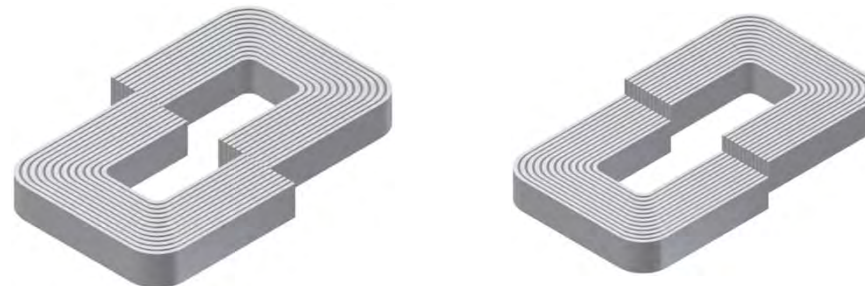
A flux orthogonal to the ribbons leads to very high eddy current losses!

## Core Loss Modeling

### Effect in Tape Wound Cores - Cause 2 : Orthogonal Flux Lines (2)

An experiment that illustrates well the loss increase due to an orthogonal flux is given here.

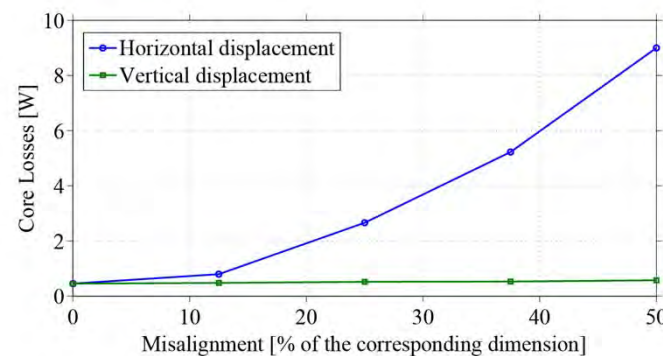
#### Displacements



Horizontal Displacement

Vertical Displacement

#### Core Loss Results

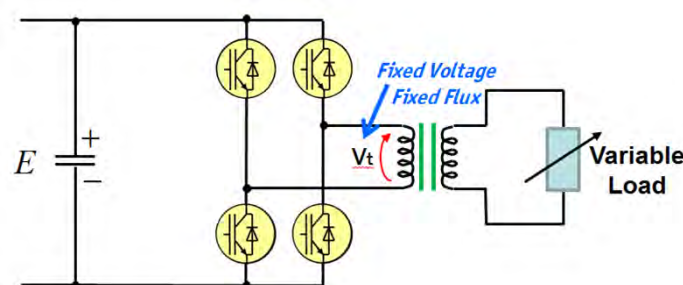
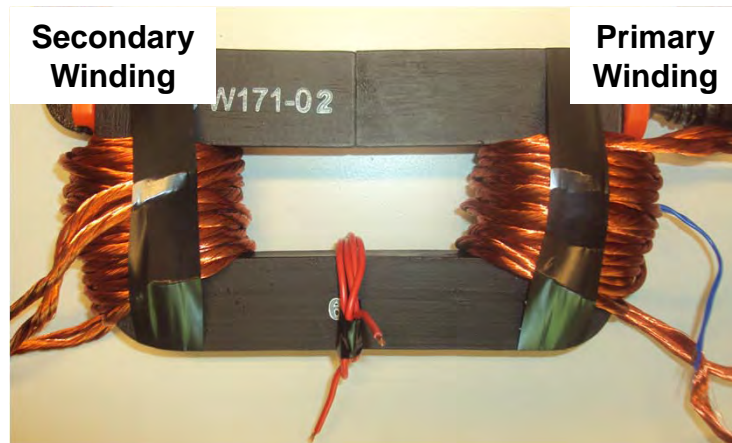


# Core Loss Modeling

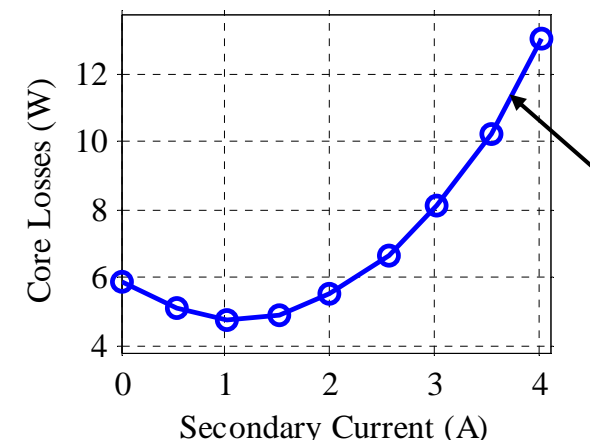
## Effect in Tape Wound Cores - Cause 2 : Orthogonal Flux Lines (3)

Core loss increase due to leakage flux in transformers.

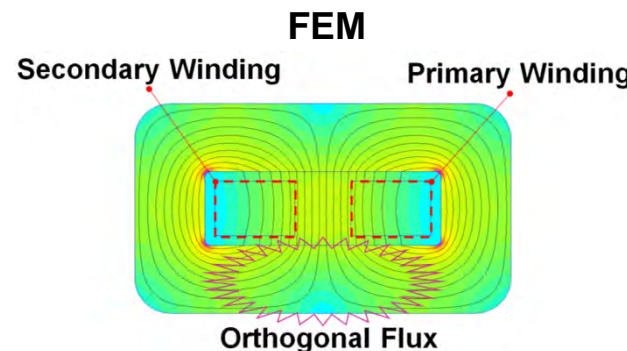
**Measurement Set Up**



**Results**



A higher load current leads to higher orthogonal flux!



## Core Loss Modeling

### Effect in Tape Wound Cores - Cause 2 : Orthogonal Flux Lines (4)

In [10] a core loss increase with increasing air gap length has been observed.

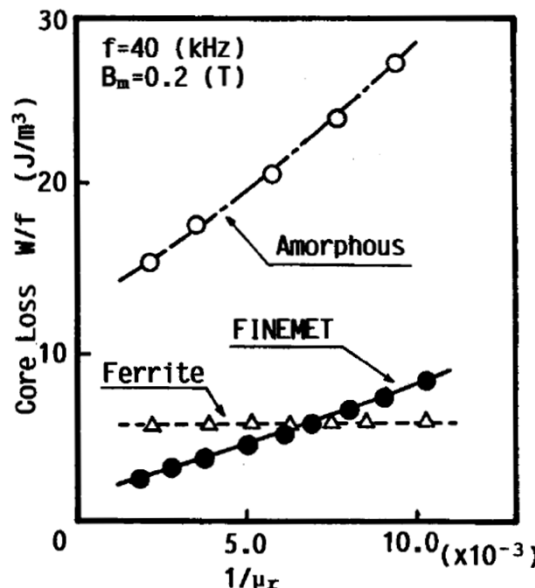


Fig.1 Core loss per cycle  $W/f$  in FINEMET, Fe-based amorphous, and ferrite cut cores as a function of inverse of the effective permeability  $\mu_r$ .

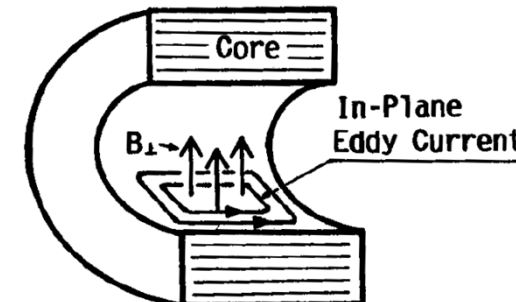


Fig.2 Schematic representation of in-plane eddy current generated by leakage flux normal to ribbon surfaces.

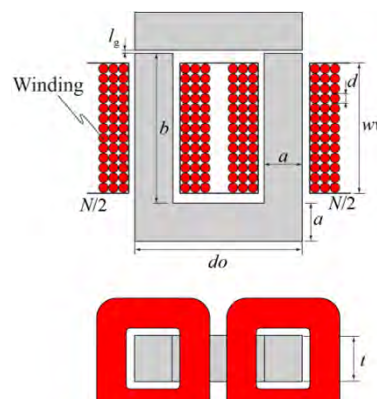
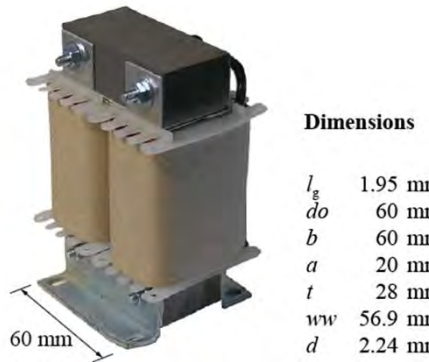
Figures from [10]

- [10] H. Fukunaga, T. Eguchi, K. Koga, Y. Ohta, and H. Kakehashi, "High Performance Cut Cores Prepared From Crystallized Fe-Based Amorphous Ribbon", in IEEE Transactions on Magnetics, vol. 26, no. 5, 1990.

## Example

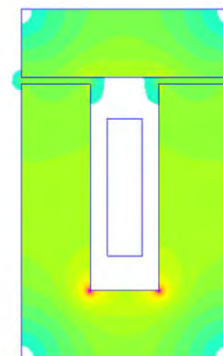
### Core Loss Modeling

#### Photo & Dimensions



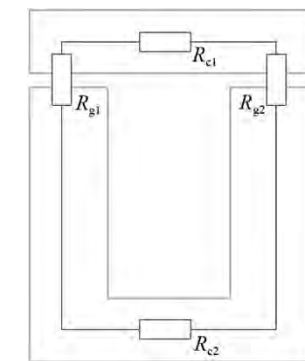
Grain-oriented steel (M165-35S)

#### Flux Density Distribution

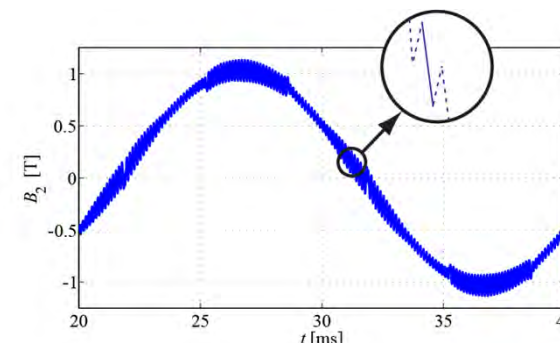


An approximately homogeneous flux density distribution inside the core.

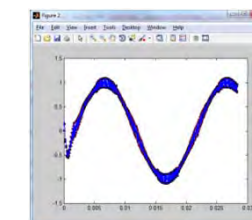
#### Reluctance Model



#### Flux Density Waveform



#### MATLAB Presentation



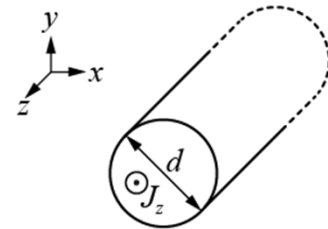
# Outline

- **Magnetic Circuit Modeling**
- **Core Loss Modeling**
- **Winding Loss Modeling**
- **Thermal Modeling**
- **Multi-Objective Optimization**
- **Summary & Conclusion**

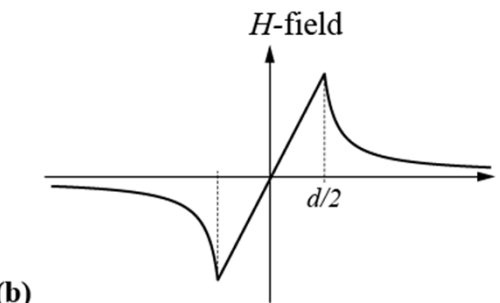
# Winding Loss Modeling

## Skin Effect (1)

**H-field in conductor**



(a)

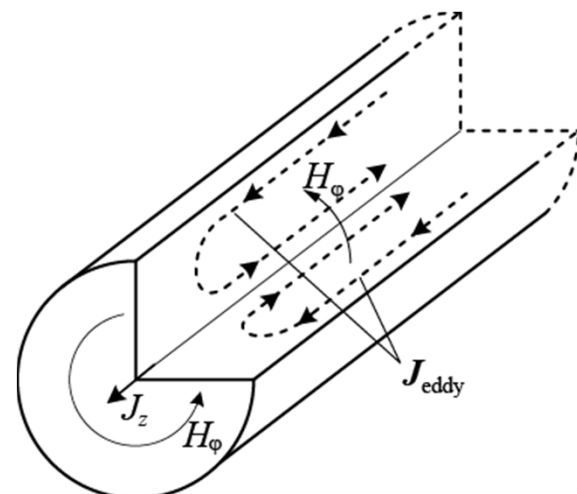


(b)

**Ampere's Law**

$$\oint \mathbf{H} d\mathbf{l} = \iint \mathbf{J} d\mathbf{A}$$

**Induced Eddy Currents**

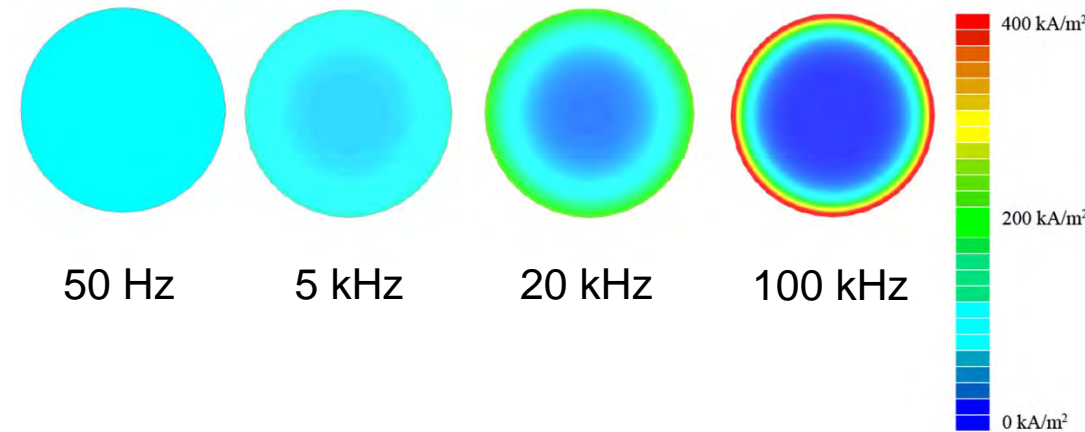


**Faraday's Law**

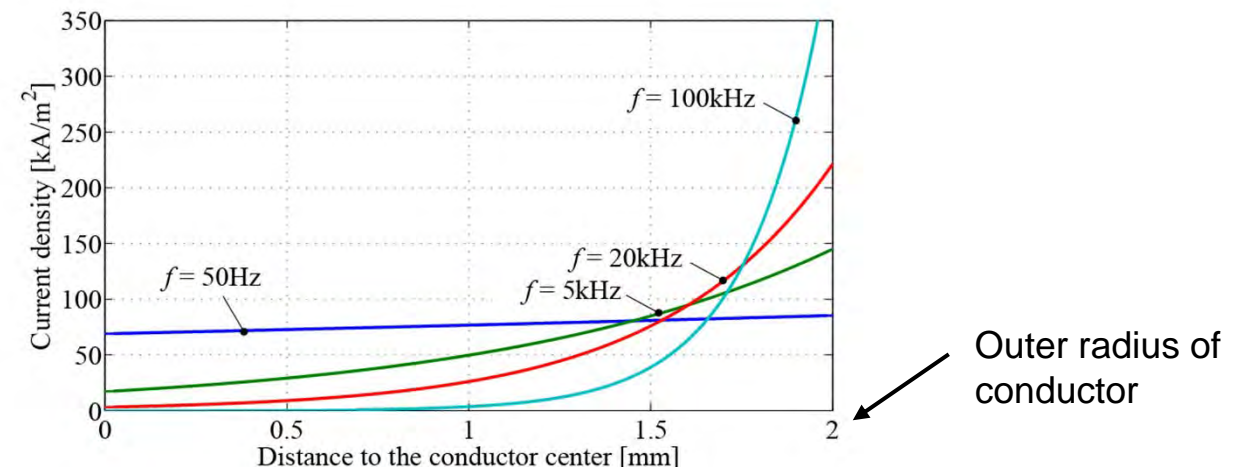
$$\oint \mathbf{E} d\mathbf{l} = - \frac{d}{dt} \iint \mathbf{B} d\mathbf{A}$$

## Winding Loss Modeling Skin Effect (2)

### FEM Simulation



### Current Distribution

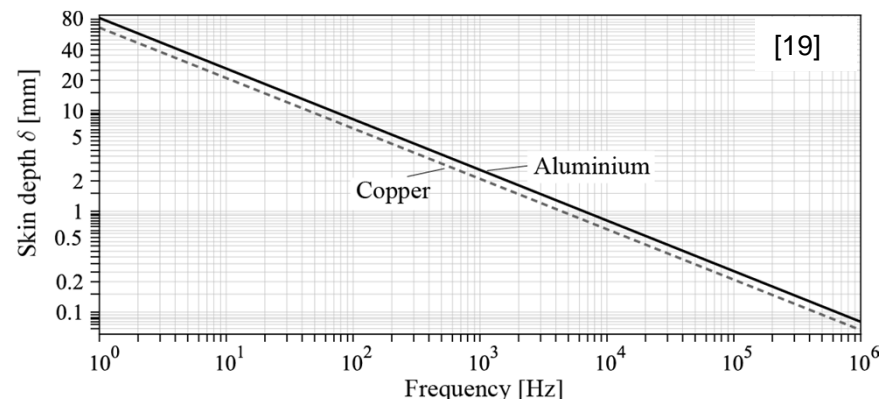
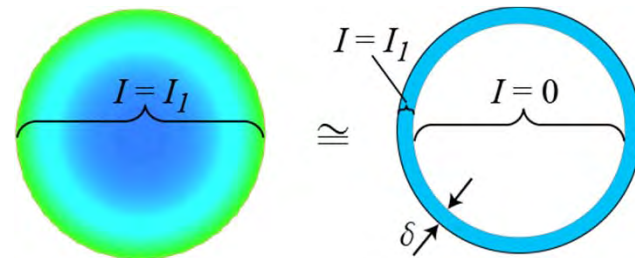


# Winding Loss Modeling

## Skin Effect (3)

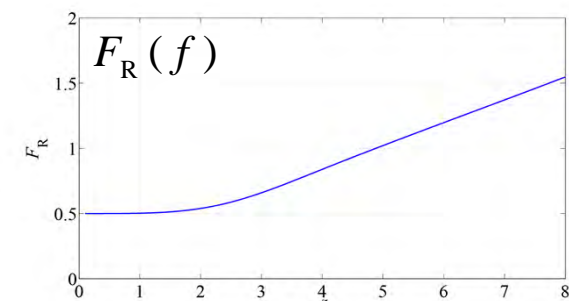
**Skin Depth** (, where the current density has  $1/e$  of surface value)

$$\delta = \frac{1}{\sqrt{\pi \mu_0 \sigma f}}$$



## Power Loss Increase with Frequency

$$P_s = F_R(f) \cdot R_{DC} \cdot \hat{I}^2$$



$$\xi = \frac{d}{\sqrt{2}\delta}$$

# Winding Loss Modeling

## Skin Effect (4)

### Current Distributions

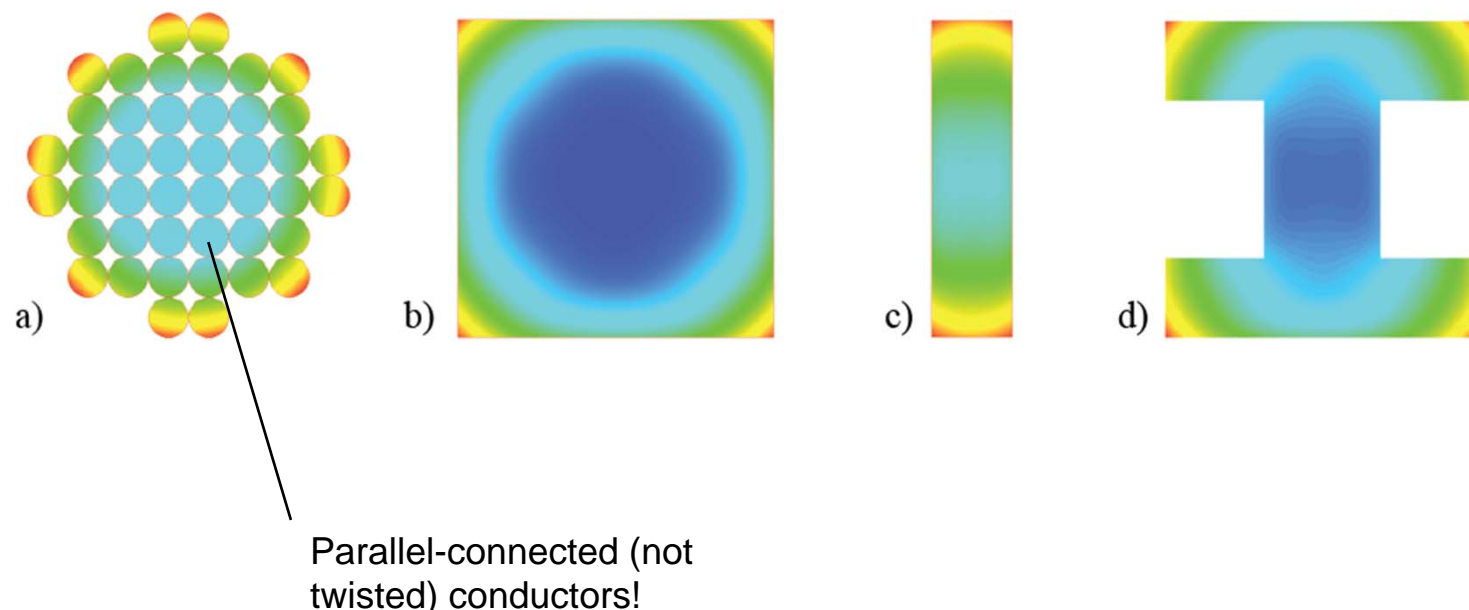
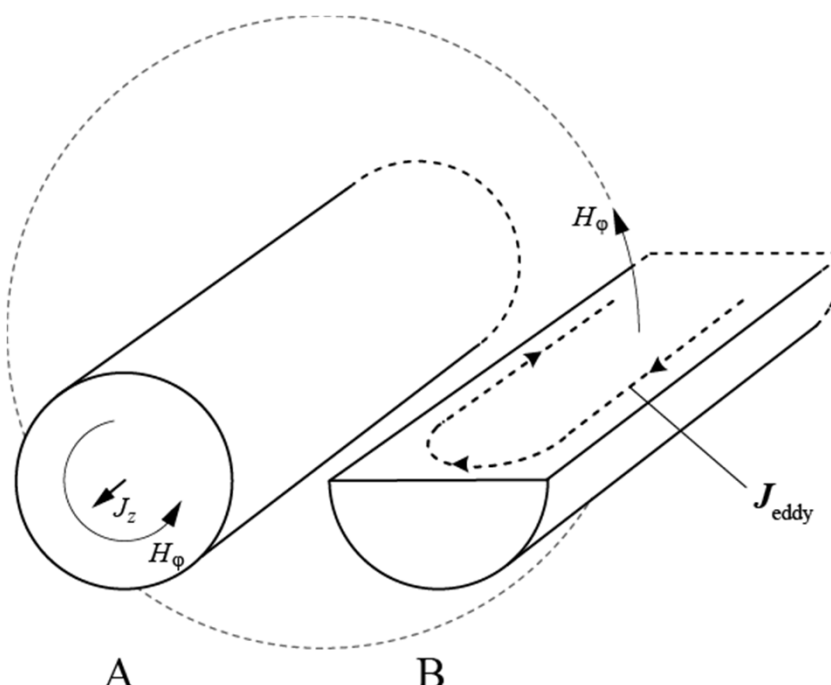


Figure from [19]

# Winding Loss Modeling

## Proximity Effect (1)

$H$ -field of neighboring conductor induces eddy currents



Ampere's Law

$$\oint \mathbf{H} d\mathbf{l} = \iint \mathbf{J} d\mathbf{A}$$

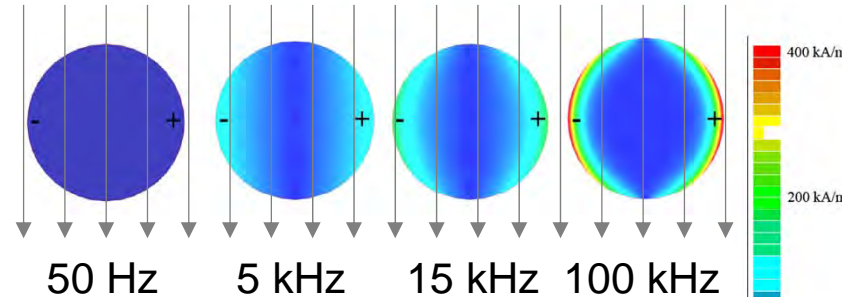
Faraday's Law

$$\oint \mathbf{E} d\mathbf{l} = -\frac{d}{dt} \iint \mathbf{B} d\mathbf{A}$$

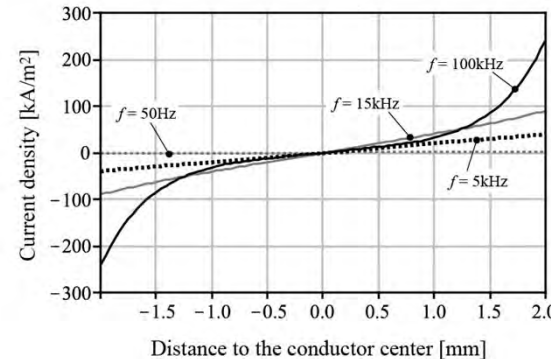
## Winding Loss Modeling

### Proximity Effect (2)

**Eddy Currents in Conductor**

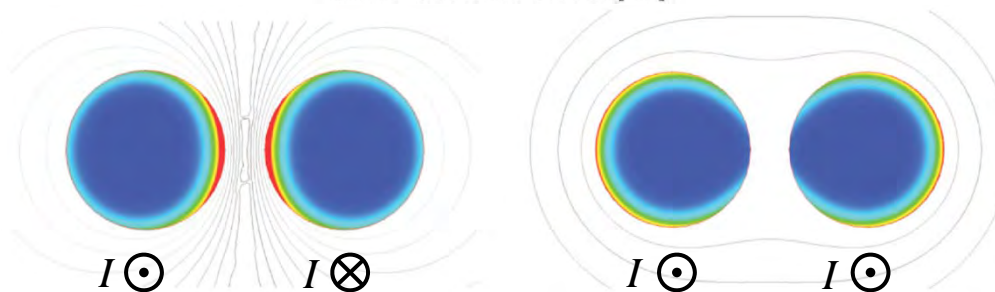


**Induced Eddy Currents**



( $H_{e,\text{rms}} = 35 \text{ A/m}$   
parallel to  
conductor)

**Current Concentration**



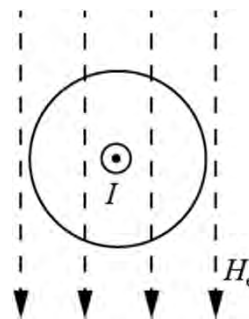
Figures from [19]

# Winding Loss Modeling

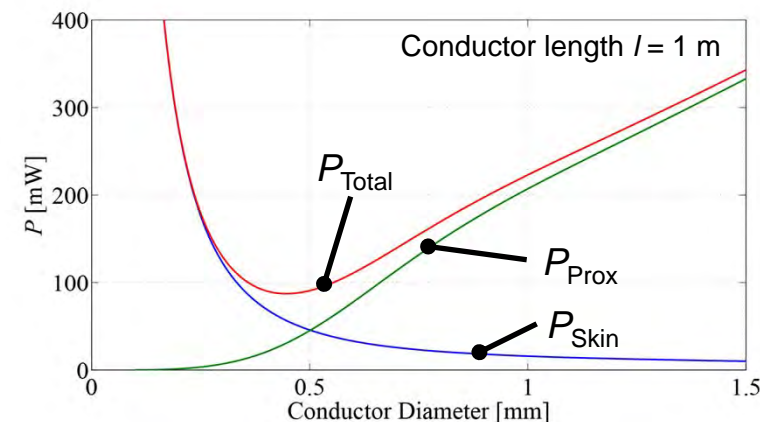
## Skin vs. Proximity Effect

### Situation

( $f = 100 \text{ kHz}$ ,  $I_{\text{peak}} = 1 \text{ A}$ ,  $H_{e,\text{peak}} = 1000 \text{ A/m}$ )



### Results



### Definition

#### Skin Effect Losses $P_{\text{Skin}}$

Losses due to current  $I$ , including loss increase due to self-induced eddy currents.

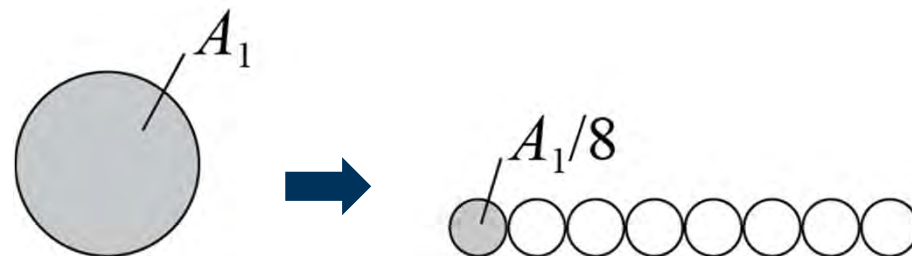
#### Proximity Effect Losses $P_{\text{Prox}}$

Losses due to eddy currents induced by external magnetic field  $H_e$ .

## Winding Loss Modeling

### Litz Wire (1) - What are Litz wires?

Idea



**Advantages of Litz wires**

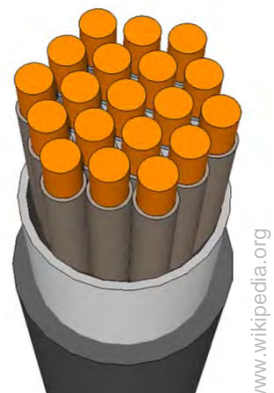
HF losses can be reduced substantially

**Disadvantages of Litz wires**

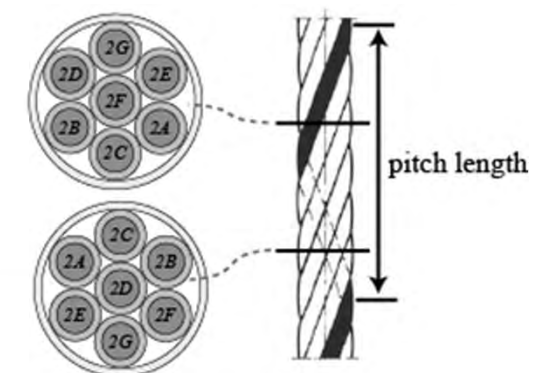
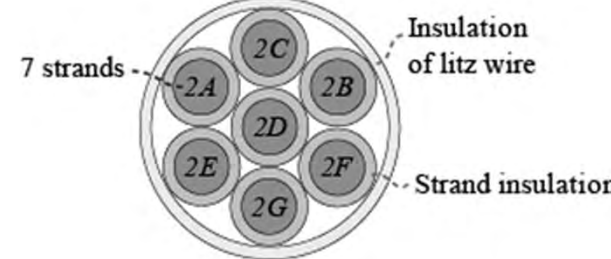
High price

Heat dissipation difficult

Implementation



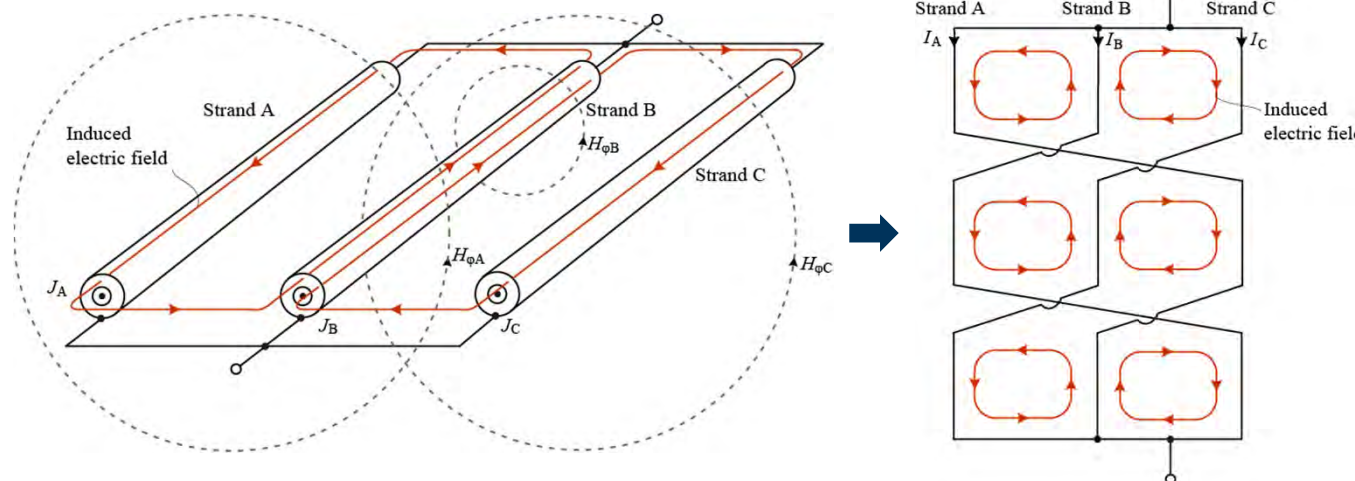
[www.wikipedia.org](http://www.wikipedia.org)



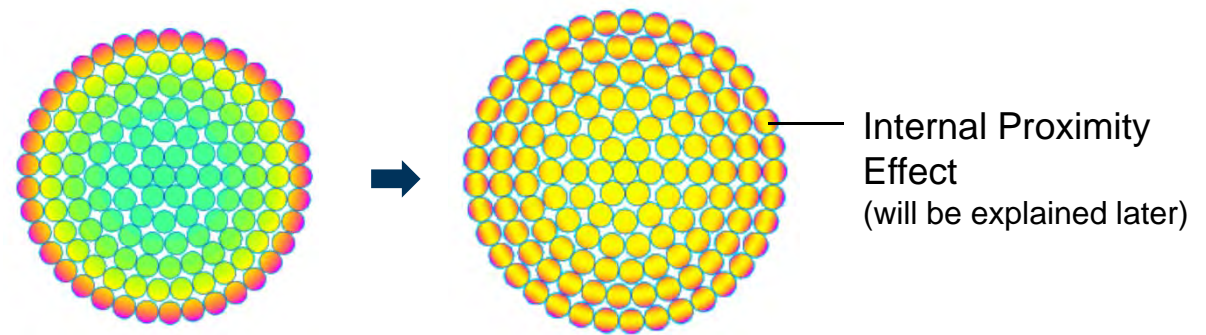
# Winding Loss Modeling

## Litz Wire (2) - Why Litz Wires Have to be Twisted? (1)

### Bundle-Level Skin Effect



### Current Distributions



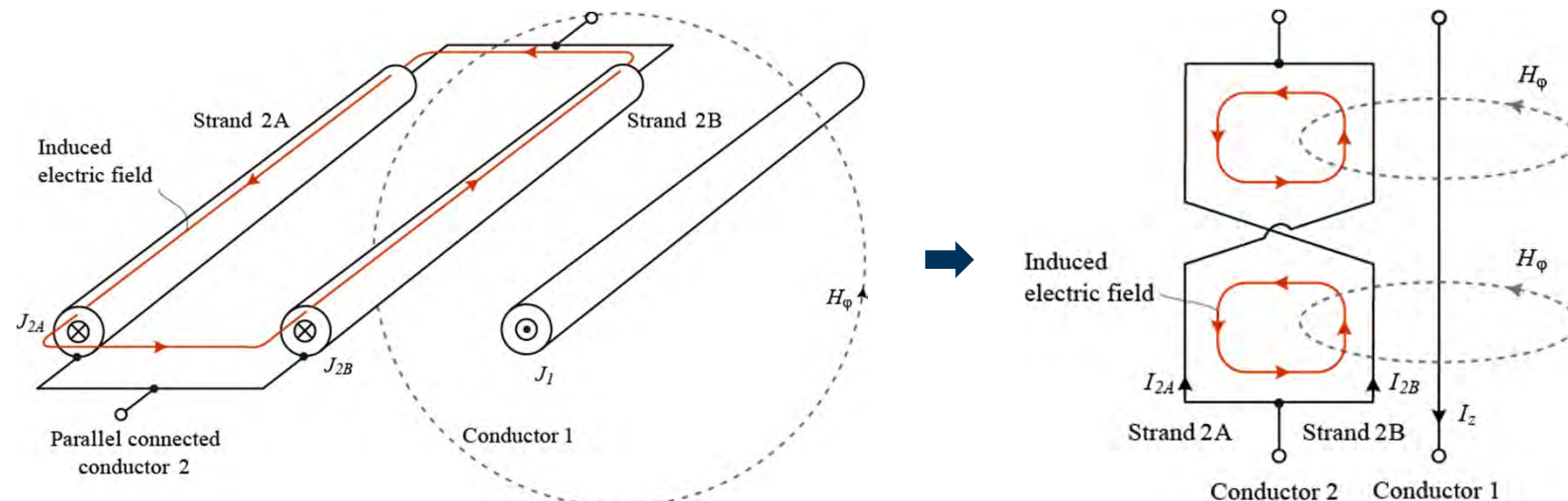
$$\oint \mathbf{H} d\mathbf{l} = \iint \mathbf{J} d\mathbf{A} \quad (\text{Ampere's Law})$$

$$\oint \mathbf{E} d\mathbf{l} = -\frac{d}{dt} \iint \mathbf{B} d\mathbf{A} \quad (\text{Faraday's Law})$$

# Winding Loss Modeling

## Litz Wire (3) - Why Litz Wires Have to be Twisted? (2)

### Bundle-Level Proximity Effect



$$\oint \mathbf{H} d\mathbf{l} = \iint \mathbf{J} d\mathbf{A} \quad (\text{Ampere's Law})$$

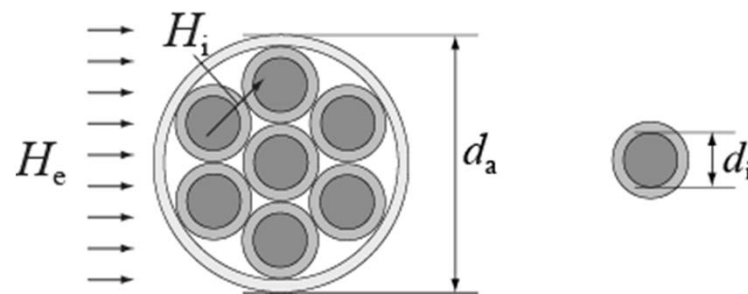
$$\oint \mathbf{E} d\mathbf{l} = -\frac{d}{dt} \iint \mathbf{B} d\mathbf{A} \quad (\text{Faraday's Law})$$

Figures from [19]

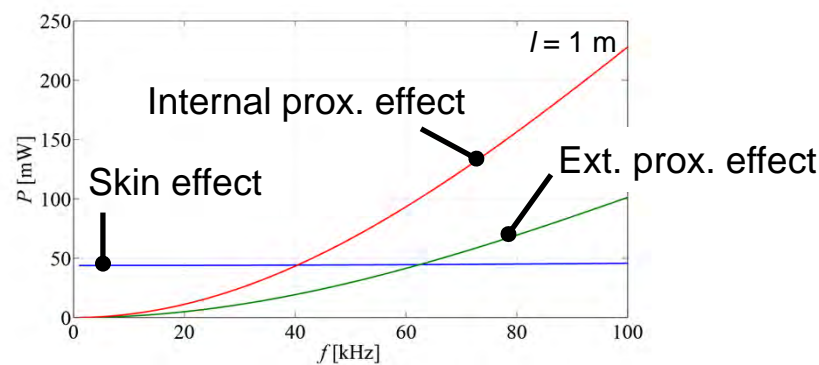
# Winding Loss Modeling

## Litz Wire (4) – Strand-Level Effects

Internal and External Fields lead to Internal and External Proximity Effects

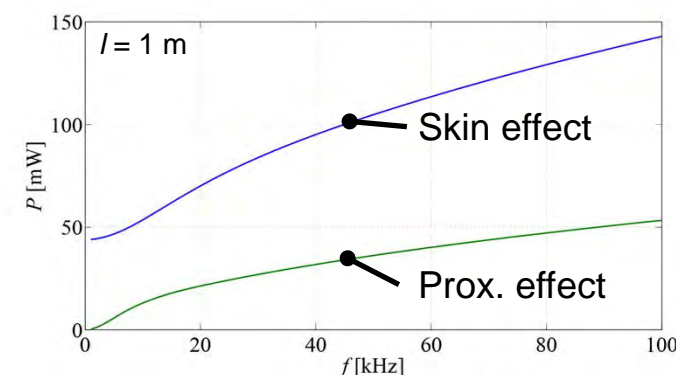


**Losses in Litz Wires**



$(25 \times d_i = 0.5 \text{ mm}, I_{\text{peak}} = 5 \text{ A}, H_{e,\text{peak}} = 300 \text{ A/m})$

**Losses in Solid Wires**



$(d = 2.5 \text{ mm}, I_{\text{peak}} = 5 \text{ A}, H_{e,\text{peak}} = 300 \text{ A/m})$

## Winding Loss Modeling

### Litz Wire (5) – Types of Eddy-Current Effects in Litz Wire

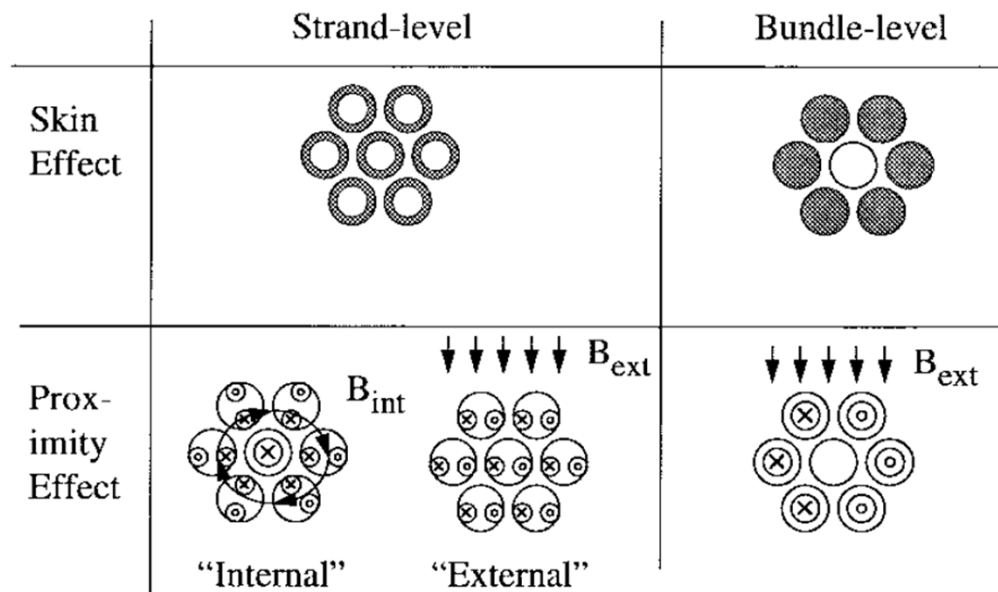
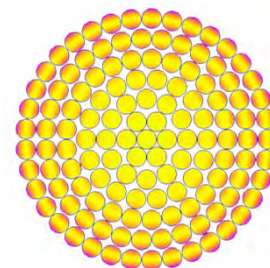


Figure from [11] Ch. R. Sullivan, "Optimal Choice for Number of Strands in a Litz-Wire Transformer Winding", in IEEE Transactions on Power Electronics, vol. 14, no. 2, 1999.

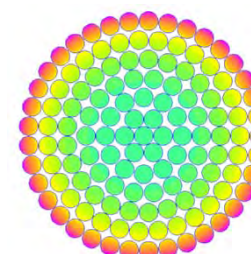
# Winding Loss Modeling

## Litz Wire (6) – Real Litz Wire

**Ideal Litz Wire**  
(ideally twisted  
strands)



**Worst Case Litz Wire**  
(parallel connected  
strands, no twisting)



**Operating Point**  
 $f = 20 \text{ kHz}$  /  $n = 130$  /  
 $d_i = 0.4 \text{ mm}$

### How do “real” Litz wires behave? [12]

Skin Effect / Internal Proximity Effect

$$R_{\text{skin},\lambda} = \lambda_{\text{skin}} R_{\text{skin,ideal}} + (1 - \lambda_{\text{skin}}) R_{\text{skin,parallel}}$$

External Proximity Effect

$$R_{\text{prox},\lambda} = \lambda_{\text{prox}} R_{\text{prox,ideal}} + (1 - \lambda_{\text{prox}}) R_{\text{prox,parallel}}$$

Litz Wire Type 1: 7 bundles with 35 strands each<sup>1)</sup>:

$$\lambda_{\text{skin}} \approx 0.5 / \lambda_{\text{prox}} \approx 0.99$$

Litz Wire Type 2: 4 bundles with 61/62 strands each<sup>1)</sup>:

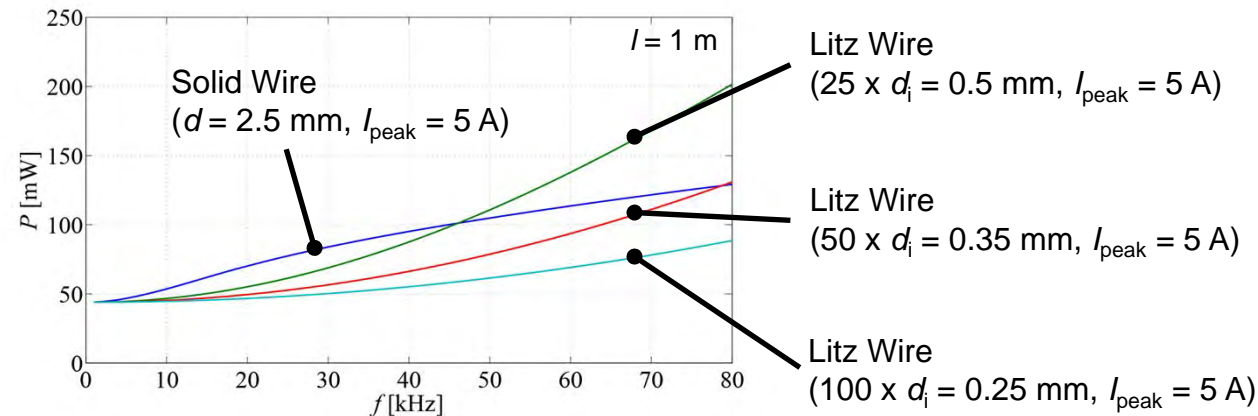
$$\lambda_{\text{skin}} \approx 0.9 / \lambda_{\text{prox}} \approx 0.99$$

[12] H. Rossmanith, M. Doebroenti, M. Albach, and D. Exner, “Measurement and Characterization of High Frequency Losses in Nonideal Litz Wires”, IEEE Transactions on Power Electronics, vol. 26, no. 11, November 2011

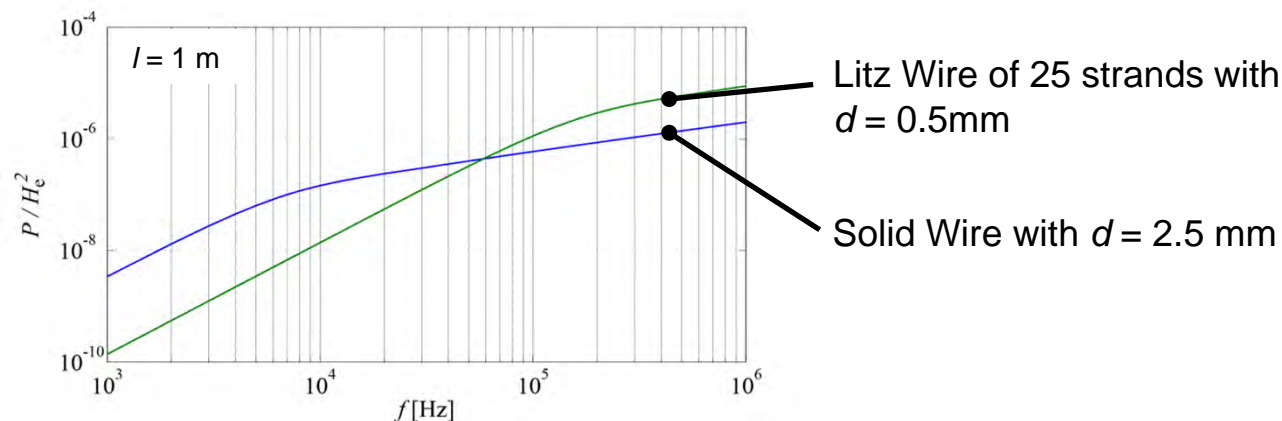
## Winding Loss Modeling

### Litz Wire (7) - Are Litz Wires Better than Solid Conductors?

#### Skin and Internal Proximity Effect

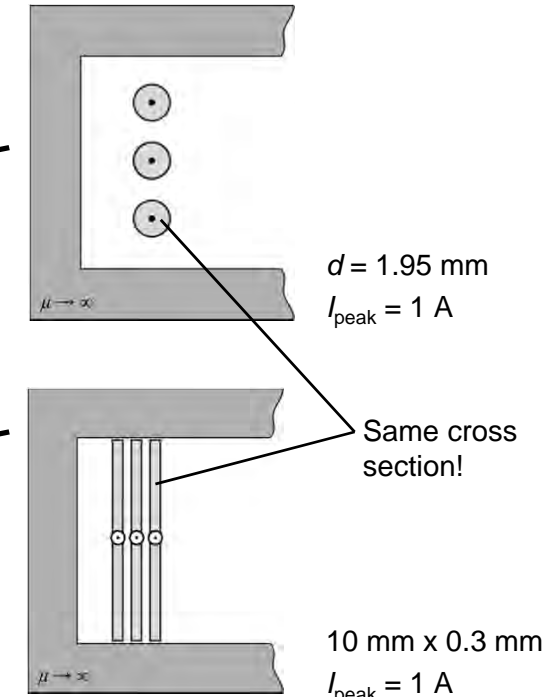
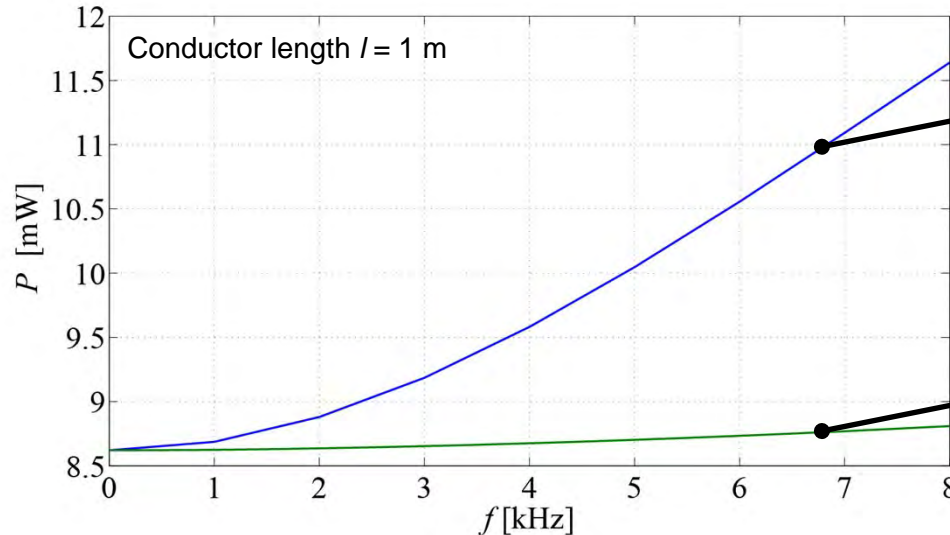


#### External Proximity Effect



## Winding Loss Modeling

### Foil Windings Enclosed by Magnetic Material



#### Advantages of foil windings

- HF losses can be reduced
- Lower price compared to Litz wire
- High filling factor

#### Disadvantages of foil windings

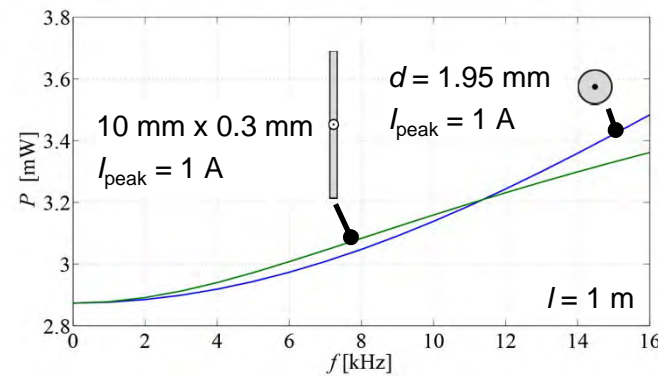
- Increased winding capacitance
- Risk of orthogonal flux

→ “Skin” of foil conductor larger than of round conductor with same cross section; hence, skin effect losses lower in foil conductor.

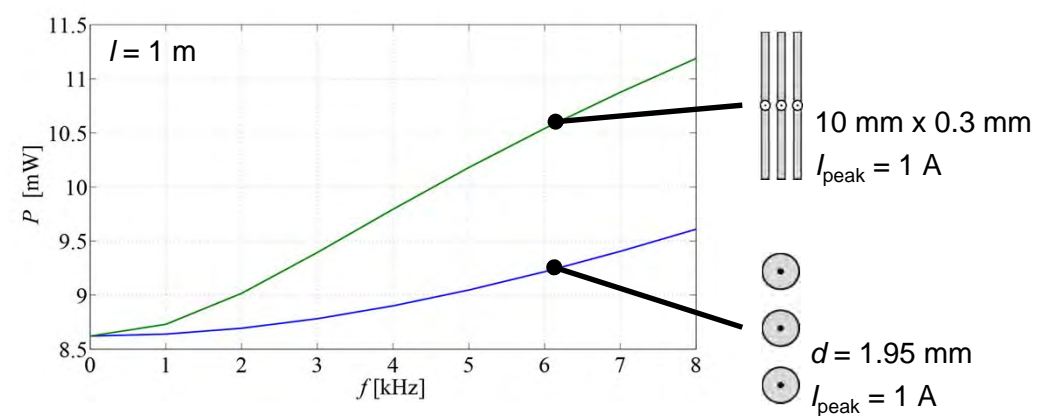
# Winding Loss Modeling

## Foil Windings Not Enclosed by Magnetic Material (1)

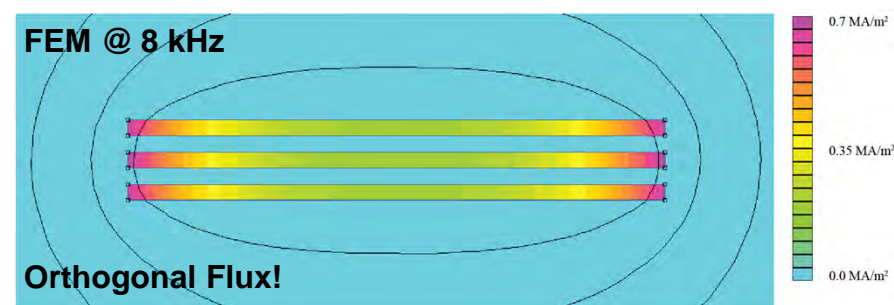
**Single Conductor**



**Three Conductors**



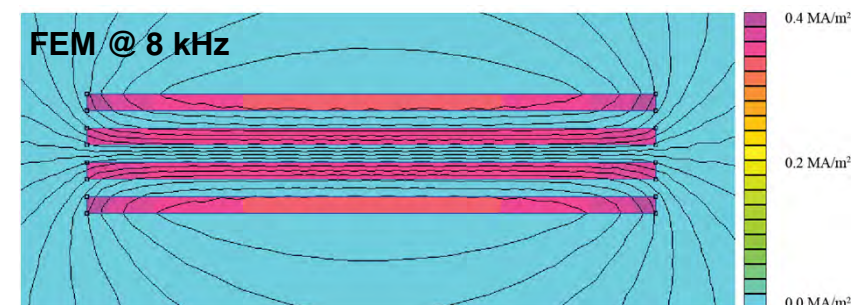
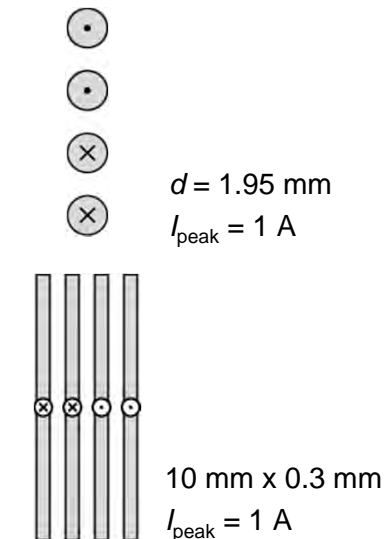
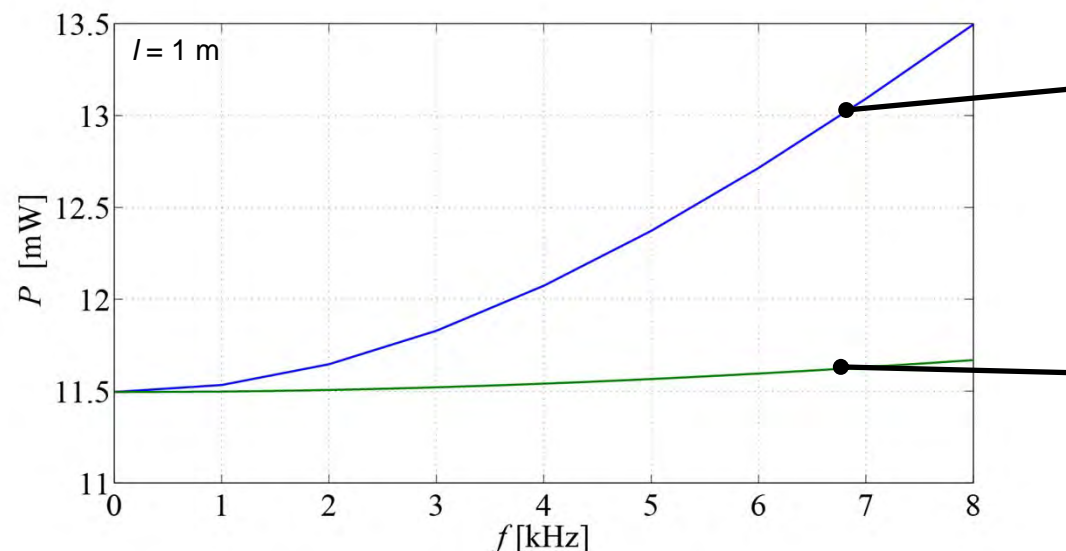
Orthogonal flux leads to increased skin and proximity effect.



## Winding Loss Modeling

### Foil Windings Not Enclosed by Magnetic Material (2)

(Foil) Windings with Return Conductors



# Winding Loss Modeling

## Overview About Different Winding Types

Type	Price	Skin & Proximity	Filling Factor	Heat Dissipation
Round Solid Wire	++	--	+	+
Litz Wire	--	++	-	--
Foil Winding	+	+	++	+
Rectangular Wire	++	-	++	+

### Rectangular Wire

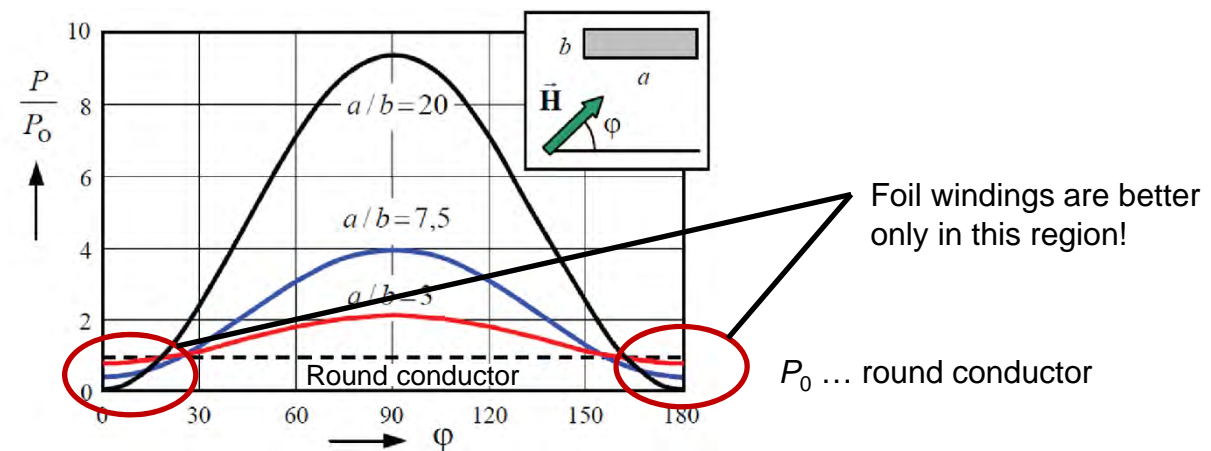
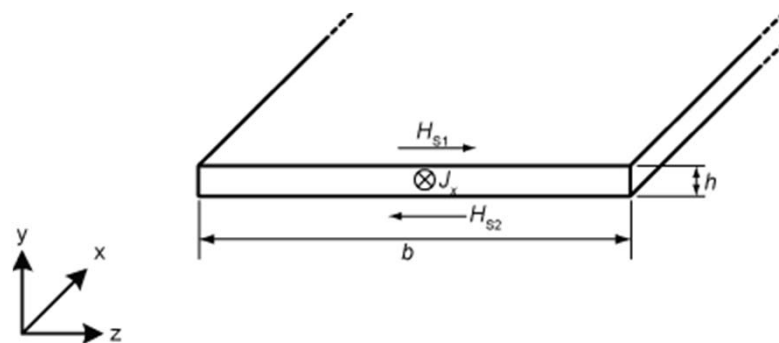


Table and Figure from [13] M. Albach, "Induktive Komponenten in der Leistungselektronik", VDE Fachtagung - ETG Fachbereich Q1 "Leistungselektronik und Systemintegration", Bad Nauheim, 14.04.2011

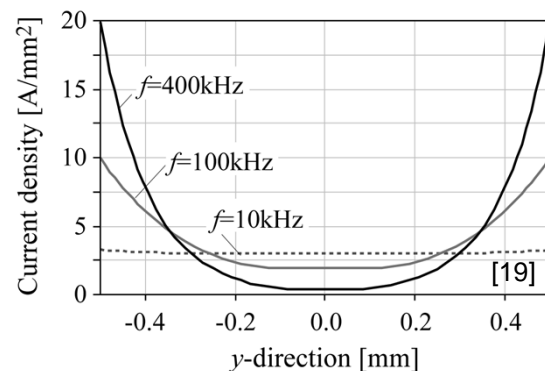
# Winding Loss Modeling

## Skin Effect of Foil Conductor

### Geometry Considered



### Current Distribution



with

$$P_s = F_F(f) \cdot R_{DC} \cdot \hat{I}^2$$

(Loss per unit length)

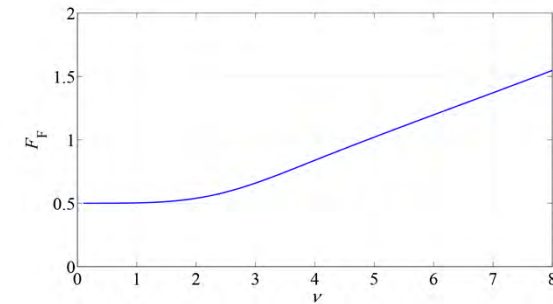
$$F_F = \frac{\nu}{4} \frac{\sinh \nu + \sin \nu}{\cosh \nu - \cos \nu}$$

$$R_{DC} = \frac{1}{\sigma b h}$$

$$\nu = \frac{h}{\delta}$$

$$\delta = \frac{1}{\sqrt{\pi \mu_0 \sigma f}}$$

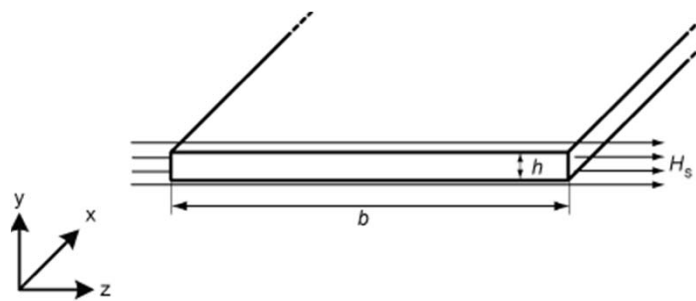
### $F_F$ evaluated



# Winding Loss Modeling

## Proximity Effect of Foil Conductor

### Geometry Considered



with

$$P_p = G_F(f) \cdot R_{DC} \cdot \hat{H}_s^2$$

(Loss per unit length)

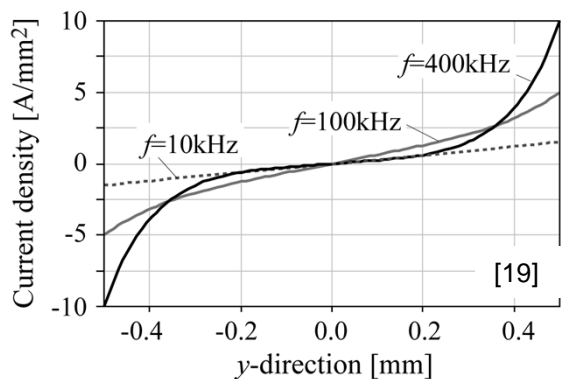
$$G_F = b^2 v \frac{\sinh v - \sin v}{\cosh v + \cos v}$$

$$R_{DC} = \frac{1}{\sigma b h}$$

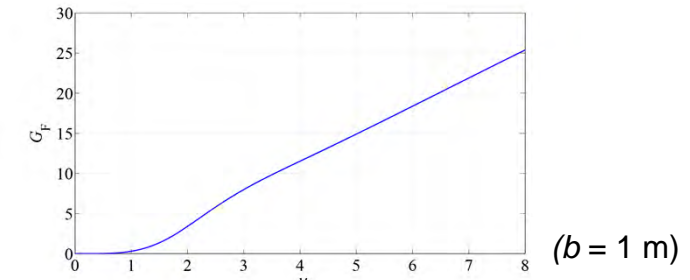
$$v = \frac{h}{\delta}$$

$$\delta = \frac{1}{\sqrt{\pi \mu_0 \sigma f}}$$

### Current Distribution



### $G_F$ evaluated



# Winding Loss Modeling

## Skin Effect of Solid Round Conductor

$$P_s = F_R(f) \cdot R_{DC} \cdot \hat{I}^2$$

(Loss per unit length)

with

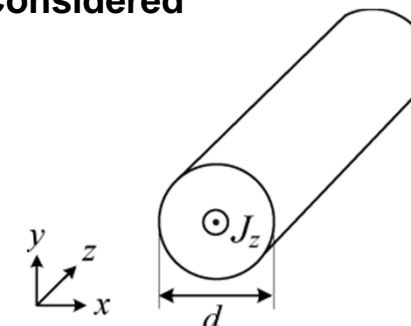
$$R_{DC} = \frac{4}{\sigma \pi d^2}$$

$$\xi = \frac{d}{\sqrt{2}\delta}$$

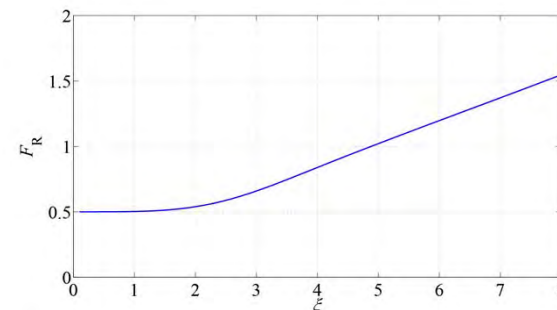
$$\delta = \frac{1}{\sqrt{\pi \mu_0 \sigma f}}$$

$$F_R = \frac{\xi}{4\sqrt{2}} \left[ \frac{\text{ber}_0(\xi)\text{bei}_1(\xi) - \text{ber}_0(\xi)\text{ber}_1(\xi)}{\text{ber}_1(\xi)^2 + \text{bei}_1(\xi)^2} - \frac{\text{bei}_0(\xi)\text{ber}_1(\xi) - \text{bei}_0(\xi)\text{bei}_1(\xi)}{\text{ber}_1(\xi)^2 + \text{bei}_1(\xi)^2} \right]$$

Geometry Considered



$F_R$  evaluated



# Winding Loss Modeling

## Proximity Effect of Solid Round Conductor

$$P_p = G_R(f) \cdot R_{DC} \cdot \hat{H}_S^2$$

(Loss per unit length)

with

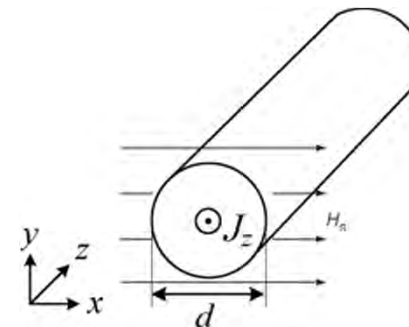
$$R_{DC} = \frac{4}{\sigma \pi d^2}$$

$$\xi = \frac{d}{\sqrt{2}\delta}$$

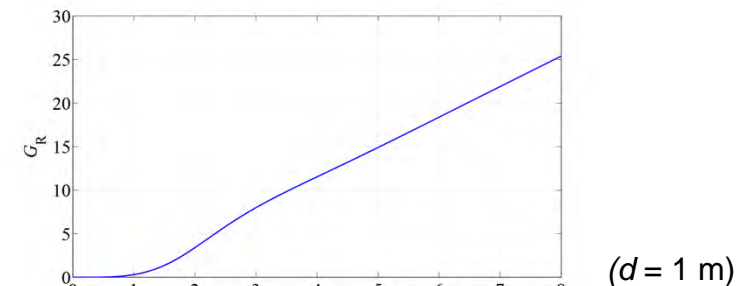
$$\delta = \frac{1}{\sqrt{\pi \mu_0 \sigma f}}$$

$$G_R = -\frac{\xi \pi^2 d^2}{2\sqrt{2}} \left[ \frac{\text{ber}_2(\xi)\text{ber}_1(\xi) + \text{ber}_2(\xi)\text{bei}_1(\xi)}{\text{ber}_0(\xi)^2 + \text{bei}_0(\xi)^2} + \frac{\text{bei}_2(\xi)\text{bei}_1(\xi) - \text{bei}_2(\xi)\text{ber}_1(\xi)}{\text{ber}_0(\xi)^2 + \text{bei}_0(\xi)^2} \right]$$

### Geometry Considered



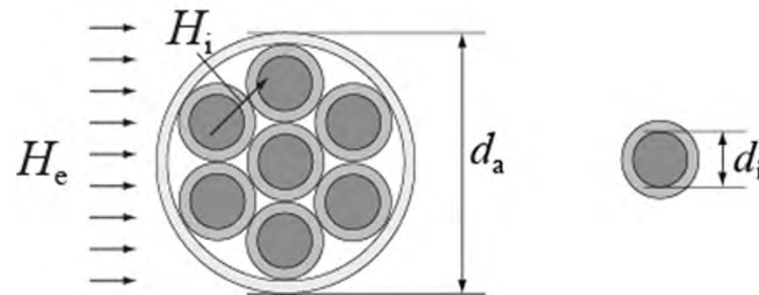
### $G_R$ evaluated



( $d = 1$  m)

# Winding Loss Modeling

## Skin and Proximity Effect of Litz Wire



### Skin Effect

$$P_S = n \cdot R_{DC} \cdot F_R(f) \cdot \left( \frac{\hat{I}}{n} \right)^2$$

(Loss per unit length)

### Proximity Effect

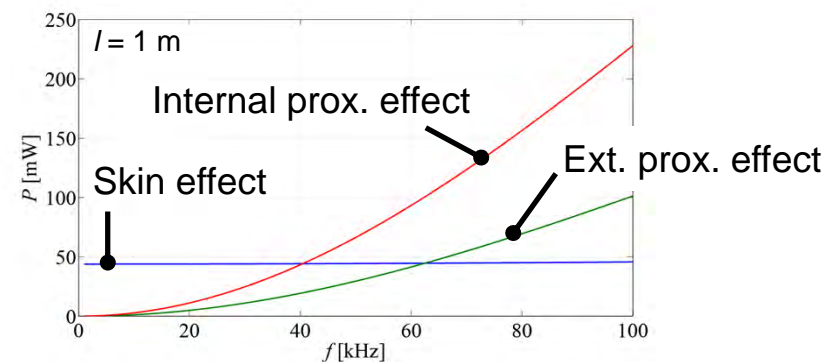
$$P_p = P_{p,e} + P_{p,i}$$

$$= n \cdot R_{DC} \cdot G_R(f) \cdot \left( H_e^2 + \frac{\hat{I}^2}{2\pi^2 d_a^2} \right)$$

(Loss per unit length)

Average internal field  $H_i$  under the assumption of a homogeneous current distribution inside the Litz wire.

### Losses in Litz Wires



( $25 \times d_i = 0.5 \text{ mm}$ ,  $I_{peak} = 5 \text{ A}$ ,  $H_{e,peak} = 300 \text{ A/m}$ )

## Winding Loss Modeling

### Orthogonality of Winding Losses

It is valid to calculate the losses for each frequency component independently and total them up.

$$P = \sum_{i=0}^{\infty} (P_{S,i} + P_{P,i})$$

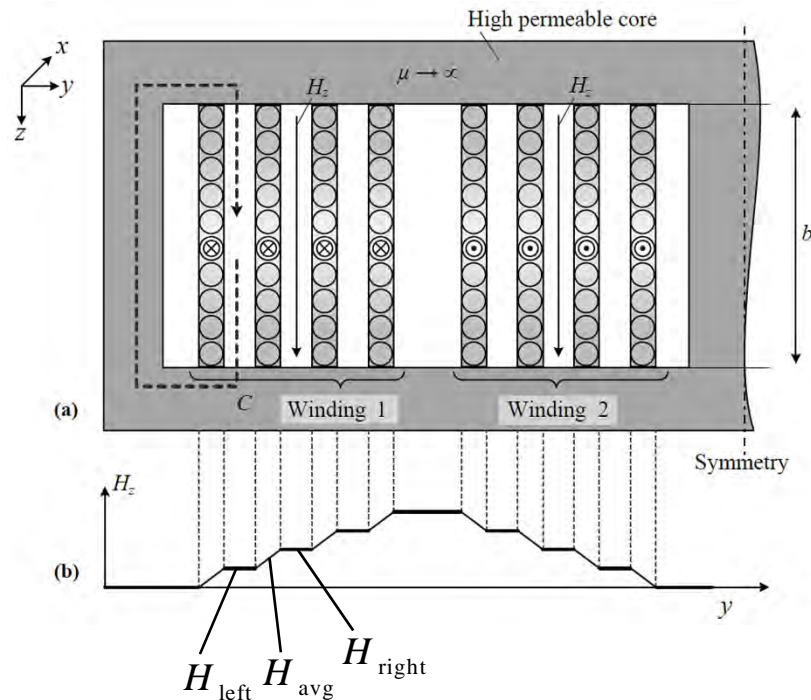
It is valid to calculate the skin and proximity losses independently and total them up.

- [14] J. A. Ferreira, "Improved analytical modeling of conductive losses in magnetic components", in IEEE Transactions on Power Electronics, vol. 9, no. 1, 1994.

# Winding Loss Modeling

## Calculation of External Field $H_e$ (1D - Approach)

### Un-Gapped Transformer Cores



$$P = R_{DC} \left( F_{R/F} \hat{I}^2 NM + NG_{R/F} \sum_{m=1}^M \hat{H}_{avg,m}^2 \right) l_m$$

with

$$H_{avg} = \frac{1}{2} (H_{left} + H_{right})$$

it is

$$P = R_{DC} \hat{I}^2 \left( F_{R/F} NM + N^3 M G_{R/F} \frac{4M^2 - 1}{12b_F^2} \right) l_m$$

where

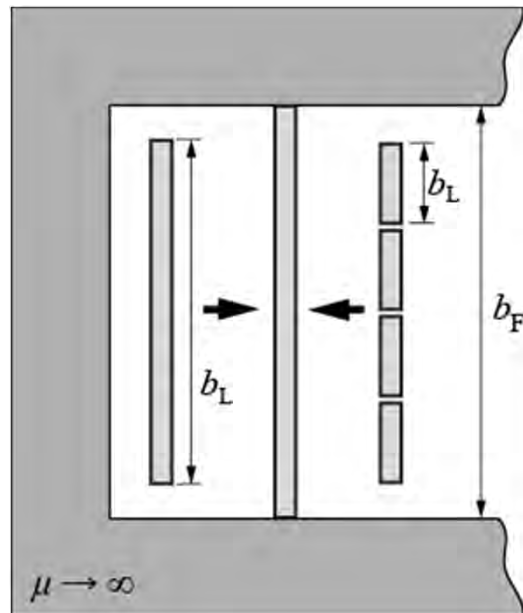
$N$  ... the number of conductors per layer  
(i.e.  $N = 1$  for foil windings)

$M$  ... the number of layers.

Figure from [19]

$$\oint \mathbf{H} d\mathbf{l} = \iint \mathbf{J} d\mathbf{A} \quad (\text{Ampere's Law})$$

## Winding Loss Modeling Short Foil Conductors



“Porosity Factor”

$$\eta = \frac{Nb_L}{b_F}$$

Redefinition of Parameters

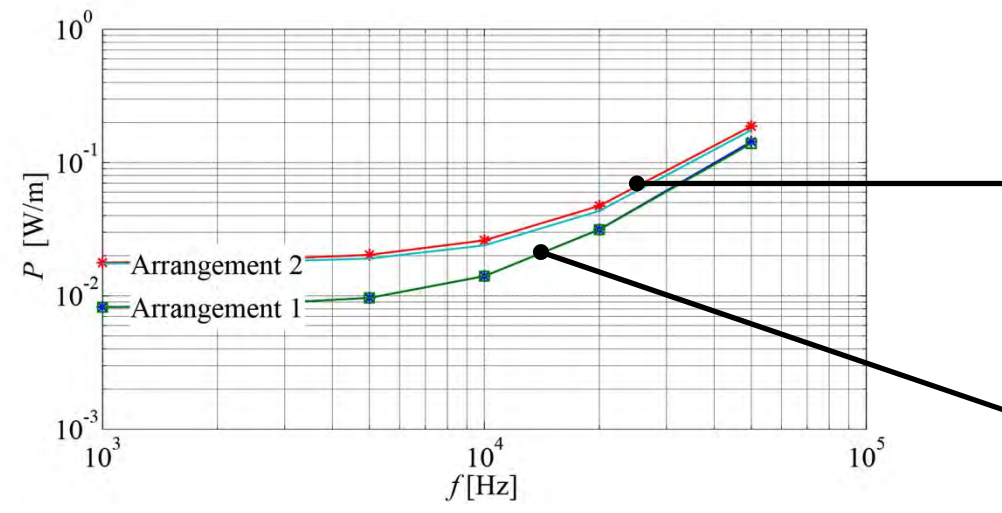
$$\sigma' = \eta \sigma$$

$$\delta' = \frac{1}{\sqrt{\pi f \sigma' \mu_0}}$$

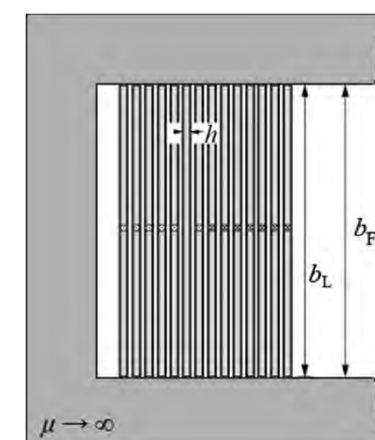
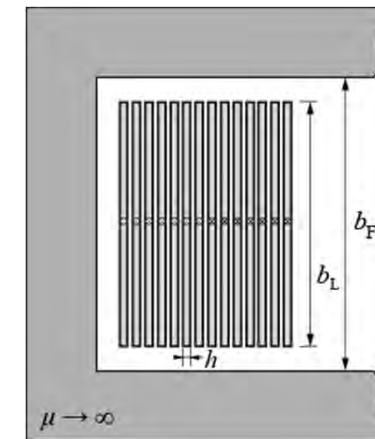
$$\nu' = \frac{h}{\delta'}$$

## Winding Loss Modeling

### FEM Simulations : Foil Windings



Error < 6.5%



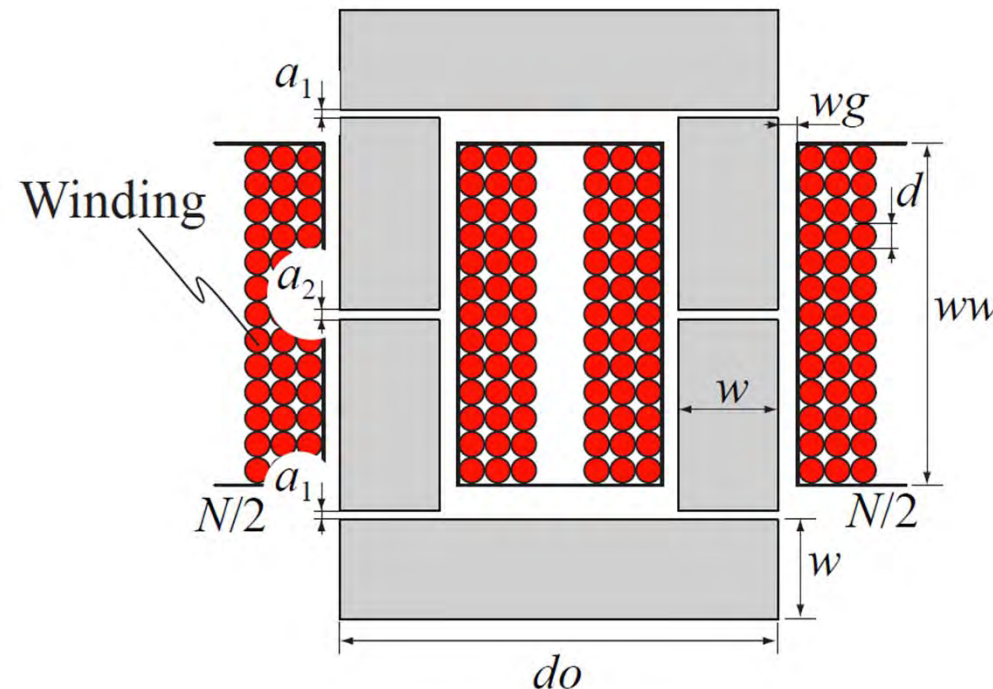
$N = 2 \times 10$   
 $h = 0.3 \text{ mm}$   
 $b_L = 33 \text{ mm}$   
 $b_F = 37 \text{ mm}$   
 $I_{\text{peak}} = 1 \text{ A}$

$N = 2 \times 7$   
 $h = 0.4 \text{ mm}$   
 $b_L = 37 \text{ mm}$   
 $b_F = 37 \text{ mm}$   
 $I_{\text{peak}} = 1 \text{ A}$

## Winding Loss Modeling

### Calculation of External Field $H_e$ (2D - Approach)

Gapped cores: 2D approach is necessary !

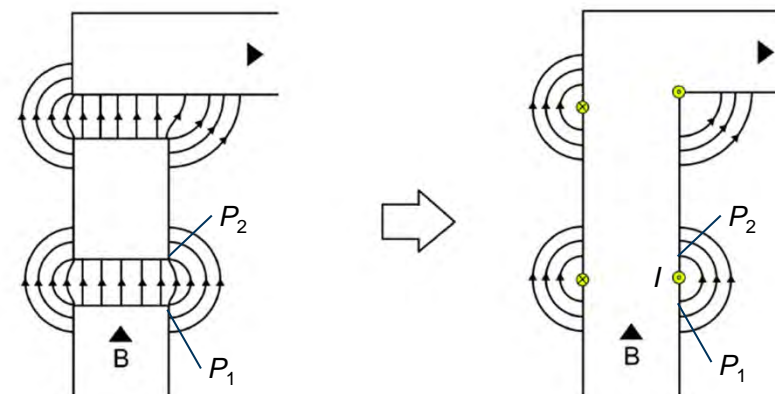


## Winding Loss Modeling

### Effect of the Air Gap Fringing Field

The air gap is replaced by a fictitious current, which ...

... has the value equal to the magneto-motive force (mmf) across the air gap.



$$V_{m,air} = \int_{P_1}^{P_2} \mathbf{H} d\mathbf{l} = \phi \cdot R_{air}$$

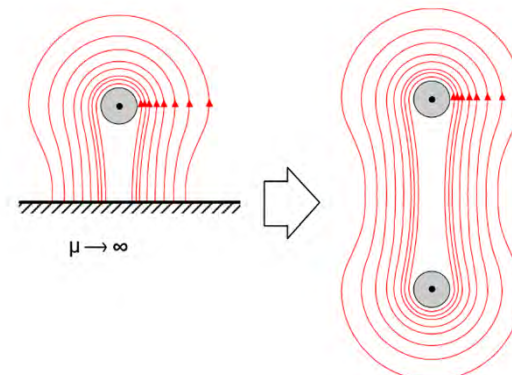
$$V_{m,air} = \int_{P_1}^{P_2} \mathbf{H} d\mathbf{l} = I$$

→ An accurate air gap reluctance model is needed!

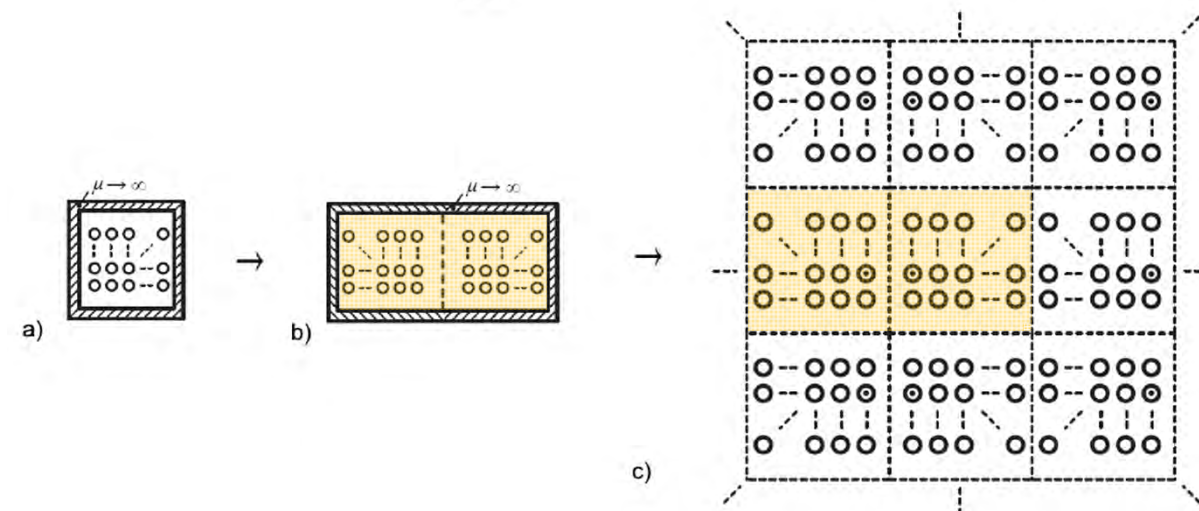
## Winding Loss Modeling

### Effect of the Core Material

The **method of images (mirroring)**



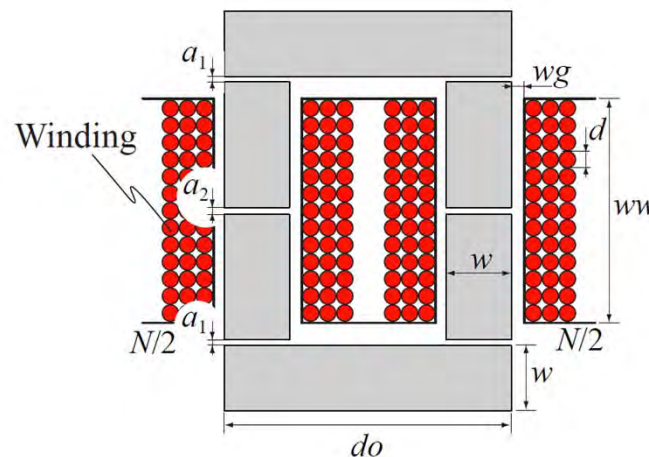
“Pushing the walls away”



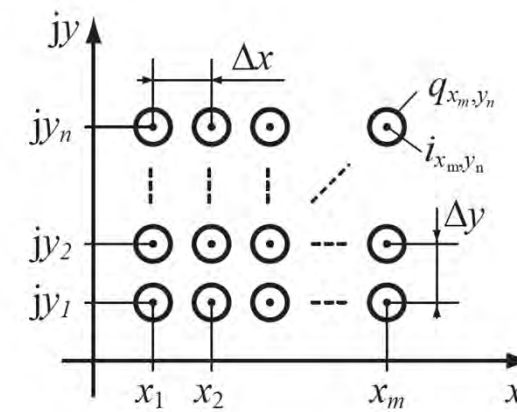
# Winding Loss Modeling

## Calculation of External Field $H_e$ (2D - Approach)

## Gapped cores: 2D approach



## **Winding Arrangement**

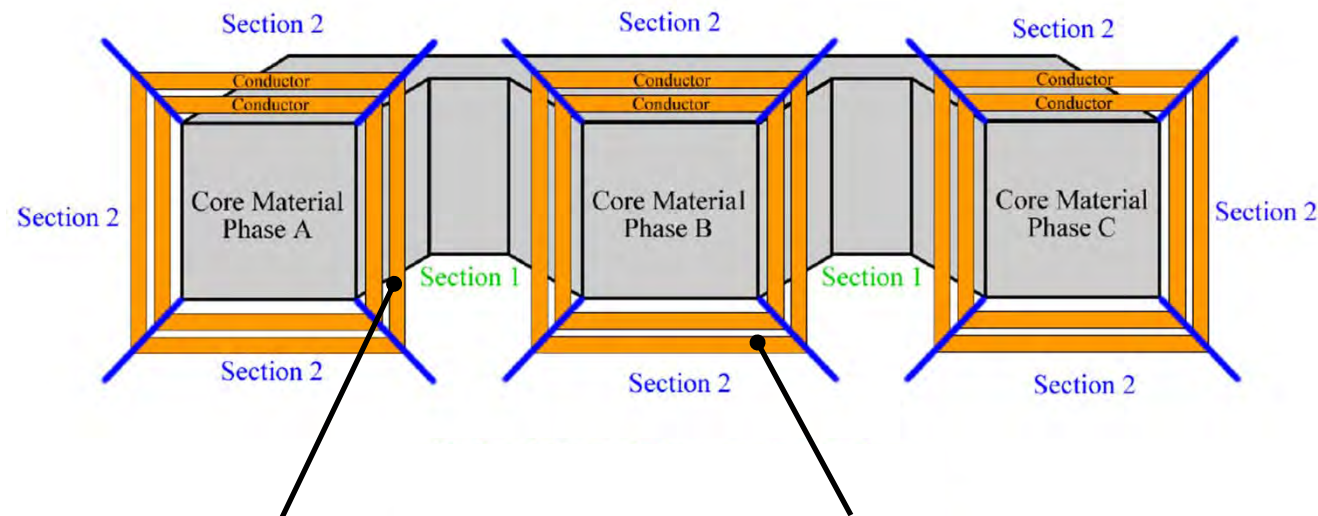


**External field vector across conductor  $q_{xi;yk}$**

$$\hat{H}_e = \left| \sum_{u=1}^m \sum_{l=1}^n \epsilon(u, l) \frac{\hat{i}_{x_u, y_l} ((y_l - y_k) - j(x_u - x_i))}{2\pi ((x_u - x_i)^2 + (y_l - y_k)^2)} \right|$$

## Winding Loss Modeling

### Different Winding Sections



#### Section 1

Many mirroring steps  
necessary in order to push  
the walls away.

#### Section 2

Only one mirroring step  
necessary (only one wall).

→ Normally, higher proximity losses in Section 1.

# Winding Loss Modeling

## FEM Simulations : Round Windings (Including Litz Wire Windings) (1)

### Major Simplification

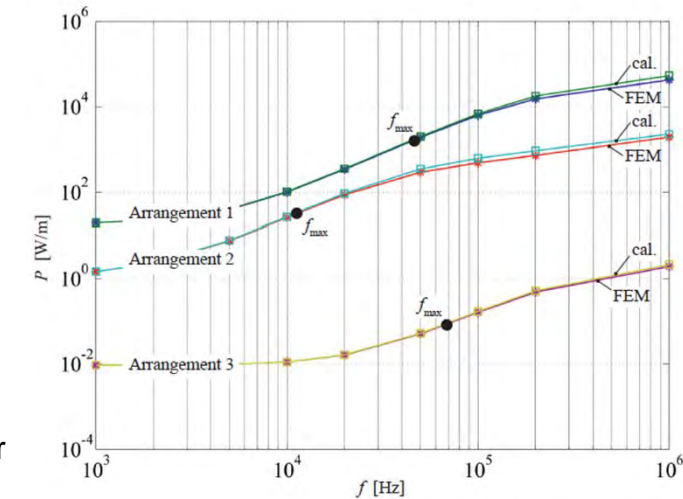
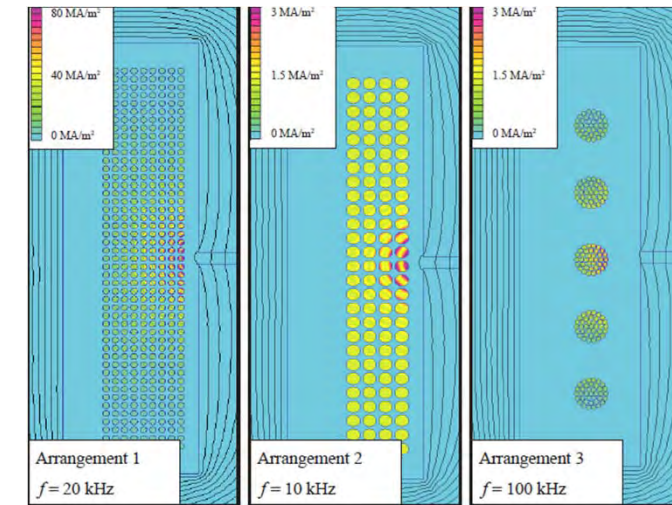
- magnetic field of the induced eddy currents neglected.
- This can be problematic at frequencies above (rule-of-thumb) [15]

$$f_{\max} = \frac{2.56}{\pi \mu_0 \sigma d^2}$$

### Results of considered winding arrangements

$f$ -range	$f < f_{\max}$	$f > f_{\max}$
Error	< 5%	> 5% (always < 25%)

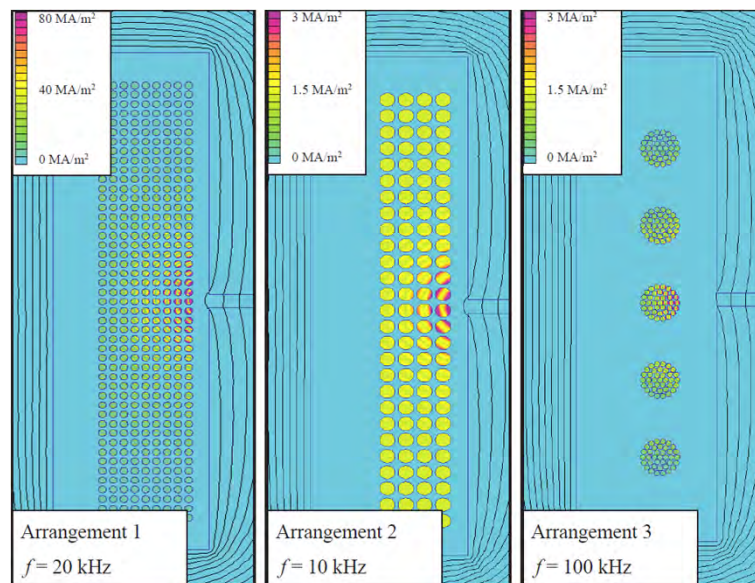
[15] A. Van den Bossche, V. C. Valchev, "Inductors and Transformers for Power Electronics", CRC Press. Taylor & Francis Group, 2005



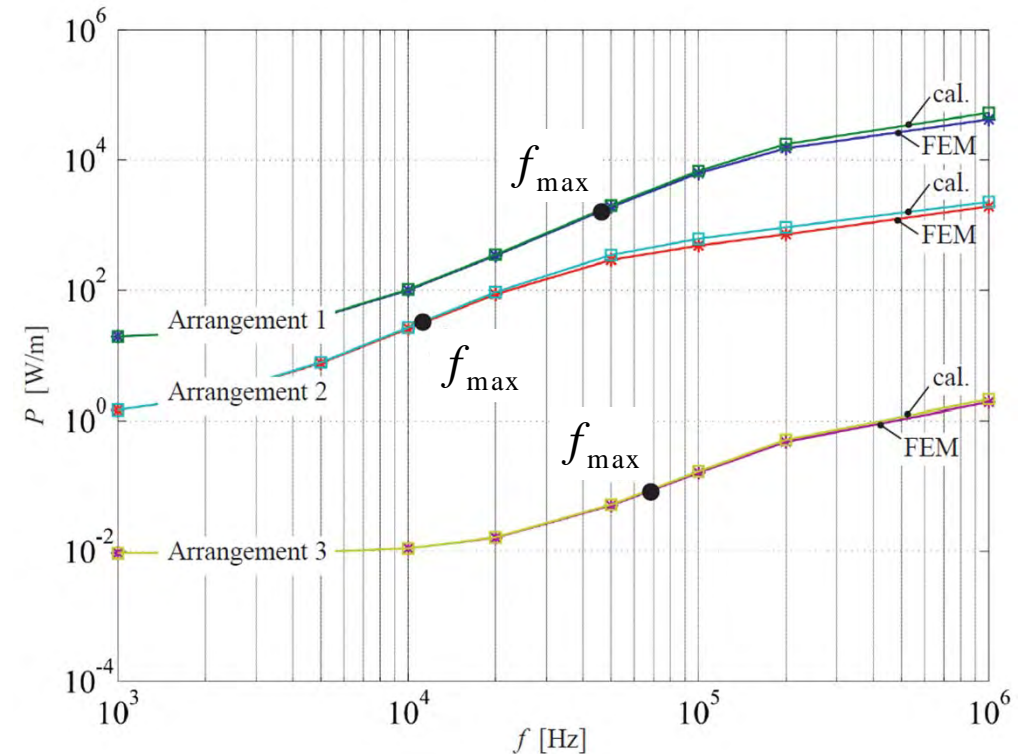
## Winding Loss Modeling

### FEM Simulations : Round Windings (Including Litz Wire Windings) (2)

#### FEM Simulation



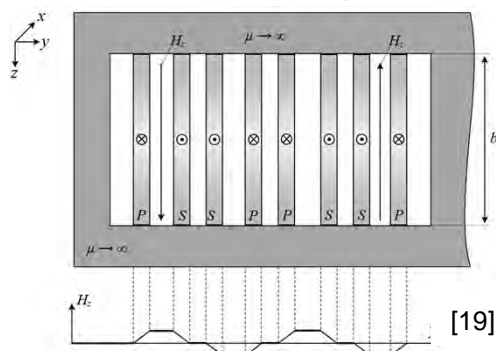
#### Results



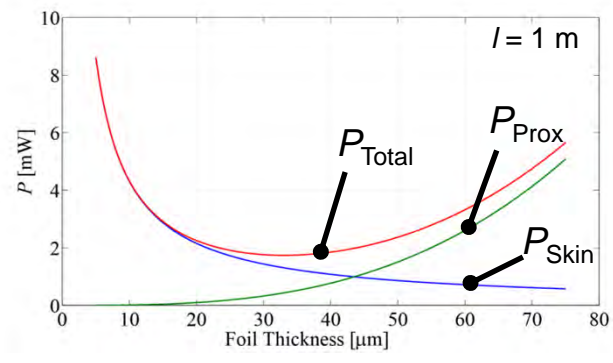
# Winding Loss Modeling

## Methods to Decrease Winding Losses (1)

### Interleaving

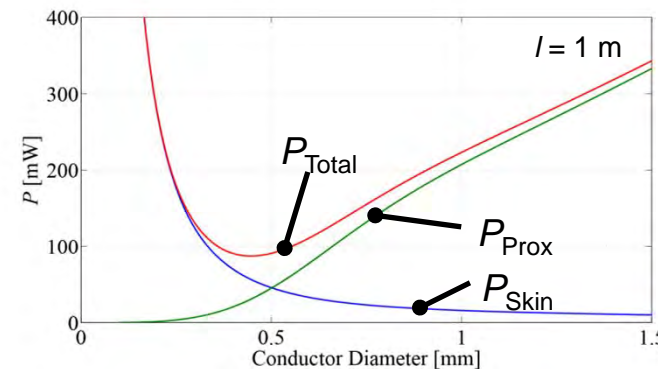


### Optimal Foil Thickness

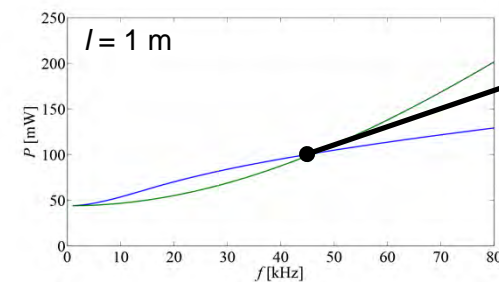


### Avoid Orthogonal Flux in Foil Windings

### Optimal Solid Wire Thickness



### Litz Wire

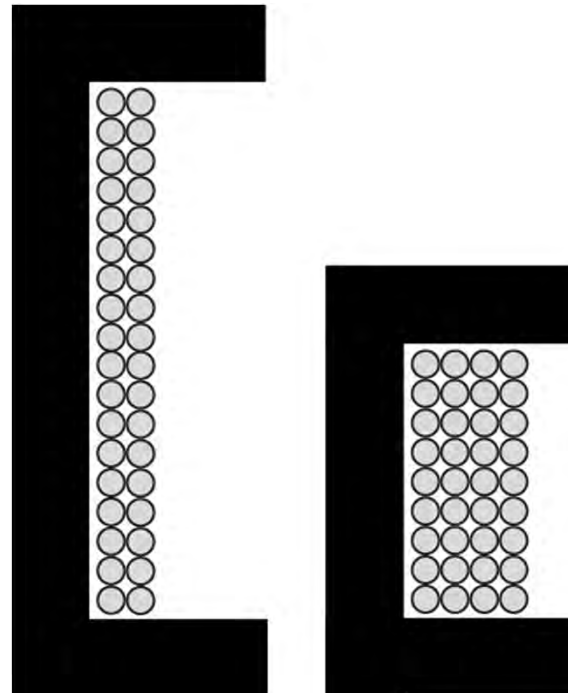


Push this point to higher frequencies!  
→ Increase number of strands.

# Winding Loss Modeling

## Methods to Decrease Winding Losses (2)

### Arrangement of Windings



Proximity losses increase in  
more compact winding  
arrangements.

# Winding Loss Modeling

## Methods to Decrease Winding Losses (3)

### Aluminum vs. Copper [13]

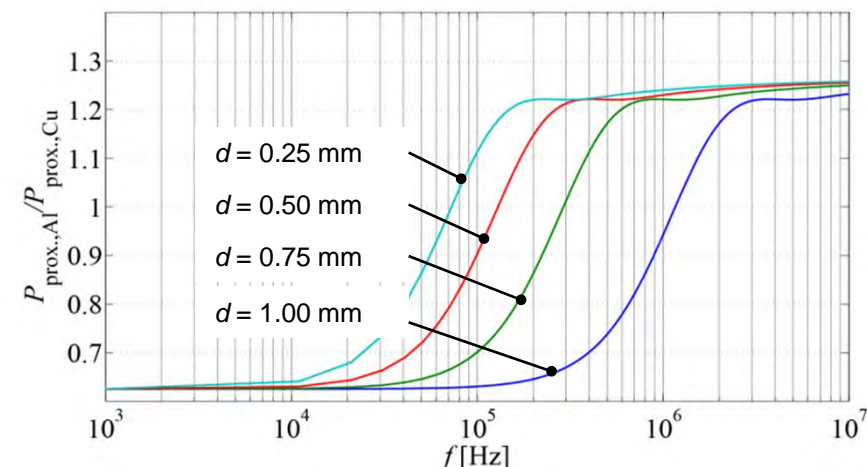
Aluminum (vs. Copper):

- Lighter
- Lower costs
- Lower Conductivity  $\sigma = 38 \cdot 10^6 \text{ } 1/(\Omega\text{m})$   
(Copper:  $\sigma = 58 \cdot 10^6 \text{ } 1/(\Omega\text{m})$ )

→ Lower Skin Depth!

Skin- and DC losses higher than in copper conductors.

Proximity losses are lower in aluminum conductors over a wide frequency range. Figure shows a comparison of single round solid conductors in external field.

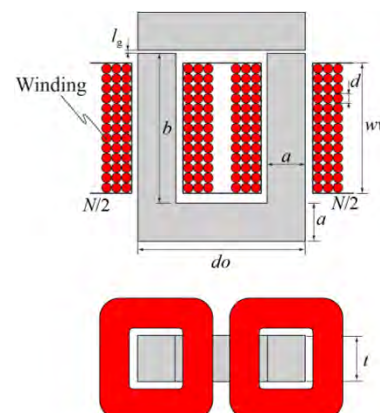
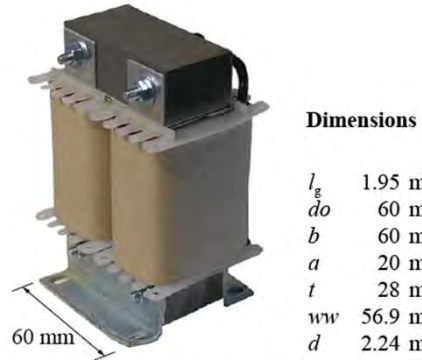


[13] M. Albach, "Induktive Komponenten in der Leistungselektronik", VDE Fachtagung - ETG Fachbereich Q1 "Leistungselektronik und Systemintegration", Bad Nauheim, 14.04.2011

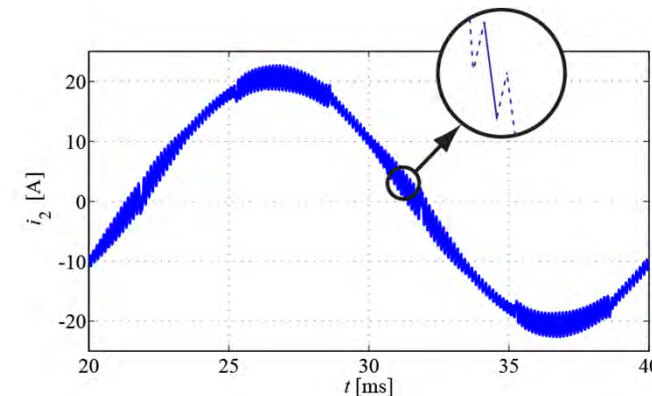
## Example

### Winding Loss Modeling

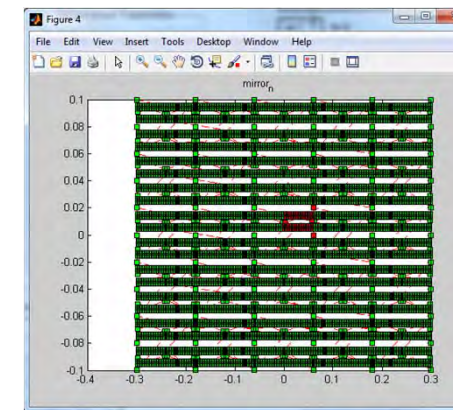
#### Photo & Dimensions



#### Current Waveform



#### Demonstration in MATLAB

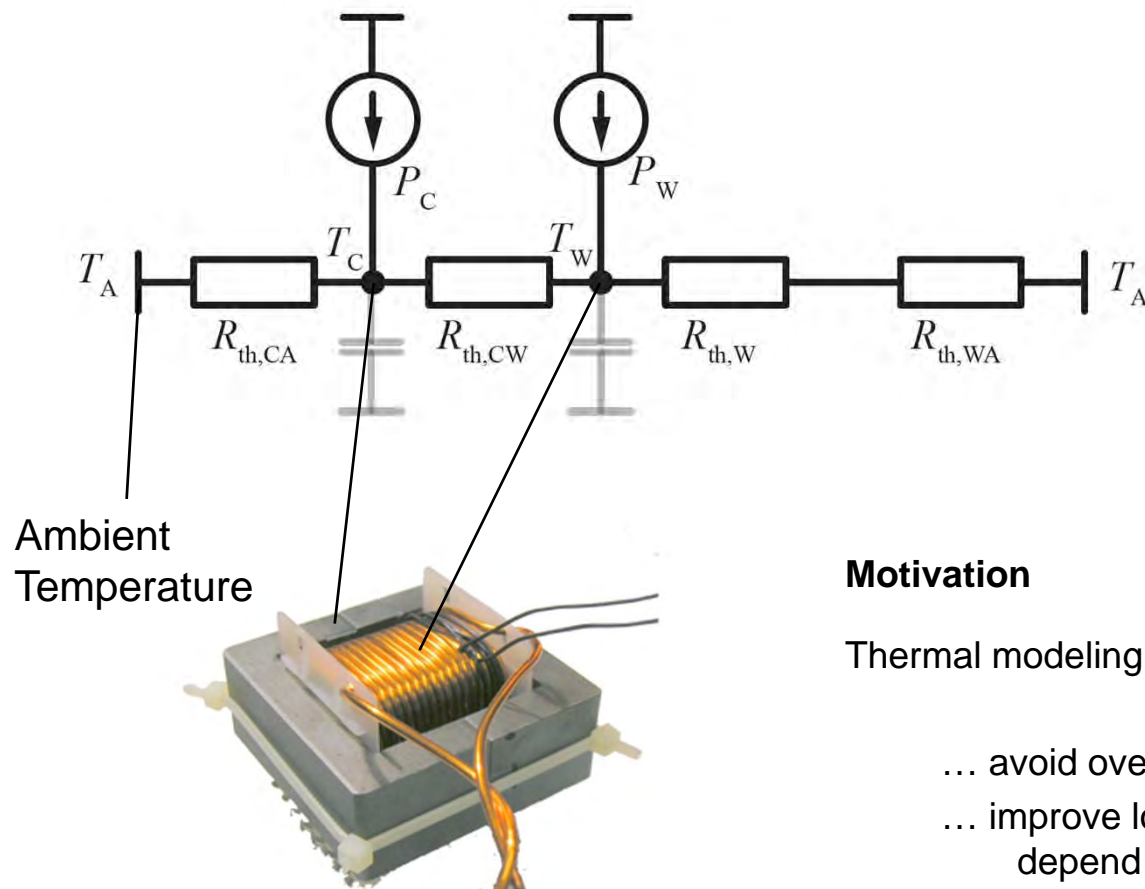


# Outline

- **Magnetic Circuit Modeling**
- **Core Loss Modeling**
- **Winding Loss Modeling**
- **Thermal Modeling**
- **Multi-Objective Optimization**
- **Summary & Conclusion**

# Thermal Modeling

## Motivation & Model (1)



### Motivation

Thermal modeling is important to ...

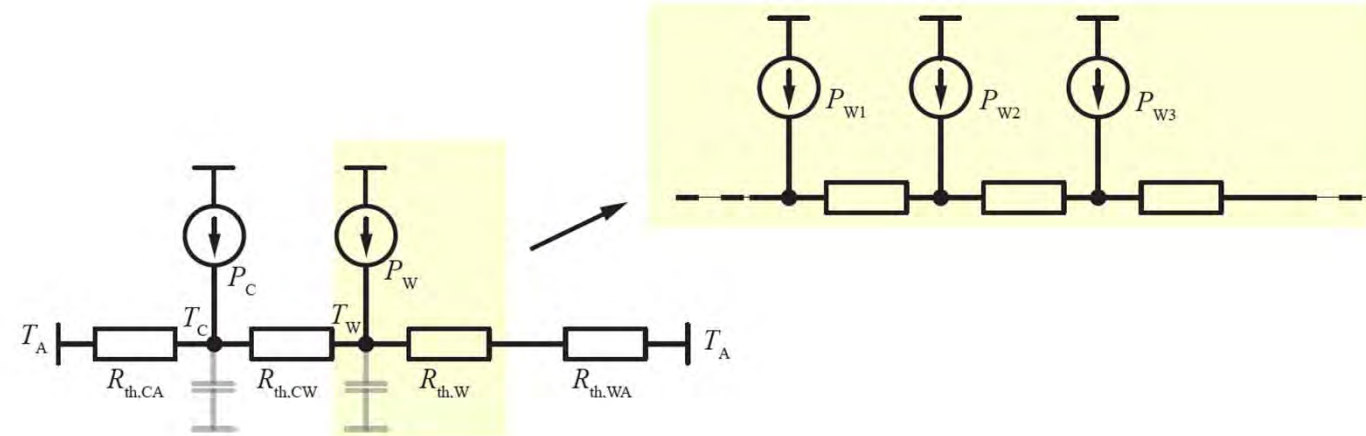
- ... avoid overheating.
- ... improve loss calculation (since the losses depend on temperature).

# Thermal Modeling

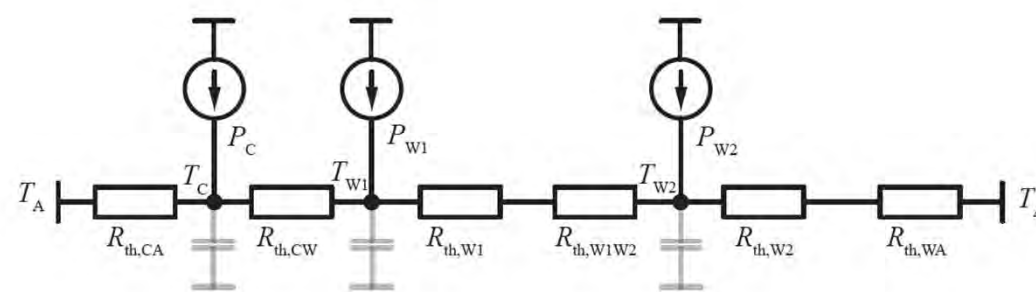
## Motivation & Model (2)

### Model

Inductor



Transformer



→ Determination of thermal resistors is challenging!

# Thermal Modeling

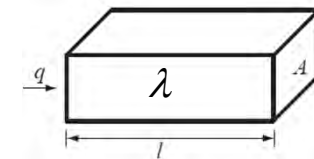
## Heat Transfer Mechanisms

$$R_{\text{th}} = \frac{\Delta T}{P} = f(T)$$

### Conduction

Independent of temperature  $T$  for most materials  
Difficult to determine interfaces between materials

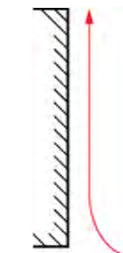
$$R_{\text{th}} = \frac{\Delta T}{P} = \frac{l}{A\lambda}$$



### Convection

Combined effect of conduction and fluid flow  
Changes with changing absolute temperature (nonlinear)  
Good empirical calculation approach available

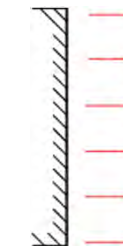
$$R_{\text{th}} = \frac{\Delta T}{P} = \frac{1}{\alpha A}$$



### Radiation

Small compared to other mechanisms  
Modeling the system is demanding  
(nonlinear eq. / to describe which components “sees”  
the other component).

$$P = \epsilon_{\text{eff}} A_l \sigma (T_b^4 - T_a^4)$$



# Thermal Modeling

## Thermal Resistance Calculation : (Natural) Convection (1)

$$R_{\text{th}} = \frac{\Delta T}{P} = \frac{1}{\alpha A}$$

**$\alpha$  is a coefficient that is influenced by ...**

- ... the absolute temperature,
- ... the fluid property,
- ... the flow rate of the fluid,
- ... the dimensions of the considered surface,
- ... orientation of the considered surface,
- ... and the surface texture.

# Thermal Modeling

## Thermal Resistance Calculation : (Natural) Convection (2)

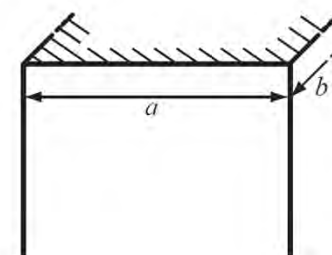
Empirical solutions known for ...

vertical plane

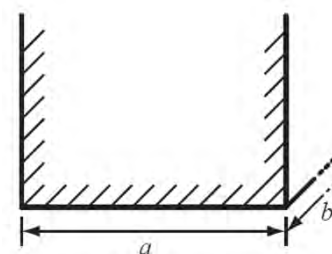


horizontal plane

- top:

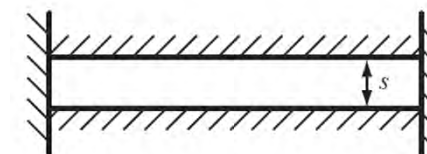


- bottom :

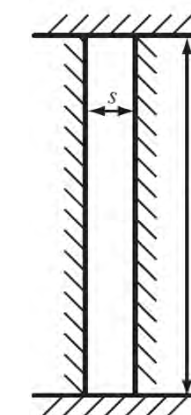


gap

- horizontal:



- vertical:



and more ...

# Thermal Modeling

## Thermal Resistance Calculation : (Natural) Convection (3)

### Structure of Empirical Solutions - Theory

$g$	gravity of earth: 9.81 m/s <sup>2</sup>
$l$	characteristic length
$\beta$	volumetric thermal expansion coefficient : 1/T (air)
$\nu$	kinematic viscosity: $162.6 \cdot 10^{-7}$ m <sup>2</sup> /s (air)

Name Measure of ...

Nusselt number  $Nu$  ... improvement of heat transfer compared to the case with hypothetical static fluid.

Grashof number  $Gr$  ... ration between buoyancy and frictional force of fluid.

Prandtl number  $Pr$  ... ratio between viscosity and heat conductivity of fluid.

Rayleigh number  $Ra$  ... flow condition (laminar or turbulent) of fluid.

$$Nu = \frac{l}{A\lambda} \sqrt{\frac{1}{\alpha A}} = \frac{\alpha l}{\lambda} = f(Gr, Pr)$$

$$Gr = \frac{gl^3}{\nu^3} \beta \Delta T$$

$$Pr = 0.7 \quad (\text{for air})$$

$$Ra = Pr \cdot Gr$$

### Procedure

$$Nu(Gr, Pr) \rightarrow \alpha = \frac{Nu(Gr, Pr)\lambda}{l} \rightarrow R_{th} = \frac{1}{\alpha A}$$

$\lambda$  is the heat conductivity of the fluid  
 $\lambda_{\text{air}} = 25.873 \text{ mW}/(\text{m K}) @ 20^\circ\text{C}$  [16]

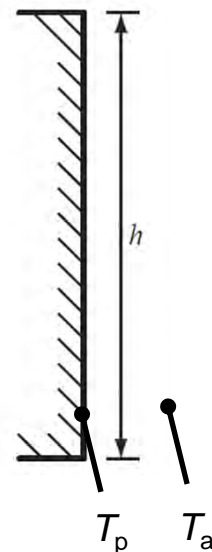
[16] VDI Heat Atlas, Springer-Verlag, Berlin, 2010

# Thermal Modeling

## Thermal Resistance Calculation : (Natural) Convection (4)

### Structure of Empirical Solutions - Example

Vertical Plane



$$Nu = \left( 0.825 + 0.387(Ra \cdot f_1(Pr))^{1/6} \right)^2$$

$$f_1 = \left( 1 + \left( \frac{0.492}{Pr} \right)^{9/16} \right)^{-16/9}$$

Reference:

[16] VDI Heat Atlas, Springer-Verlag, Berlin, 2010

$$\alpha = \frac{Nu(Gr, Pr)\lambda}{l} \quad (l = h)$$

$$R_{th} = \frac{\Delta T}{P} = \frac{1}{\alpha A}$$

### Example

( $h = 10 \text{ cm}$ ,  $T_p = 60^\circ\text{C}$ ,  $T_a = 20^\circ\text{C}$ ,  $A = h \cdot h$ )  
 $\rightarrow R_{th} = 16.6 \text{ K/W}$

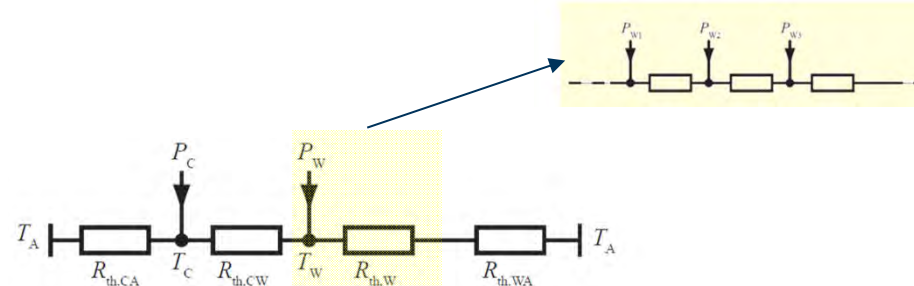
### Increase of Winding Surface



# Thermal Modeling

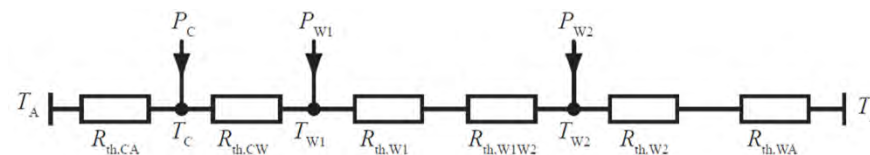
## Thermal Resistance Calculation : Conduction

### Overview

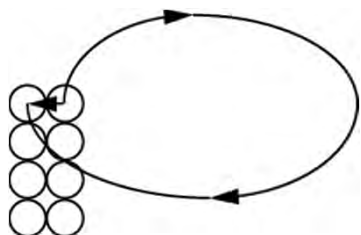


Normally, with natural convection it is

$$R_{th,W} \ll R_{th,WA}$$



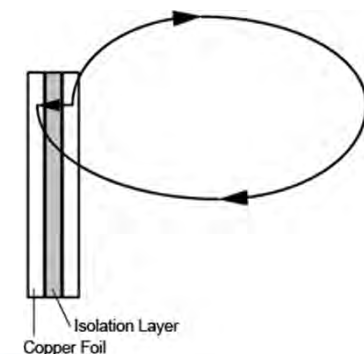
### Round Conductor



$R_{th,W}$  is difficult to determine. One difficulty is, e.g., to model the influence of pressure on the thermal resistance.

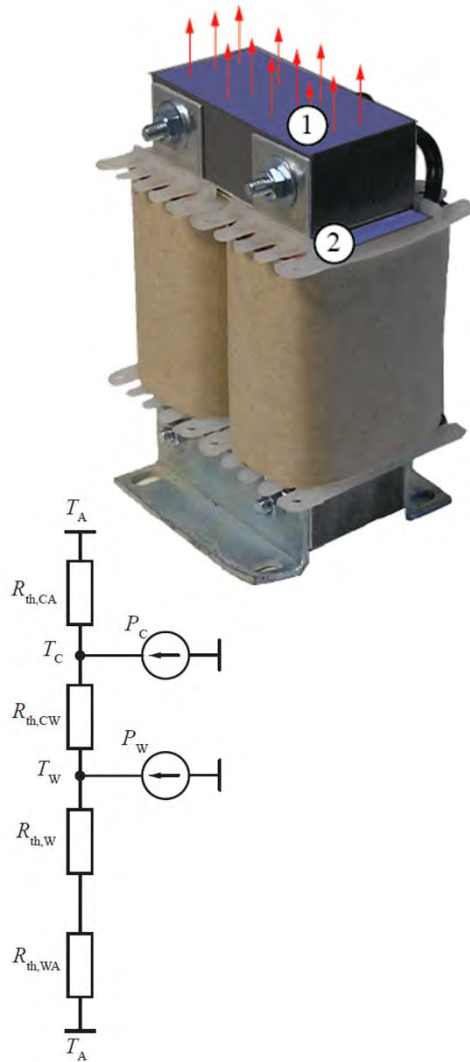
Litz wire shows low thermal conductivity.

### Foil Conductor

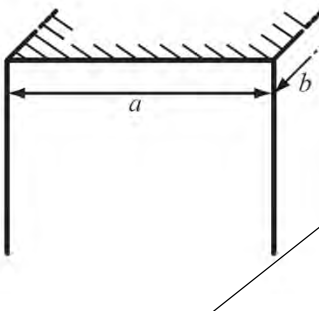


## Example

### Thermal Modeling (1)



#### (1) Horizontal Plane - Top



$g$  gravity of earth:  $9.81 \text{ m/s}^2$   
 $l$  characteristic length:  $l = a \cdot b / (2(a+b))$   
 $\beta$  volumetric thermal expansion coefficient:  $1/T$  (air)  
 $\nu$  kinematic viscosity:  $162.6 \cdot 10^{-7} \text{ m}^2/\text{s}$  (air)

$$Gr = \frac{gl^3}{\nu^3} \beta \Delta T$$

$$Pr = 0.7 \quad (\text{for air})$$

$$Ra = Pr \cdot Gr$$

$$Nu = \begin{cases} 0.766 (Ra \cdot f_2(Pr))^{1/5} & \text{for } Ra \cdot f_2(Pr) \leq 7 \cdot 10^4 \quad (\text{laminar}) \\ 0.15 (Ra \cdot f_2(Pr))^{1/3} & \text{for } Ra \cdot f_2(Pr) > 7 \cdot 10^4 \quad (\text{turbulent}) \end{cases}$$

with

$$f_2 = \left( 1 + \left( \frac{0.322}{Pr} \right)^{11/20} \right)^{-20/11}$$

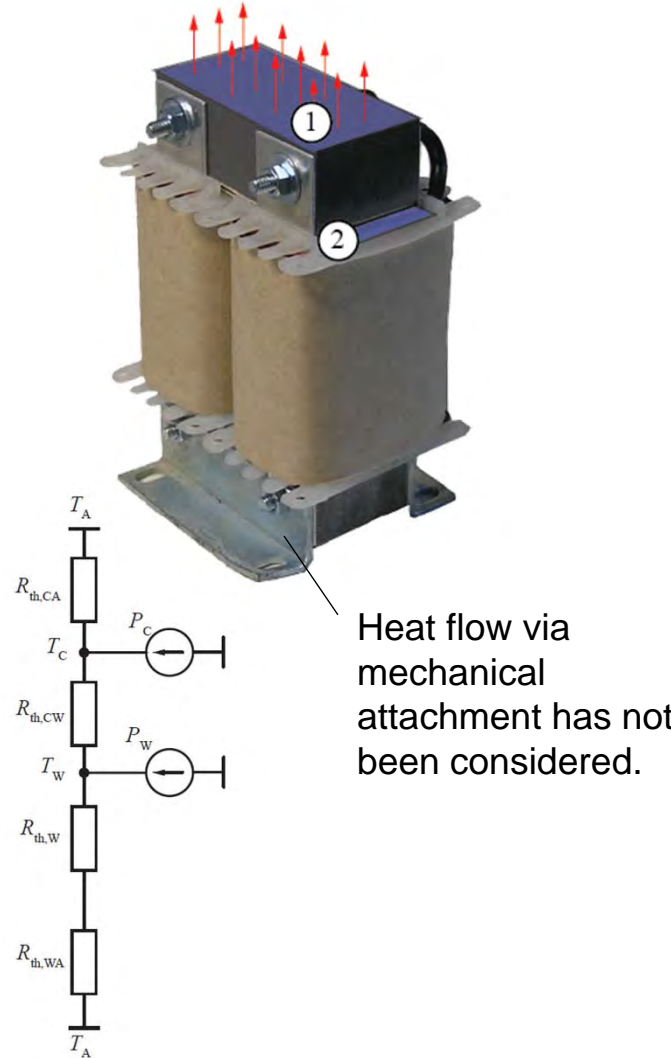
$$\alpha = \frac{Nu(Gr, Pr)\lambda}{l}$$

$$R_{th} = \frac{\Delta T}{P} = \frac{1}{\alpha A}$$

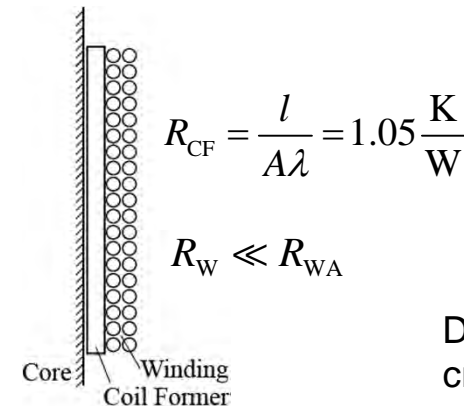
Resistor  $R_{th}$  is now calculated for one operating point!  
 ( $\rightarrow$  more iterations are necessary!)

## Example

### Thermal Modeling (2)



### (2) Core to Winding



Drawing represents the cross-section of one coil former side (there are total 2 x 4 coil former sides).

### Measurement Results

( $\Delta B=0.18$  T,  $f = 10$  kHz, triangular)

	Calc.	Meas.
$P_{core}$	107 °C	112 °C
$P_{winding}$	100 °C	104 °C

### Quantity Values

$$R_{th,CA} = 3.6 \text{ K/W}$$

$$R_{th,WA} = 4.7 \text{ K/W}$$

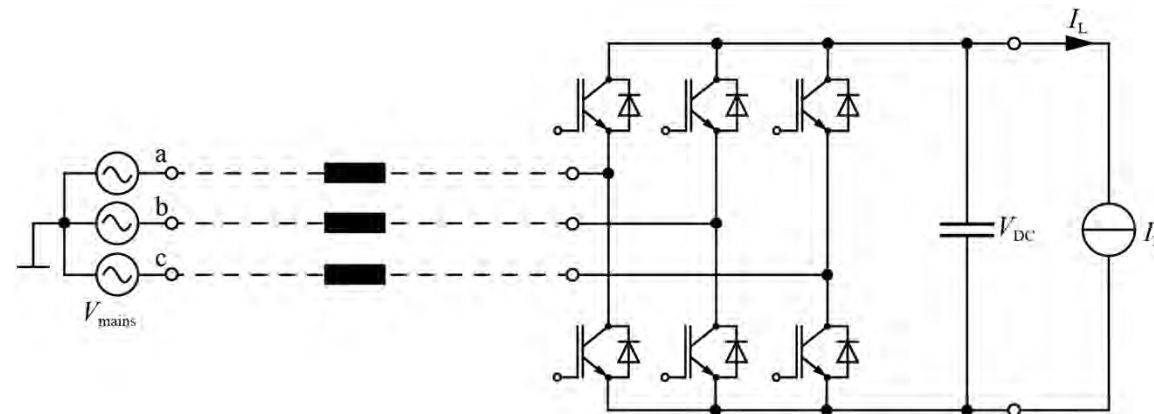
# Outline

- **Magnetic Circuit Modeling**
- **Core Loss Modeling**
- **Winding Loss Modeling**
- **Thermal Modeling**
- **Multi-Objective Optimization**
- **Summary & Conclusion**

# Multi-Objective Optimization – Volume vs. Losses

## Introduction to the PFC Rectifier (1)

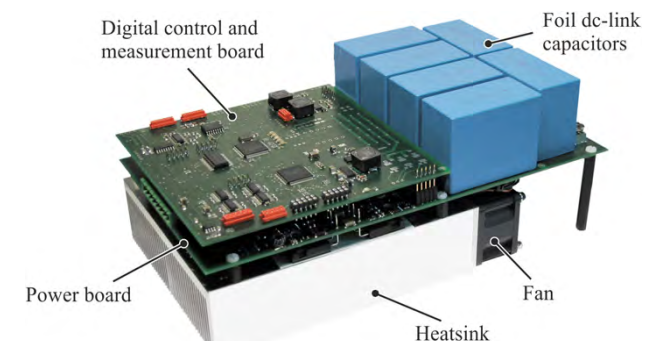
Simplified Schematic



Converter Specifications

Parameter	Variable	Value	
Input Voltage AC	$V_{\text{mains}}$	230	V
Mains Frequency	$f_{\text{mains}}$	50	Hz
DC-Voltage	$V_{\text{DC}}$	650	V
Load Current	$I_L$ (nominal)	15.4	A
Switching Frequency	$f_{\text{sw}}$	8	kHz

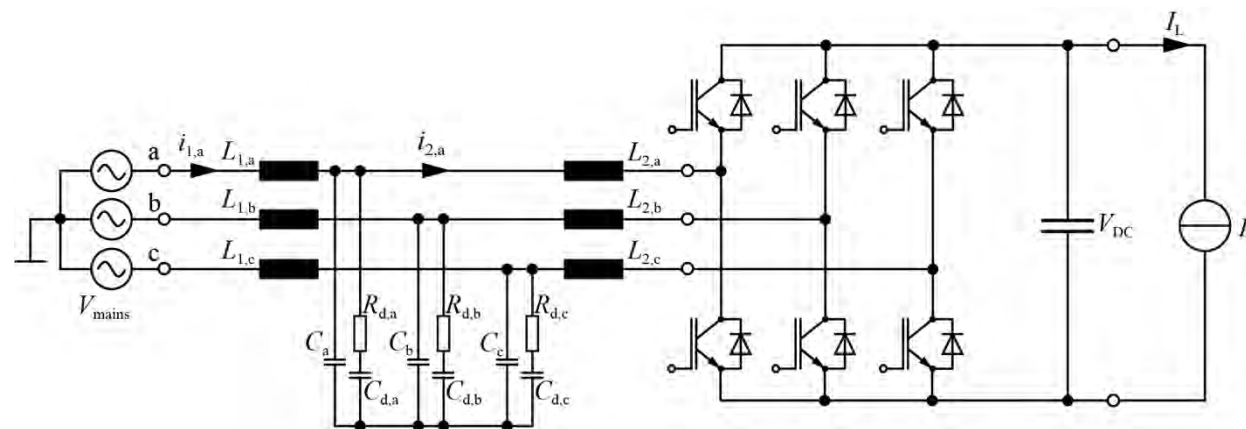
Photo of Converter



# Multi-Objective Optimization – Volume vs. Losses

## Introduction to the PFC Rectifier (2)

**Simplified Schematic**



### Filter Specifications

Input Current THD  $\leq 4\%$

Max. current ripple in boost inductors 4 A

**LCL filter consists of**

three boost inductors

and a damped three-phase *LC* filter.

# Multi-Objective Optimization – Volume vs. Losses

## Introduction to the PFC Rectifier (3)

**Selected Inductor Shape**

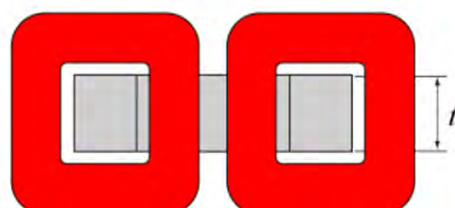
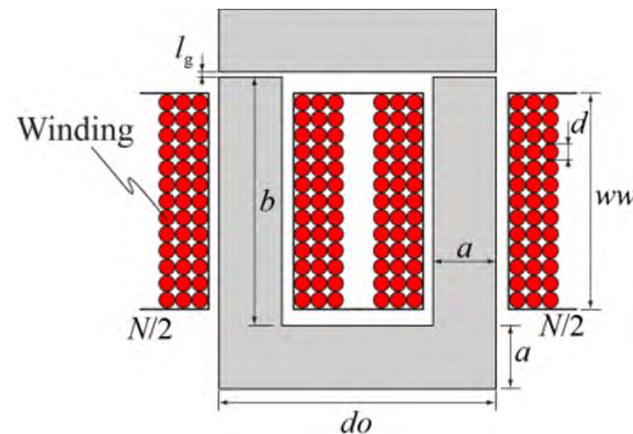


**Photo of Inductor**



**Degrees of Freedom**

$$\begin{pmatrix} l_g \\ a \\ N \\ do \\ b \\ t \\ ww \\ d \end{pmatrix}$$

**Material**

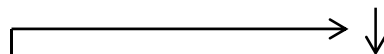
Grain-oriented steel  
(M165-35S,  
lam. thickness 0.35 mm)

# Multi-Objective Optimization – Volume vs. Losses

## Modeling LCL Filter (1)

### Procedure

- 1) A reluctance model is introduced to describe the electric / magnetic interface, i.e.  $L = f(i)$ .



- 2) Core losses are calculated.



- 3) Winding losses are calculated.



- 4) Inductor temperature is calculated.



### Considered effects

- Air gap stray field
- Non-linearity of core material
- DC Bias
- Different flux waveforms
- Wide range of flux densities and frequencies
- Skin and proximity effect
- Stray field proximity effect
- Effect of core to magnetic field distribution

## Multi-Objective Optimization – Volume vs. Losses

### Modeling LCL Filter (2)

**EPCOS X2 MKP Film  
Capacitor**  
(Rated voltage 305 V)



#### Volume Calculation

$$0.18 \mu\text{F}/\text{cm}^3$$

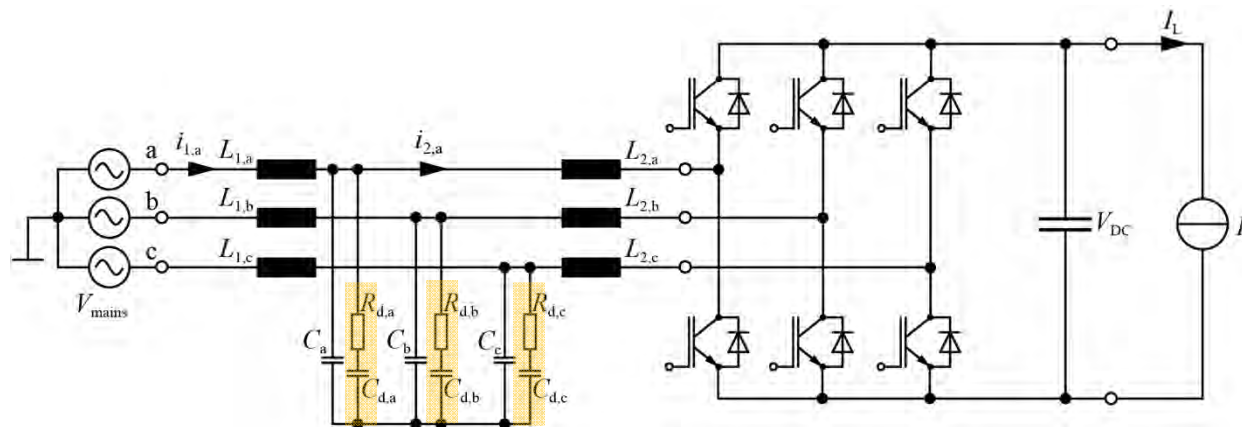
#### Power Loss Calculation

$$P = 2\pi f C \tan\delta V^2$$

## Multi-Objective Optimization – Volume vs. Losses

### Modeling LCL Filter (3)

Simplified Schematic



Trade-off between damping capacitor size and damping achieved

$$\rightarrow C = C_d$$

Optimal damping achieved with [17]

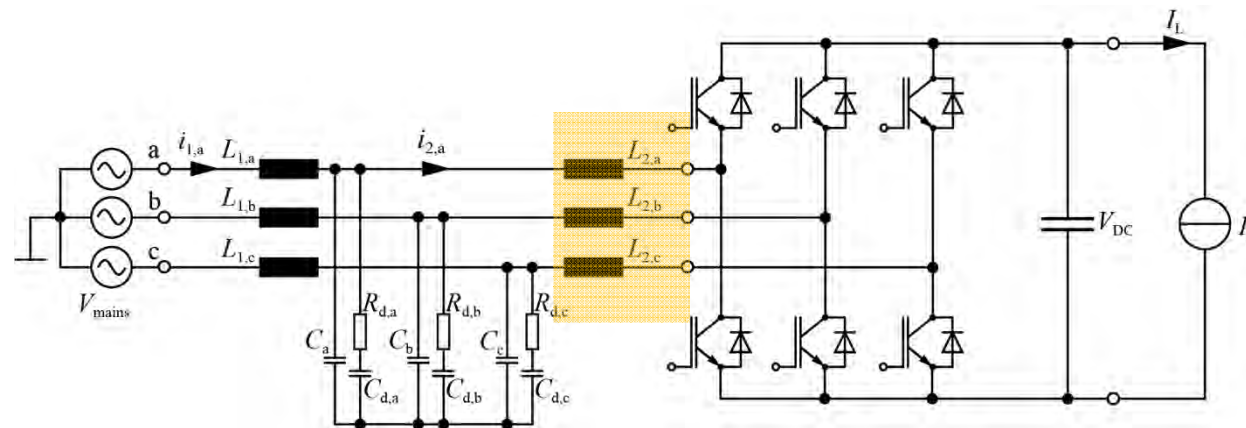
$$R_d = \sqrt{2.1 \frac{L_1}{C}}$$

[17] R. W. Erickson and D. Maksimovic, "Fundamentals of Power Electronics", Springer Science+Business Media, LLC, 2004

# Multi-Objective Optimization – Volume vs. Losses

## Optimization of LCL Filter (1)

Simplified Schematic



### Constraints concerning boost inductors

max. current ripple  $I_{HF,pp,max}$

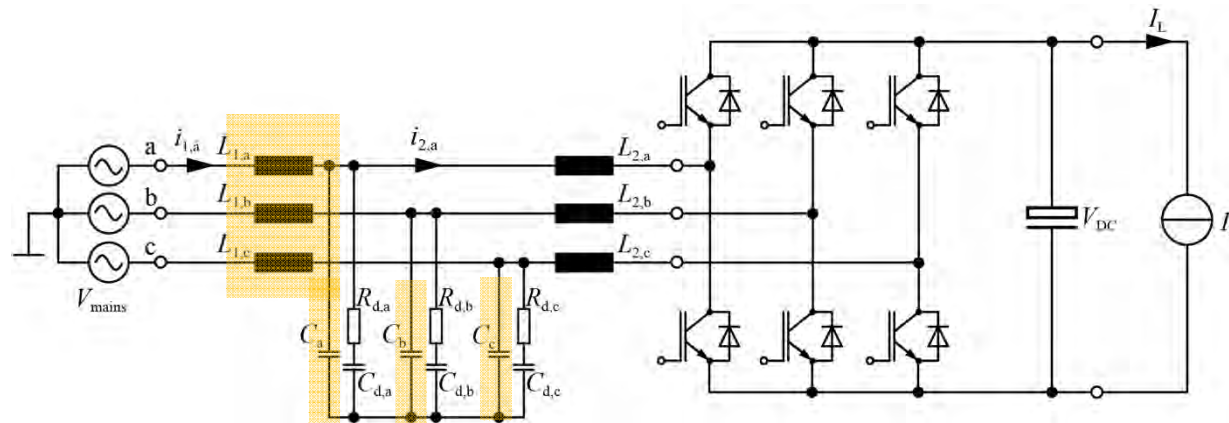
max. temperature  $T_{max}$

max. volume  $V_{max}$

## Multi-Objective Optimization – Volume vs. Losses

### Optimization of LCL Filter (2)

Simplified Schematic



### Constraints concerning LC filter

max. THD of mains current

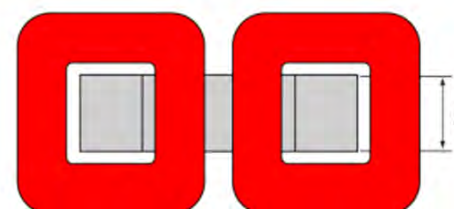
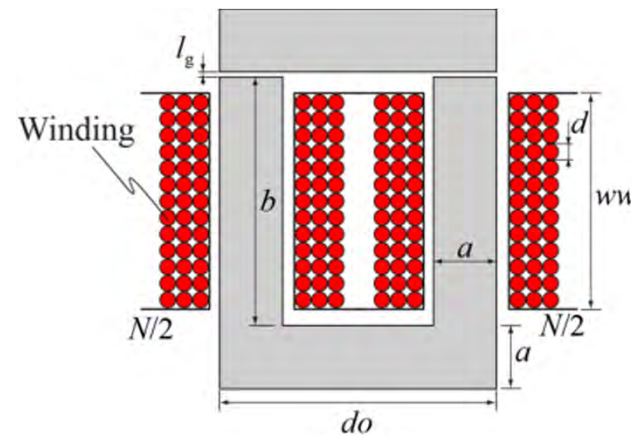
max. temperature  $T_{\max}$

max. volume  $V_{\max}$

## Multi-Objective Optimization – Volume vs. Losses

### Optimization of LCL Filter (3)

#### Selected Inductor Shape



#### Filter Design Parameterization

$$X = \begin{pmatrix} l_{g,L1} & l_{g,L2} \\ a_{L1} & a_{L2} \\ N_{L1} & N_{L2} \\ do_{L1} & do_{L2} \\ b_{L1} & b_{L2} \\ t_{L1} & t_{L2} \\ ww_{L1} & ww_{L2} \\ d_{L1} & d_{L2} \end{pmatrix}$$

#### Filter C Calculation

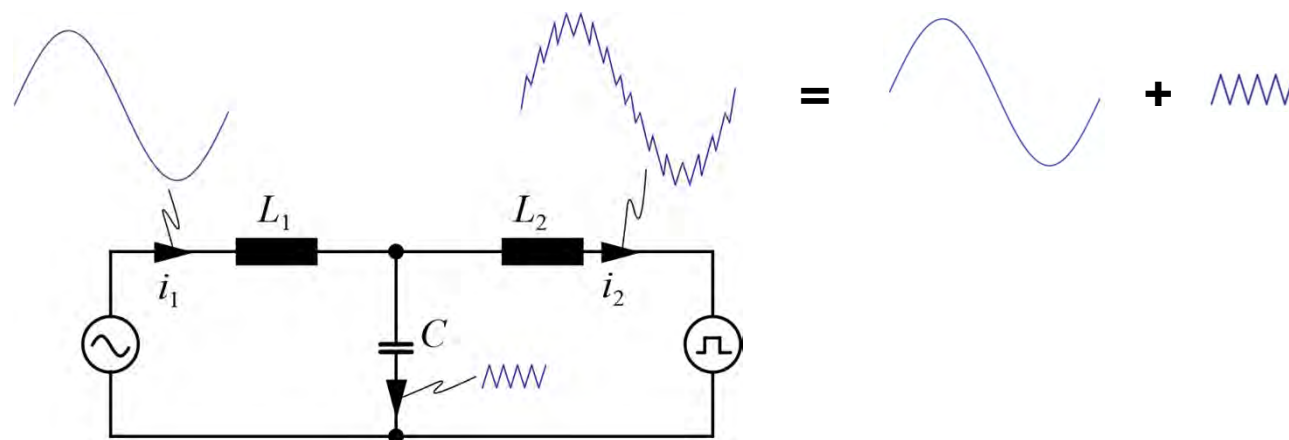
$$C = \frac{1}{L_1 \omega_0^2} = \frac{1}{L_1 (2\pi f_{sw} \cdot 10^{\frac{A}{40 \text{dB}}})^2}$$

- The filter capacitance is calculated to meet the THD constraint.

## Multi-Objective Optimization – Volume vs. Losses

### Optimization of LCL Filter (4)

Simplified current / voltage waveforms for optimization procedure



### Expectations

Loss overestimation in  $L_2$  expected.

Loss underestimation in  $L_1$  expected.

# Multi-Objective Optimization – Volume vs. Losses

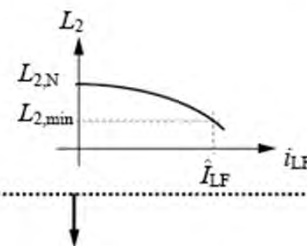
## Optimization of LCL Filter (5)

### Optimization Flow Chart (1)

#### Optimization Constraints and Conditions

- max.  $I_{HF,pp,max}$  in boost inductors  $L_2$  4 A
- max. THD of mains current 4 %
- max. temperature  $T_{max}$  125 °C
- max. volume  $V_{max}$  10 dm<sup>3</sup>
- switching frequency  $f_{sw}$  8 kHz
- DC link voltage  $V_{DC}$  650 V
- load current  $I_L$  15.4 A

#### → Calculate $L_2$



(I) Next slide

#### Boost Inductor

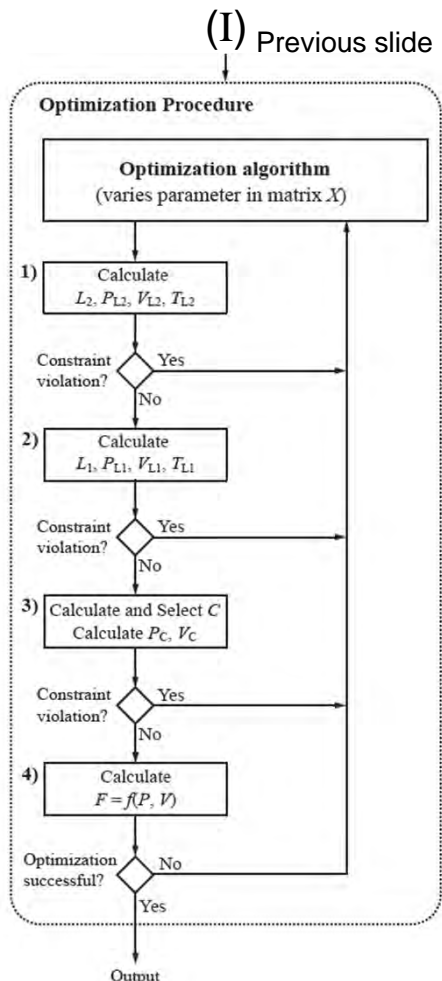
$$L_{2,min} = \frac{\sqrt{2}|V_{mains}|}{V_{DC}/\sqrt{3}} \cos(\pi/6) \cdot \frac{\frac{2}{3}V_{DC} - \sqrt{2}V_{mains}}{I_{HF,pp,max} \cdot f_{sw}}$$

$L_{2,min}$  can be calculated based on the constraint  $I_{HF,pp,max}$ . The maximum current ripple  $I_{HF,pp,max}$  occurs when the fundamental current peaks.

# Multi-Objective Optimization – Volume vs. Losses

## Optimization of LCL Filter (6)

### Optimization Flow Chart (2)



### Cost Function

$$F = k_{\text{Loss}} P + k_{\text{Volume}} V$$

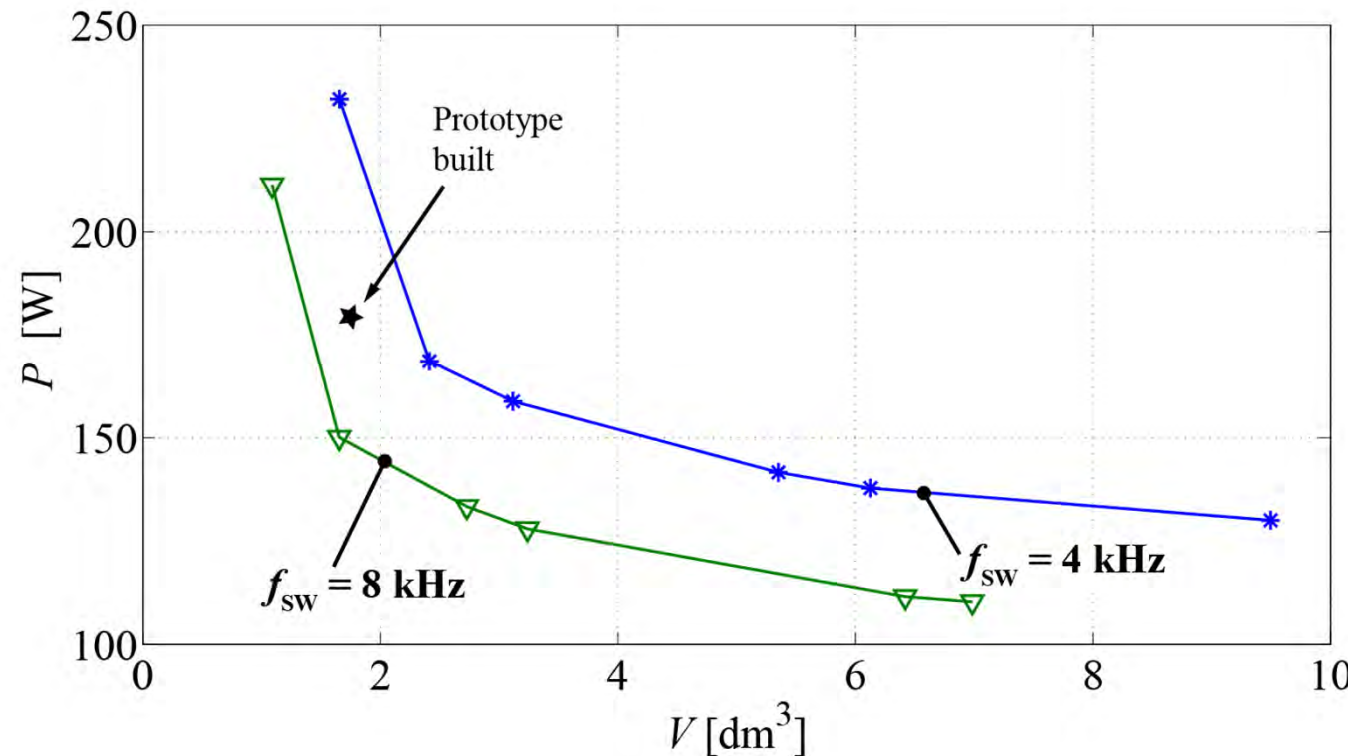
### Filter C Calculation

$$C = \frac{1}{L_1 \omega_0^2} = \frac{1}{L_1 (2\pi f_{\text{sw}} \cdot 10^{\frac{A}{40 \text{dB}}})^2}$$

## Multi-Objective Optimization – Volume vs. Losses

### Results – LCL Filter (1)

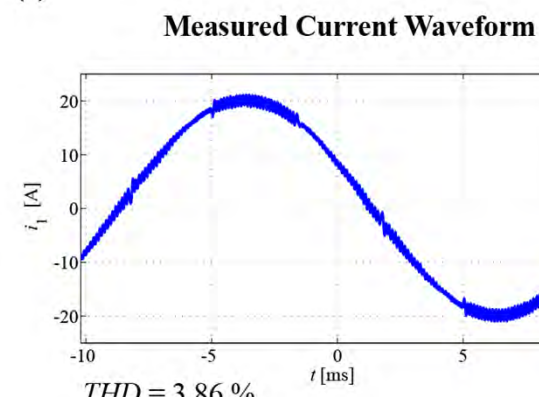
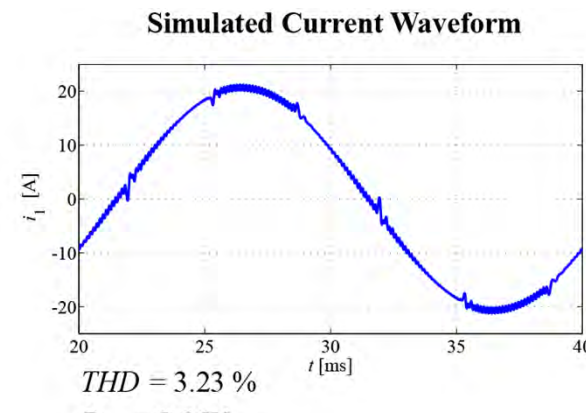
Filter Losses vs. Filter Volume  
**Pareto Front**



# Multi-Objective Optimization – Volume vs. Losses

## Results – LCL Filter (2)

Results  $L_1$



Photo



### Dimensions

(cf. Fig. 1)

$N$	44
$l_g$	4.7 mm
$do$	60 mm
$b$	60 mm
$a$	20 mm
$t$	8.2 mm
$ww$	56.9 mm
$d$	3.15 mm

### Conclusion

Loss modeling accurate.

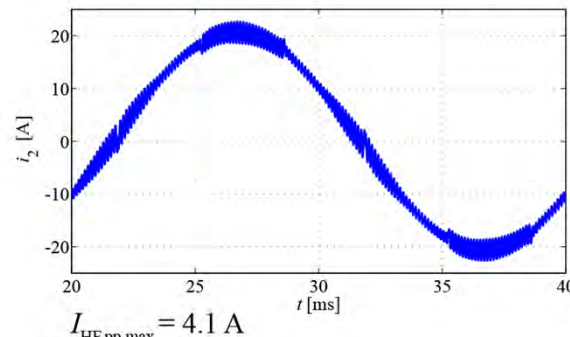
THD underestimated  
(frequency modeling necessary).

# Multi-Objective Optimization – Volume vs. Losses

## Results – LCL Filter (3)

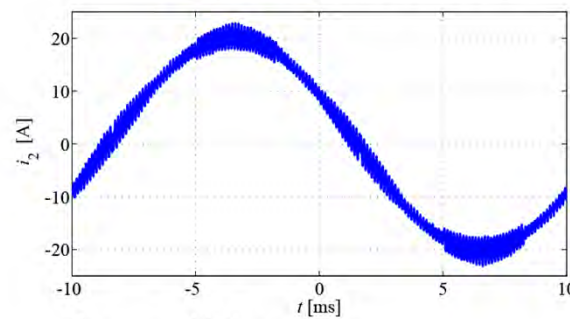
Results  $L_2$

Simulated Current Waveform



(a)

Measured Current Waveform



(b)

Photo



Dimensions

$l_g$	1.95 mm
$do$	60 mm
$b$	60 mm
$a$	20 mm
$t$	28 mm
$ww$	56.9 mm
$d$	2.24 mm

## Conclusion

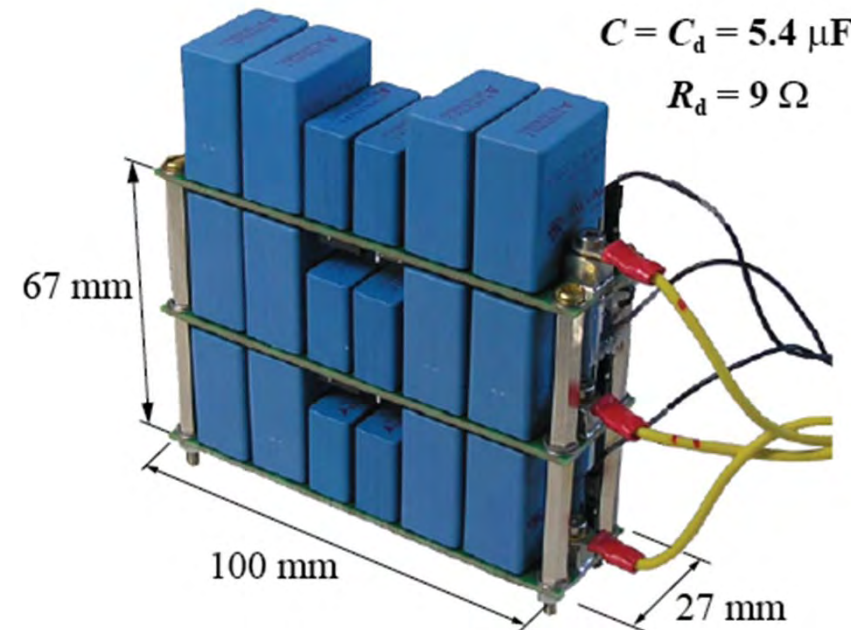
Loss modeling very accurate.

Current ripple underestimated  
(frequency modeling necessary).

## Multi-Objective Optimization – Volume vs. Losses

### Results – LCL Filter (4)

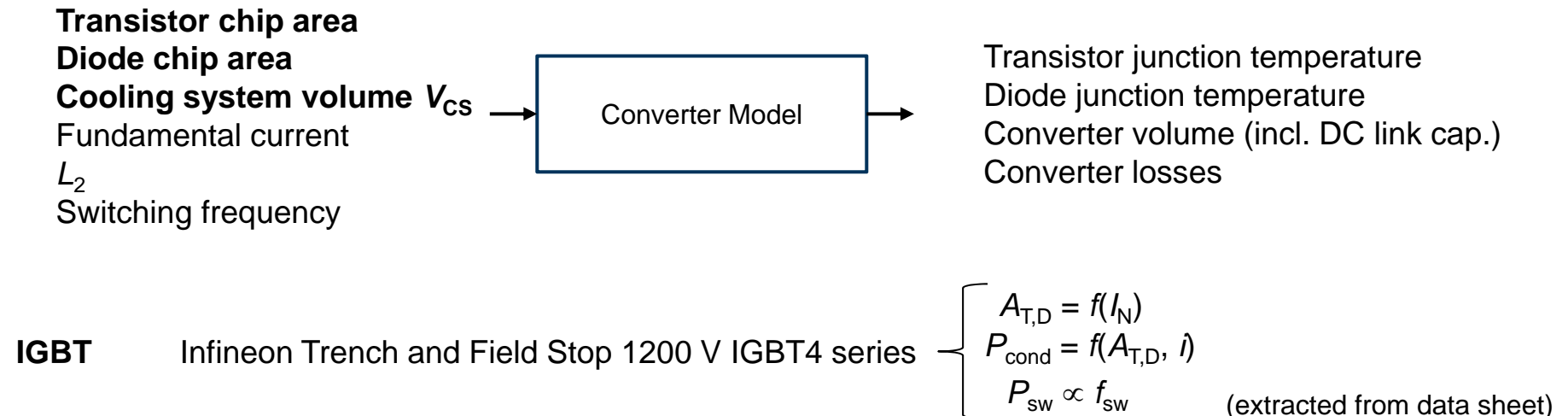
Photo of Capacitors



# Multi-Objective Optimization – Volume vs. Losses

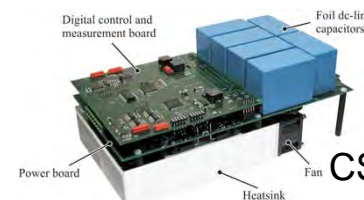
## Overall System Optimization (1) – Converter Model

### Converter Model



### Cooling System Performance Index (CSPI) [18]

$$R_{th} = \frac{1}{CSPI \cdot V_{cs}}$$



$CSPI \approx 15 \text{ W / (K liter)}$

[18] U. Drozenik, G. Laimer, J. W. Kolar, "Theoretical converter power density limits for forced convection cooling", Proc. of. PCIM Europe, Nuremberg, 2005

## Multi-Objective Optimization – Volume vs. Losses

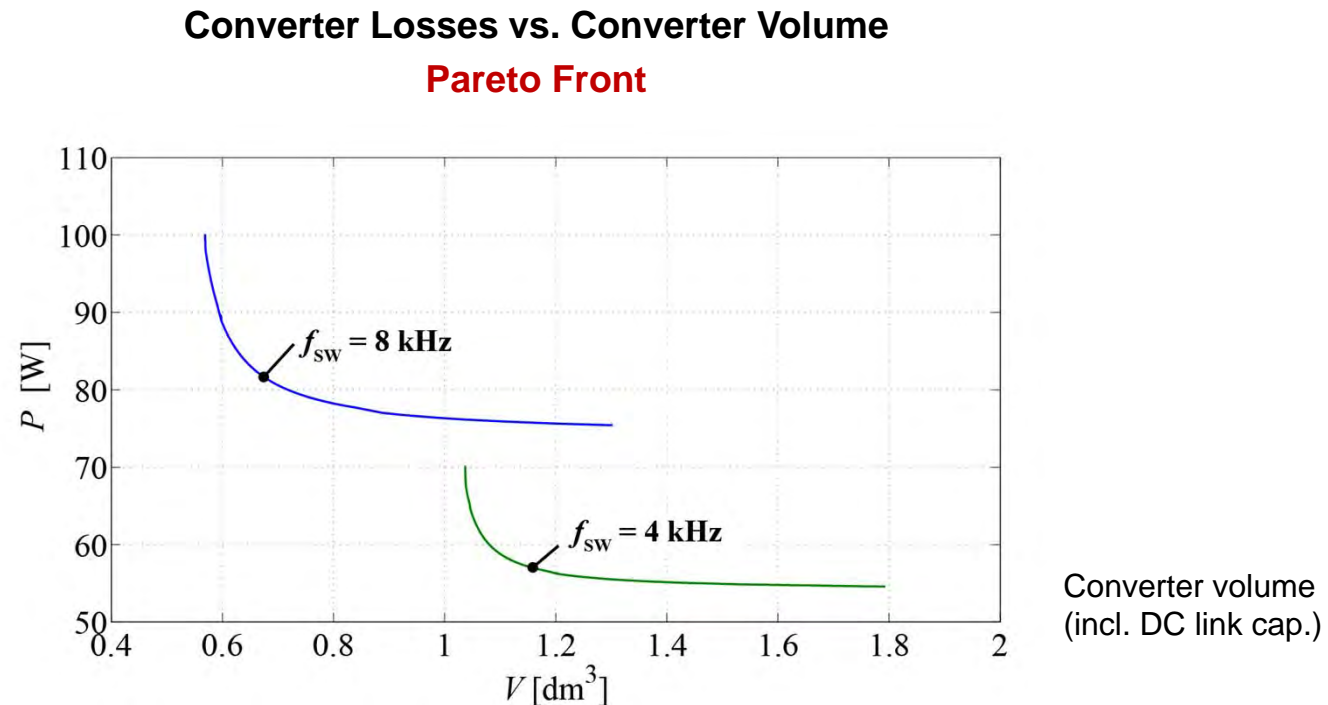
### Overall System Optimization (2) – Optimization Constraints

#### Optimization Constraints

Parameter	Variable	Value	
Max. junction temp.	$T_{j,\max}$	125	°C
Max. cooling system vol.	$V_{CS,\max}$	0.8	dm <sup>3</sup>
Heatsink height		4	cm
Max. area per chip	$A_{T,\max}/A_{D,\max}$	1	cm <sup>2</sup>
DC link voltage	$V_{DC}$	650	V
max. DC link voltage overshoot	$\Delta V_{DC}$	50	V
Fund. peak-peak current	$I_{(1),pp}$	20.5	A

## Multi-Objective Optimization – Volume vs. Losses

### Overall System Optimization (3) – Converter Pareto Front

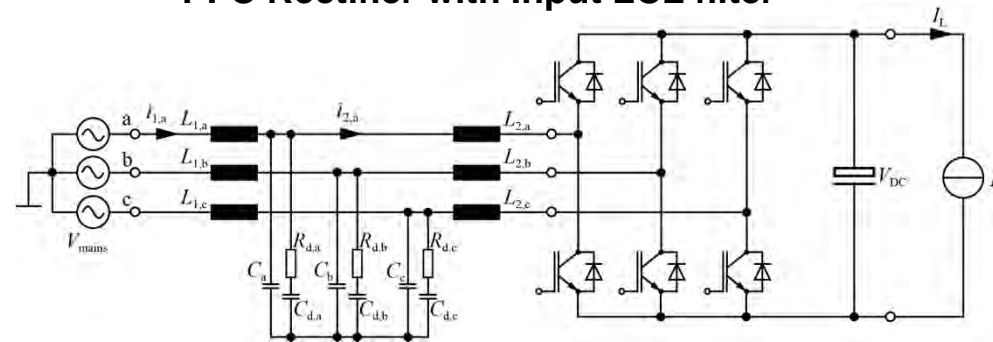


A decreasing switching frequency leads to lower losses!

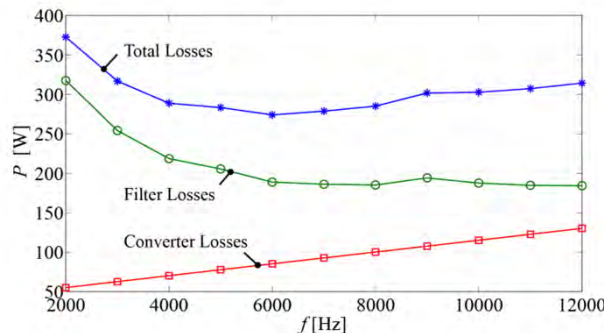
## Multi-Objective Optimization – Volume vs. Losses

### Overall System Optimization (3) – Optimal Designs

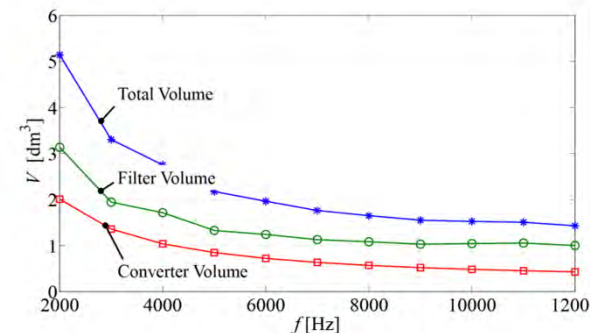
PFC Rectifier with Input LCL filter



Losses of loss-optimized designs



Volume of volumetric-optimized designs



- In order to get an optimal system design, an overall system optimization has to be performed.
- It is (often) not enough to optimize subsystems independently of each other.

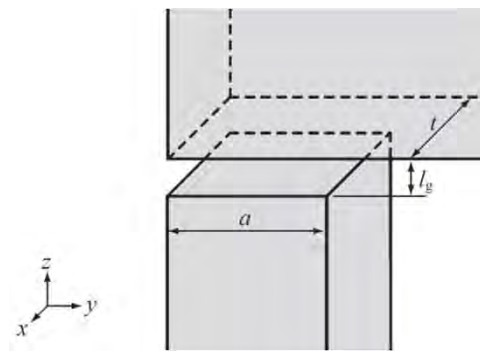
# Outline

- **Magnetic Circuit Modeling**
- **Core Loss Modeling**
- **Winding Loss Modeling**
- **Thermal Modeling**
- **Multi-Objective Optimization**
- **Summary & Conclusion**

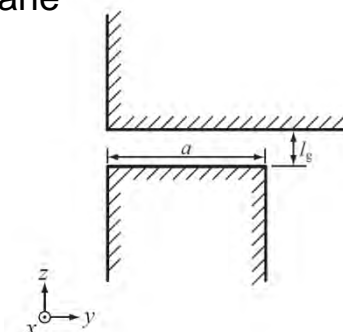
# Summary & Conclusion

## Magnetic Circuit Modeling

### Air Gap Reluctance Calculation



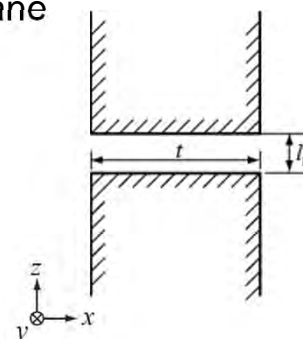
zy-plane



Air gap per unit length

$$\rightarrow R'_{zy} \rightarrow \sigma_y = \frac{R'_{zy}}{\frac{l_g}{\mu_0 a}}$$

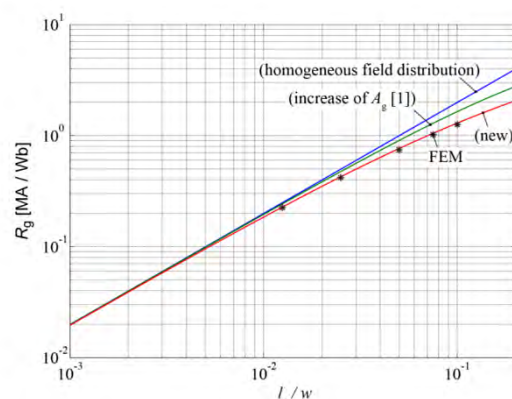
zx-plane



$$\rightarrow R'_{zx} \rightarrow \sigma_x = \frac{R'_{zx}}{\frac{l_g}{\mu_0 t}}$$

$$\rightarrow R_g = \sigma_x \sigma_y \frac{l_g}{\mu_0 a t}$$

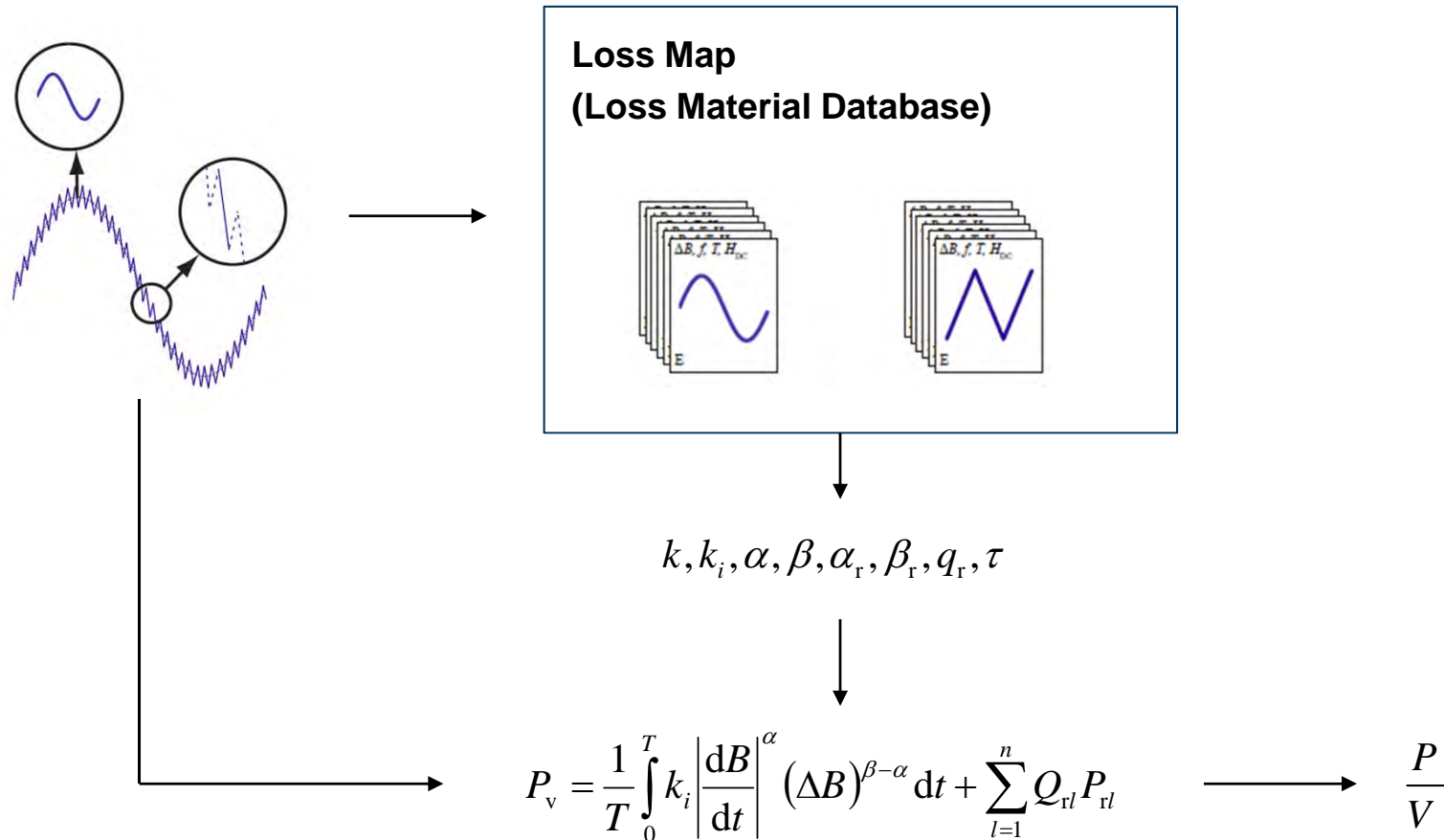
### Results



# Summary & Conclusion

## Core Loss Modeling

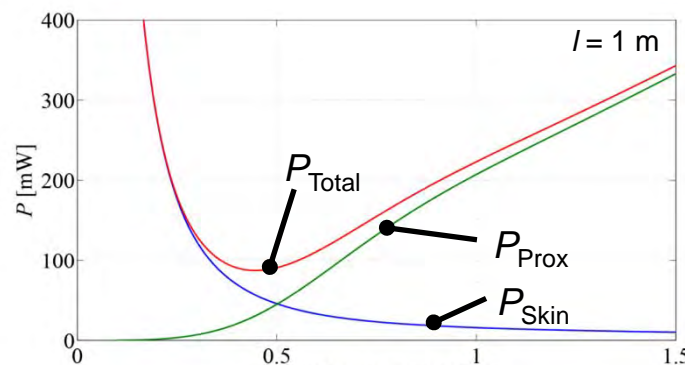
“The best of both worlds” (Steinmetz & Loss Map approach)



# Summary & Conclusion

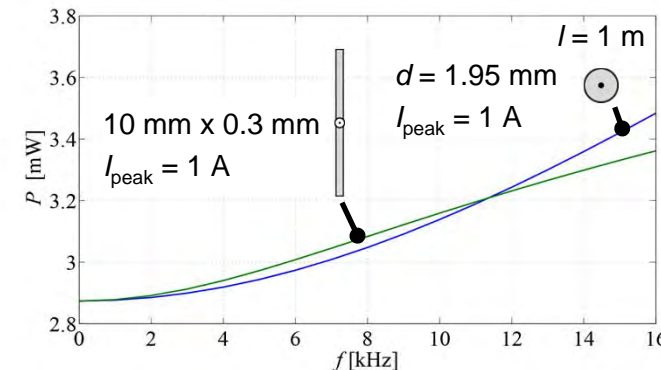
## Winding Loss Modeling

### Optimal Solid Wire Thickness

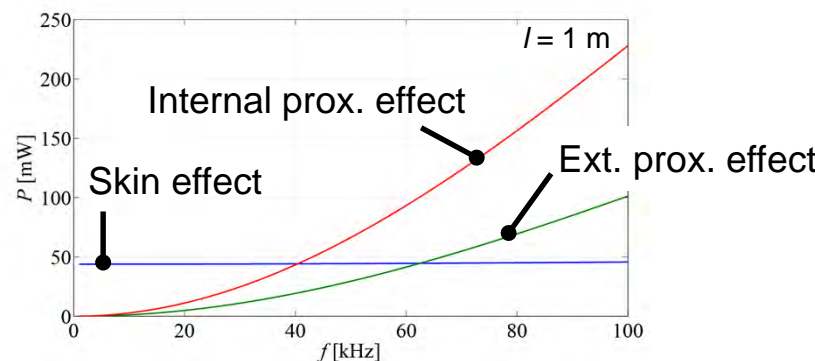


$(f = 100 \text{ kHz}, I_{\text{peak}} = 1 \text{ A}, H_{e,\text{peak}} = 1000 \text{ A/m})$

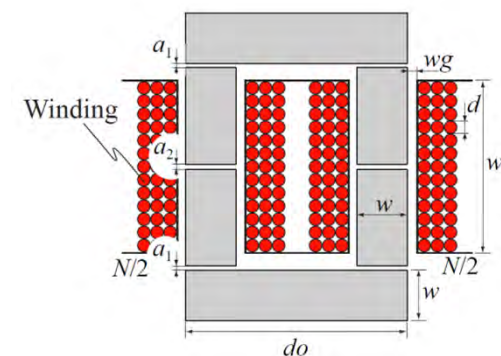
### Foil vs. Round Conductors



### Losses in Litz Wires



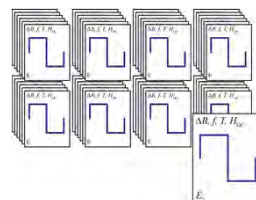
### Gapped cores: 2D approach



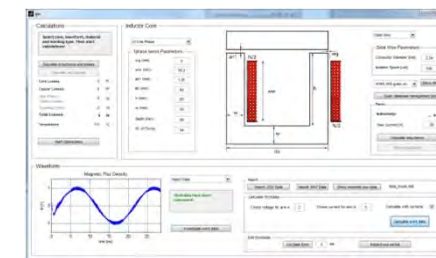
# Summary & Conclusion

## Magnetic Design Environment

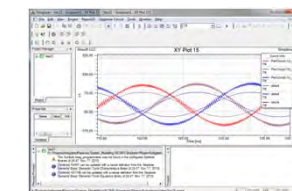
### Core Material Database



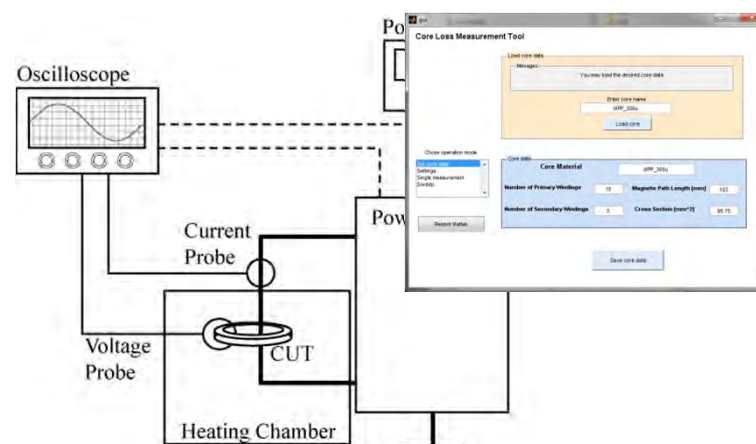
### Magnetics Design Software



### Circuit Simulator



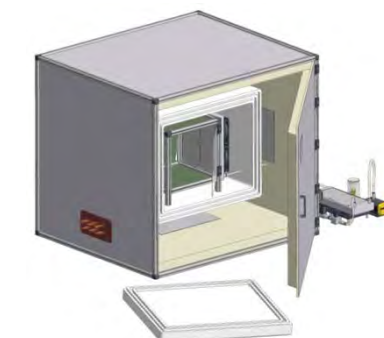
### Automated Measurement System



### Prototype



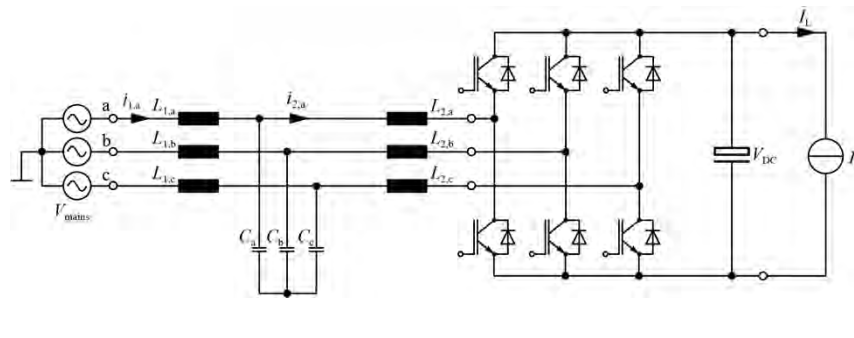
### Verification (e.g. with Calorimeter)



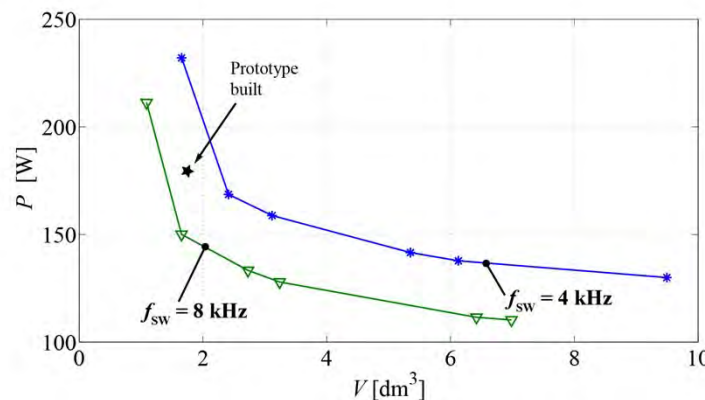
# Summary & Conclusion

## Multi-Objective Optimization - Next Steps

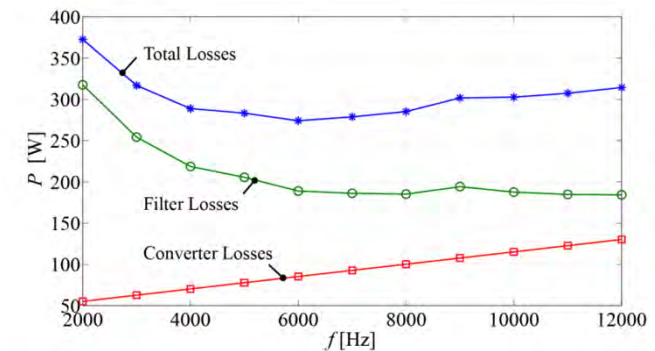
PFC Rectifier with Input LCL filter



Filter Pareto Front



Losses of loss-optimized designs



## Next Steps

Comparison of different rectifier topologies (2-level, 3-level), modulation schemes, etc. on filter size, filter losses.

# Thank you !

## Additional References

- [6] J. Mühlethaler, J.W. Kolar, and A. Ecklebe, "A Novel Approach for 3D Air Gap Reluctance Calculations", in Proc. of the ICPE - ECCE Asia, Jeju, Korea, 2011
- [9] J. Mühlethaler, J. Biela, J.W. Kolar, and A. Ecklebe, "Improved Core Loss Calculation for Magnetic Components Employed in Power Electronic Systems", in Proc. of the APEC, Ft. Worth, TX, USA, 2011.
- [19] Jürgen Biela, "Wirbelstromverluste in Wicklungen induktiver Bauelemente", Part of script to lecture Power Electronic Systems 1, ETH Zurich, 2007
- [20] J. Mühlethaler, J.W. Kolar, and A. Ecklebe, "Loss Modeling of Inductive Components Employed in Power Electronic Systems", in Proc. of the ICPE - ECCE Asia, Jeju, Korea, 2011
- [21] J. Mühlethaler, J. Biela, J.W. Kolar, and A. Ecklebe, "Core Losses under DC Bias Condition based on Steinmetz Parameters", in Proc. of the IPEC - ECCE Asia, Sapporo, Japan, 2010.
- [22] B. Cougo, A. Tüysüz, J. Mühlethaler, J.W. Kolar, "Increase of Tape Wound Core Losses Due to Interlamination Short Circuits and Orthogonal Flux Components", in Proc. of the IECON, Melbourne, 2011.
- [23] J. Mühlethaler, M. Schweizer, R. Blattmann, J.W. Kolar, and A. Ecklebe, "Optimal Design of LCL Harmonic Filters for Three-Phase PFC Rectifiers", in Proc. of the IECON, Melbourne, 2011

## Contact

**Jonas Mühlethaler**  
[muehlethaler@lem.ee.ethz.ch](mailto:muehlethaler@lem.ee.ethz.ch)  
[www.pes.ee.ethz.ch](http://www.pes.ee.ethz.ch)